

UVM ScholarWorks

Catalytic Main Group Element Bond Formation Reactions Toward the Preparation of Conjugated Materials

Item Type	dissertation;article
Authors	Mucha, Neil
Download date	2026-06-18 08:08:34
Link to Item	https://hdl.handle.net/20.500.14849/4432

CATALYTIC MAIN GROUP ELEMENT BOND FORMATION REACTIONS
TOWARD THE PREPARATION OF CONJUGATED MATERIALS

A Dissertation Presented

by

Neil Thomas Mucha

to

The Faculty of the Graduate College

of

The University of Vermont

In Partial Fulfillment of the Requirements
for the Degree of Doctor of Philosophy
Specializing in Chemistry

October, 2015

Defense Date: July 23, 2015
Dissertation Examination Committee:

Rory Waterman, Ph. D., Advisor
Qingbin Wang, Ph. D., Chairperson
Christopher C. Landry, Ph. D.
Adam C. Whalley, Ph. D.
Cynthia J. Forehand, Ph. D., Dean of the Graduate College

ABSTRACT

Polymers incorporating main group elements offer different and interesting properties compared to their all carbon analogues. For example, π -conjugated polymers incorporating phosphorus in the main chain of the polymer have generated interest due to their unique thermal and electronic properties, which primarily result from delocalization of the phosphorous lone pair within aromatic units. Similarly, interest in polysilanes stems from conductivity resulting from σ electron delocalization, though current methods of preparation for both of these types of materials are lacking. In this dissertation, both early and late transition-metal compounds were used to dehydrocouple phosphine and silane substrates. The use of dehydrocoupling catalysis as a method for the synthesis of main group element-linked polymers was explored utilizing substrates designed to engender solubility in their polymeric products. Progress towards the preparation of silane- and phosphine-based conjugated materials via dehydrocoupling catalysis is reported.

Catalytic reactions of bisphosphinite pincer-ligated iridium compounds p - $X^R(\text{POCOP})\text{IrHCl}$ ($\text{POCOP} = 2,6\text{-}(\text{R}_2\text{PO})_2\text{C}_6\text{H}_3$, $R = {}^i\text{Pr}, {}^t\text{Bu}$, $X = \text{H}, \text{COOMe}, \text{H}, \text{NMe}_2$) with primary and secondary silanes have been performed. Compounds featuring the less sterically demanding ${}^i\text{Pr}$ -substituted ligands facilitate silane redistribution reactions, but dehydrocoupling catalysis is observed for more encumbered silane substrates or with aggressive removal of H_2 . The bulkier ${}^t\text{Bu}$ -substituted compounds are silane dehydrocoupling precatalysts that also undergo competitive redistribution with less hindered substrates. Products generated from reactions utilizing ${}^t\text{Bu}$ ligated Ir include low molecular weight oligosilanes with varying degrees of redistribution present or disilanes when employing more sterically demanding substrates. The interplay of steric and electronic effects of the POCOP ligand on the silane product distribution will be presented.

In previous work by our group, a triamidoamine-supported zirconium catalyst, $[\kappa^5\text{-}(\text{Me}_3\text{SiNCH}_2\text{CH}_2)_2\text{NCH}_2\text{CH}_2\text{NSiMe}_2\text{CH}_2]\text{Zr}$, **1** has been shown to be effective in catalyzing the formation of phosphorus–element bonds via dehydrocoupling. Substrates including 2,5-bisphosphinofuran and 1,4-bisphosphinobenzene were dehydrocoupled to yield hyperbranched polyphosphine products. Efforts to characterize these products have been limited due to poor solubility. Rational substrate design incorporating aliphatic side chains in primary phosphine linker molecules to engender solubility has been accomplished. Treatment of these second generation substrates with **1** or $[\text{Cp}^*\text{ZrH}_3]\text{Li}$, **2** leads to sluggish reactions reaching moderate conversions to diphosphine products. The working hypothesis is that steric congestion during the bond forming step hinders additional bond-formation. Efforts toward the characterization and utilization of these insoluble materials as metal ion scavengers will be presented.

CITATIONS

Material from this dissertation has been published in the following form:

Mucha, N.T.; Waterman, R.. (2015). Iridium Pincer Catalysts for Silane Dehydrocoupling: Ligand Effects on Selectivity and Activity. *Organometallics*, 34, 3865–3872.

DEDICATION

To my parents, grandparents and family

ACKNOWLEDGEMENTS

This work was supported by a US National Science Foundation grant (CHE-1265608) to R.W. I would also like to thank the Vermont Space Grant Consortium for support through a NASA Experimental Program to Stimulate Competitive Research Graduate Research Fellowship. The last five years have flown by. Looking back, my career at UVM has been a rollercoaster ride littered with moments of hope, sadness, frustration, and elation which ultimately culminated in a rewarding and formative experience. During my time in Vermont, many people and experiences helped shape me both as a scientist and as a person; the work presented in this dissertation would not be possible without their continued support and friendship. With all aspects of life to find fulfillment in whatever you do, it's always "all about the people".

I would first like to thank my advisor, Dr. Rory Waterman. Choosing a graduate advisor is the one time in a person's life where they can pick their own boss. I committed to UVM specifically to work with you, and in retrospect I wouldn't change a thing. I just wish I wasn't so intimidated by your incredibly quick wit during the first three years. Thank you for being an excellent advisor, mentor, and role model. I am in continued awe at how hard you work at your craft, and no doubt it will continue to lead to your future success.

Thank you to the many Waterman group graduate students and undergrads that I've had the pleasure of working with over the years. I specifically thank Dr. Mike Ghebreab for teaching me Schlenk technique and taking me under his wing as a first year. "Young" Anthony Ramuglia also deserves credit for being an awesome protégé, great lab mate, and for always being amenable to my coaching.

Thank you to Dr. Matt Sheridan for reminding me to always make time for “drinking and thinking”. You’re the man, even if no one cares about electrode modification 😊. Always remember the good times down by the river. Dr. Natalie Machamer deserves special thanks for the many conversations that kept me sane and for continually reminding me how awesome PA is. Thank you for being a great example of a graduate student who doesn’t procrastinate, and for being a great friend. PA 4 EVA.

Thank you to “The B Team”: Matt, Shaun, Nina, Heather, Dan, and Lindsey for never talking about chemistry and for forcing me to go out. You all are great people who I am proud to call my friends. I have truly grown as a person because of the experiences we’ve shared together.

Douglas, thank you for being you. Though we are brothers, I’ve always thought it’s really cool how different we both are. Thank you for always being willing to listen, calling me out on occasional BS, and for the countless hours of conversation at the Legion. Let’s go sign the book when I’m back in The Valley.

To my parents Tom and Diane: what can I say? Anything I write here is a severe understatement. Thank you for everything you’ve done for me to this point. Thank you for believing in me even when I didn’t believe in myself. Thank you both for being shining examples of great parents and for always placing emphasis on doing the right thing.

TABLE OF CONTENTS

	Page
CITATIONS	ii
DEDICATION.....	iii
ACKNOWLEDGEMENTS.....	iv
LIST OF TABLES.....	ix
LIST OF FIGURES	xi
LIST OF ABBREVIATIONS.....	xiv
CHAPTER 1: GENERAL INTRODUCTION	1
1.1. Conjugated Polymers.....	1
1.2. π -Conjugated Materials	3
1.2.1. Design Considerations	5
1.2.2. Heteroatom Substitution	6
1.3. Phosphorus in Conjugated Materials.....	9
1.4. Polysilanes and σ -Conjugated Polymers	14
1.4.1. σ Electron Delocalization	15
1.4.2. Substituent and Conformational Effects.....	17
1.5. Dehydrocoupling	19
1.5.1. Mechanisms of Metal-Catalyzed Dehydrocoupling Reactions	21
1.6. Phosphine Dehydrocoupling.....	25

1.6.1. Early Transition-Metal Catalysts	26
1.6.2. Late Metal Catalysts	28
1.6.3. Main Group Catalysts	30
1.7. Silane Dehydrocoupling	31
1.7.1. Early Transition Metal Catalysts	32
1.7.2. Late Transition-Metal Catalysts	34
1.8. Pincer Compounds.....	39
1.8.1. Catalysis with Iridium Pincer Compounds	40
1.9. References.....	41
CHAPTER 2: ZIRCONIUM-CATALYZED PHOSPHINE DEHYDROCOUPLING: EFFORTS TOWARD SOLUBLE POLYPHOSPHINES	50
2.1. Introduction.....	50
2.2. Results	58
2.2.1. Synthesis of Linker Molecules Incorporating Long-Chain Alkoxy Groups .	62
2.2.2. Dehydrocoupling Reactions of Second Generation Bisphosphine Substrates	67
2.3. Conclusions	73
2.4. Experimental Methods.....	74
2.5. References.....	80
CHAPTER 3: IRIDIUM-CATALYZED SILANE DEHYDROCOUPLING: LIGAND EFFECTS ON PRODUCT SELECTIVITY	83
3.1. Introduction.....	83
3.2. Results	89

3.2.1. Synthesis and Characterization of Pincer Compounds	89
3.2.2. Sealed NMR-Scale Reactions with PhSiH ₃ and Catalytic Siloxane Formation	93
3.2.3. Reactions of PhSiH ₃ Open to N ₂ Atmosphere	99
3.2.4. Reactions of Primary Silanes Open to N ₂ Atmosphere	106
3.2.5. Reactions of Secondary Silanes	112
3.3. Conclusions	115
3.4. Experimental Methods.....	116
3.5. References.....	122
CHAPTER 4: FUTURE STUDIES AND CONCLUSIONS	126
CHAPTER 5: COMPREHENSIVE BIBLIOGRAPHY	128
APPENDIX 1: CRYSTALLOGRAPHY DATA	138
APPENDIX 2: MASTER LIST OF SILANE ¹ H AND ²⁹ Si NMR δ.....	139
APPENDIX 3: PHOSPHINE SUBSTRATE NMR DATA FROM CHAPTER 2.....	141

LIST OF TABLES

Table	Page
Table 1.1 Properties of metalloles containing group 16 elements	8
Table 1.2 Relative rates of dehydrocoupling and hydrosilation reactions catalyzed by platinum group metals	35
Table 1.3 Comparison of PhSiH ₃ dehydrocoupling using zirconium and nickel catalysts	38
Table 3.1 Diagnostic NMR data (δ) for compounds 18–21 in benzene- <i>d</i> ₆ solution.	91
Table 3.2 Select bond lengths (Å) and angles (deg) for compounds 18–21	93
Table 3.3 Product distributions of NMR tube scale reactions of PhSiH ₃ with catalytic 18–21	98
Table 3.4 Product distributions for reaction of PhSiH ₃ with catalytic 18–21 under N ₂	101
Table 3.5 Product distributions of preparative scale reactions of (<i>o</i> -tol)SiH ₃ with catalytic 18–21 under N ₂	106
Table 3.6 Product distributions of preparative scale reactions of NapSiH ₃ with catalytic 18–21 under N ₂	108
Table 3.7 Product distributions of preparative scale reactions of MesSiH ₃ with catalytic 18–21 under N ₂	109
Table 3.8 Product distributions of preparative scale reactions of 18–21	

with PhMeSiH ₂ open to a N ₂ atmosphere.	112
Table A.1 Crystallographic Data for <i>p</i> -X ^R [Ir] Compounds	138
Table A.2 Mucha's Master Silane List.....	139

LIST OF FIGURES

Figure	Page
Figure 1.1 Schematic of band structures in materials	2
Figure 1.2 Examples of common structural motifs in conjugated polymers	4
Figure 1.3 Parameters that influence the bandgap of polythiophene	6
Figure 1.4 Motifs incorporating phosphorus in π -conjugated systems	10
Figure 1.5 Orbital interactions in phosphole.....	11
Figure 1.6 Silicon $3sp^3$ orbital interactions in a polysilane.....	16
Figure 1.7 Conformations of sp^3 orbitals of an oligosilane	17
Figure 1.8 Brookhart's (A) and Tilley's (B) rhodium dehydrocoupling catalysts.....	29
Figure 1.9 Various substitution modes in a pincer ligand.....	39
Figure 2.1 Triamidoamine ligated zirconium (N_3N)Zr, 1 studied by the Waterman group.....	53
Figure 2.2 Insoluble hyperbranched polyphosphine products from dehydrocoupling reactions with 1	58
Figure 2.3 TGA data for polymers 4 and 5	61
Figure 2.4 PPV-based synthetic target 6 for phosphine dehydrocoupling.....	63
Figure 2.5 Small molecule synthetic targets for phosphine dehydrocoupling	65
Figure 2.6 Diphosphine products produced in reactions catalyzed by 1 and 2	67
Figure 2.7 Proposed major product for unknown ^{31}P $\delta = -60.9$ s, observed in dehydrocoupling reactions catalyzed by 11	69

Figure 2.8 Comparison of product distributions in NMR-scale reactions highlighting the higher activity of 2 (SM= starting material).....	70
Figure 2.9 Polyphosphine material 17 in toluene solution (left) and after precipitation from hexanes (right)	71
Figure 2.10 Solid-state MAS ³¹ P NMR spectrum of 17	72
Figure 3.1 The four pincer compounds chosen for silane dehydrocoupling studies	89
Figure 3.2 Proposed chloro-bridged dimeric compound from initial attempts at preparing ^{iPr} (POCOP)IrHCl, 18	90
Figure 3.3 Molecular structure of 18 , 19 , and 21 (clockwise from top left) with thermal ellipsoids drawn at the 30% probability level. Hydrogen atoms, except the hydride located on iridium, are omitted for clarity.....	92
Figure 3.4 ¹ H NMR spectra in benzene- <i>d</i> ₆ solution of 16 hour reactions of 20 with PhSiH ₃ at ambient temperature. (A) No added H ₂ O (B) One hour after H ₂ O addition (C) 16 hours after H ₂ O addition	96
Figure 3.5 Proposed siloxane products resulting from incomplete catalyst removal	97
Figure 3.6 ¹ H NMR spectra in benzene- <i>d</i> ₆ solution of reactions of 18 with PhSiH ₃ both sealed and open to a N ₂ atmosphere and reactions of 19–21 open to a N ₂ atmosphere after 16 hours. Redistribution products are seen with 18 , while dehydrocoupling products are primarily seen with 19 , 20 , and 21	100
Figure 3.7 ²⁹ Si{ ¹ H} DEPT ($\theta = 90^\circ, 135^\circ$) NMR spectra in benzene- <i>d</i> ₆	

solution of reaction of 19 with PhSiH ₃ open to a N ₂ atmosphere after 16 hour reaction time. Three distinct regions are visible and correspond to the number of H and Ph groups present.....	104
Figure 3.8 Reactions of 18 with (<i>n</i> -oct)SiH ₃ under both N ₂ and reduced pressure conditions and reactions of 19–21 under N ₂	111
Figure 3.9 Reaction of 2 mol % 18 with PhMeSiH ₂ after (A) 50 minutes and (B) 16 hours of reaction time	113
Figure A3.1 ³¹ P NMR spectrum of the diethylaminophosphine precursor to 13 in benzene- <i>d</i> ₆	141
Figure A3.2 ¹ H NMR spectrum of the diethylaminophosphine precursor to 13 in benzene- <i>d</i> ₆	142
Figure A3.3 ¹³ C NMR spectrum of the diethylaminophosphine precursor to 13 in benzene- <i>d</i> ₆	143
Figure A3.4 ³¹ P NMR spectrum of 13 in benzene- <i>d</i> ₆	144
Figure A3.5 ¹ H NMR spectrum of 13 in benzene- <i>d</i> ₆	145
Figure A3.6 ¹³ C NMR spectrum of 13 in benzene- <i>d</i> ₆	146
Figure A3.7 ³¹ P NMR spectrum of 10 in benzene- <i>d</i> ₆	147
Figure A3.8 ¹ H NMR spectrum of 10 in benzene- <i>d</i> ₆	148
Figure A3.9 ¹³ C NMR spectrum of 10 in benzene- <i>d</i> ₆	149
Figure A3.10 ³¹ P NMR spectrum of 11 in benzene- <i>d</i> ₆	150
Figure A3.11 ¹ H NMR spectrum of 11 in benzene- <i>d</i> ₆	151
Figure A3.12 ¹³ C NMR spectrum of 11 in benzene- <i>d</i> ₆	152

LIST OF ABBREVIATIONS

$(\text{N}_3\text{N})^{3-}$	$[(\text{Me}_3\text{SiNCH}_2\text{CH}_2)_3\text{N}]^{3-}$
Ar	Aryl
Bz	Benzyl
COD	1,5-Cyclooctadiene
COE	<i>cis</i> -Cyclooctene
Cp	Cyclopentadiene ($\eta^5\text{-C}_5\text{H}_5$)
Cp*	1,2,3,4,5,-pentamethylcyclopentadiene ($\eta^5\text{-C}_5\text{Me}_5$)
CV	Cyclic voltammetry
Cy	Cyclohexyl
DEPT	Distortionless enhancement by polarization transfer
dippe	1,2-Bis(diisopropylphosphino)ethane
DP	Degree of polymerization
DSC	Differential scanning calorimetry
E	Element
E_{cl}	Conjugation path length
E_{g}	Energy bandgap
E_{res}	Aromatic resonance
E_{sub}	Substituent effects
E_{θ}	Torsion angle
Fc	Ferrocenyl
FET	Field effect transistor
GC	Gas chromatography
GOOB	Greasy octyloxybenzene
GPC	Gel permeation chromatography
Hex	Hexyl
HOMO	Highest occupied molecular orbital
HSQC	Heteronuclear single quantum coherence
ⁱ Pr	Isopropyl
IR	Infrared

KIE	Kinetic Isotope Effect
L	Ligand
LUMO	Lowest unoccupied molecular orbital
M	Metal
MAS	Magic-angle spinning
Me	Methyl
Mes	Mesityl
MGE	Main group element
M_n	Number average molecular weight
MO	Molecular orbital
MS	Mass spectrometry
Nap	Naphthyl
N-oct	<i>N</i> -octyl
OLED	Organic light emitting diode
O-tol	<i>O</i> -tolyl
Ph	Phenyl
POCOP	κ^3 -1,3-(R ₂ PO) ₂ C ₆ H ₃
PPP	Poly(<i>p</i> -phenylene phosphalkene)
PPV	Poly(<i>p</i> -phenylene vinylene)
R	Alkyl or aryl
SBM	σ -Bond metathesis
^t Bu	Tert-butyl
TGA	Thermogravimetric analysis
THF	Tetrahydrofuran
TMS	Trimethylsilyl
UPE	Ultraviolet photoelectron spectroscopy
UV	Ultraviolet
X	Anionic ligand

CHAPTER 1: GENERAL INTRODUCTION

1.1. Conjugated Polymers

Despite the fact that naturally-occurring polymeric materials have been used for millennia, the concept of polymer science was developed by Hermann Staudinger less than a century ago, during the 1920s. In 1935, the advent of nylon demonstrated the commercial and industrial potential that new types of synthetic polymers could provide, and indeed, their development and commercialization as materials has since flourished. In the 1950s, the field of polymer chemistry was dominated by the work of Ziegler and Natta following their discoveries regarding metal-based polymerization catalysts that would become the basis of the modern plastics industry.

Though the field of polymer science advanced exponentially during this time, these polymers are viewed as uninteresting from the view of molecular electronics. Such materials act as insulators due to their saturated nature (sp^3 hybridized carbon) and poor electrical conductivity.¹ In 1976, it was shown that after treatment with chemical dopants, polyacetylene films could act as organic semiconductors and increase their conductivity up to values comparable to metals.² This work ultimately led to the 2000 Nobel Prize in Chemistry, which recognized Alan Heeger, Alan Mac Diarmid, and Hideki Shirakawa “for their discovery and development of conductive polymers”.³

Nearly four decades since their discovery, conjugated polymers continue to be of great interest due to their unique optical and electronic properties.⁴ For organic semiconductors, the highest occupied molecular orbital (HOMO) / lowest unoccupied molecular orbital (LUMO) bandgap in conjugated polymers can best be regarded as spanning the region from wide band gap semiconductors down to insulators (Figure 1.1).⁵

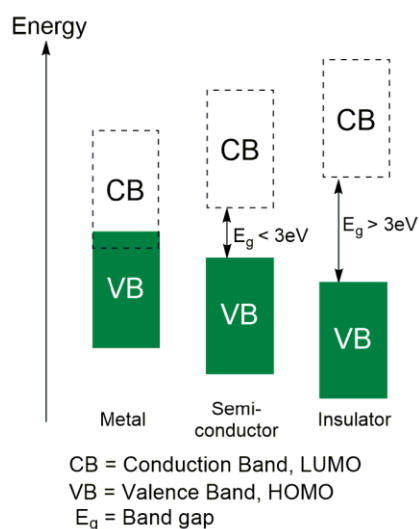


Figure 1.1 Schematic of band structures in materials

Because of the wide range of conductivities these materials can possess, substantial effort has been directed at tailoring their electronic properties (i.e., molecular orbital levels, effective conjugation length, band gap) in such a way to meet the desired function of the material.⁶

The most well-known class of conjugated materials are those that exhibit π -conjugation resulting from the delocalization of electrons in overlapping p-orbitals (c.f., polyacetylene). A second type of conjugation has been demonstrated for homopolymers of heavier main group elements such as silicon and tin. σ -Conjugation is a consequence of increased s electron orbital overlap in polymers of heavier main group elements (MGEs). As the number of atoms in the polymer backbone increases, additional bonding and antibonding orbital states are formed.⁷ The overall effect results in the formation of bands associated with the σ and σ^* orbitals states and results in σ electron delocalization along a chain of singly-bonded atoms.⁸ In π -conjugated and σ -conjugated materials, the bandgaps are π - π^* and σ - σ^* transitions, respectively. In this dissertation, transition-metal compounds were used as dehydrogenative coupling (dehydrocoupling) catalysts in reactions with silanes and phosphines. Efforts toward the preparation and characterization of phosphorus- and silicon-based materials using iridium- and zirconium-based catalysts will be presented.

1.2. π -Conjugated Materials

π -Conjugated materials have attracted the attention of research groups because their discovery and development lead to a new generation of polymers that offer the semiconducting abilities of metals while maintaining the ease of characterization and synthetic versatility that are associated with organic small molecules.⁹ These advantages

over their inorganic counterparts make them well suited for applications in photonic and electronic devices. To date, conjugated materials have been studied for applications such as organic or polymer-based light emitting diodes (OLEDs/PLEDs),¹⁰ field-effect transistors (FETs),¹¹ and plastic lasers.¹² However, the “holy grail” of this area of research is the development of plastic electronics based on molecular wires (Figure 1.2).¹³

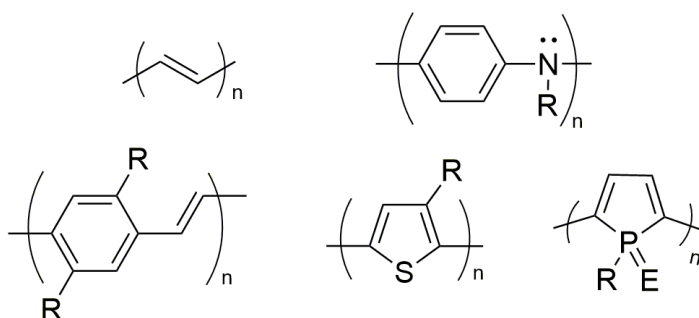


Figure 1.2 Examples of common structural motifs in conjugated polymers

In contrast to the saturated, insulator polymers mentioned earlier, the chemical bonding in π -conjugated polymers leads to a system of connected p orbitals with delocalized electrons resulting from alternating single and unsaturated bonds. Furthermore, when sp^2 hybridized orbitals on successive carbon atoms overlap, electron delocalization can occur along the backbone of a polymer. This electronic delocalization provides the pathway for charge mobility along the backbone of the polymer.

1.2.1. Design Considerations

In general, the electronic properties of conjugated polymers are determined by their chemical structure and their organization in the solid state.¹⁴ With this in mind, several design features have emerged as essential for conjugated polymers to be useful in OLED and FET applications. The first is a π -conjugated backbone capable of facilitating charge mobility. The second structural consideration is the installation of alkyl or alkoxy substituents to the main backbone chain, though these side chains are generally only necessary for characterization and manufacture by solution-based methods.⁵ Beyond these design features, a p-type component that can conduct positive charges or an n-type component for negative charge transport are frequently present if the parent material does not have a suitable bandgap.¹⁵

Indeed, conjugation of the polymer backbone is not the sole requirement to render a material conductive.¹⁶ In fact, most organic conjugated materials act as insulators in their neutral state. However the introduction of charge carriers into the backbone in the form of extra electrons or “holes” (i.e., n- or p-doped, respectively) can narrow the bandgap in these materials and render them semiconducting. Chemical modification of conjugated polymers directly influences the bandgap of these materials and is a powerful technique for tailoring the electronic properties of these systems.¹⁴ The bandgap energy (E_g) of a conjugated polymer is dependent on several factors that include the resonance stabilization via aromaticity (E_{res}), the conjugated path length (E_{cl}), the torsion angle

between monomers (E_{θ}), and steric/electronic effects from substituents (E_{sub}) (Figure 1.3).^{16,17}

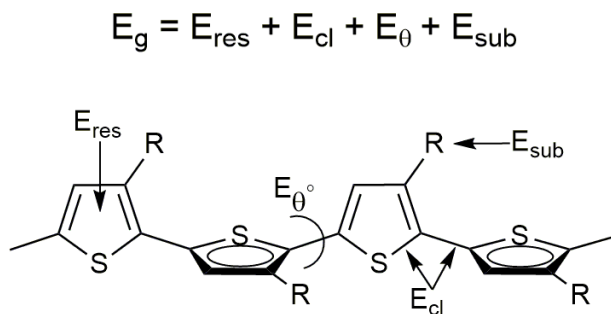


Figure 1.3 Parameters that influence the bandgap of polythiophene

One approach for engineering bandgap energies of these materials is tuning steric effects to vary the effective conjugation length.¹⁶ Sterically demanding substituents can cause twisting of the conjugated backbone, which reduces the conjugation length by decreasing the planarity of the polymer. Similarly, the rational design and use of rigid ladder-like monomers such as fluorene in conjugated materials can increase the conjugation length and thus reduce the bandgap.¹⁸

1.2.2. Heteroatom Substitution

An alternate approach towards bandgap tuning in conjugated materials is decorating the polymer backbone with functional groups. These side-chain substituents

influence the properties of materials via steric (planarity, conjugation length, supramolecular organization, etc.) and electronic effects. The incorporation of electron-donating substituents such as amino, alkyl, or alkoxy groups raise the HOMO (highest occupied molecular orbital) of aromatic monomers. Conversely, electron-withdrawing substituents such as fluorine, imines, nitriles, esters, or amides increase electron affinity and thus result in lower LUMO (lowest unoccupied molecular orbital) levels.⁶ Several methods of doping using chemical, photochemical, and electrochemical methods have been developed to introduce charge carriers into conjugated materials.⁶

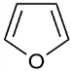
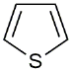
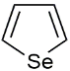
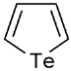
Besides functionalization of the backbone, a powerful approach to bandgap modification is to vary the chemical composition of the main chain through heteroatom incorporation/substitution.¹⁹ This strategy is attractive and popular because of the synthetic versatility offered by organic molecules and the substantial effects heteroatoms can impart on conjugated systems. Heteroatoms that possess lone pairs of electrons or vacant p-orbitals can participate in π -conjugation and further influence the bandgap of these materials and potentially obviate the need for post-synthetic doping.

One of the largest classes of heteroatom substituted conjugated materials are based on metalloles.²⁰ Within this class, thiophenes have garnered the most attention due to the early success of poly(3-hexylthiophene)¹⁴ (P3HT) and the commercial availability of functionalized thiophenes. In recent years, there have been reports of conjugated polymers based on the incorporation of other group 16 elements into heterocycles.²⁰

Metallole-based polymers offer different and potentially useful properties relative to their all carbon analogues. Considering group 16 element substitution as an example,

increasing the size of the heteroatom results in both elongation of the E–C bond and a decrease in the C–E–C bond angle due to increased steric demands imparted by the incorporation of larger heteroatoms (Table 1.1).²¹ Therefore, the smaller atomic radius of oxygen in furan can facilitate planarity and more efficient conjugation between neighboring monomers.²² Substitution of oxygen with larger, more polarizable selenium or tellurium leads to stronger intermolecular interactions and increased rigidity.²³

Table 1.1: Properties of metalloles containing group 16 elements²⁴

	 Furan	 Thiophene	 Selenophene	 Tellurophene
Heteroatom Atomic Radius (Å)	0.64	1.04	1.18	1.36
Heteroatom Electronegativity (Pauling scale)	3.5	2.5	2.4	2.1
Dipole moment (D)	0.67	0.55	0.40	0.19
Aromaticity (I ₅ index)	43	66	59	48

The aromaticity of conjugated systems influences the band gap in materials by affecting the extent of electron delocalization along the polymer backbone.¹⁶ Though the values often vary depending on the method used, the aromaticity of conjugated heterocycles is typically evaluated through comparison of resonance energies. A popular method to evaluate aromaticity is a statistical treatment called the I₅ index, which reflects the bond order uniformity in aromatic systems based on individual bond lengths.²⁵ Among the group 16 metalloles, polyfuran has a larger band gap than polythiophene as

a result of the lower aromaticity of furan. Furthermore, polyselenophene has a smaller band gap than polythiophene due to selenium's lower electronegativity.²⁴

In addition to group 16 metalloles, the photophysical and electronic properties of metalloles based on group 14 elements have also been examined.²⁶ It was determined that the substitution of heavier group 14 elements (Si, Ge, Sn) affected the metalloles LUMO energy levels of the systems to virtually the same extent through $\sigma^*-\pi^*$ conjugation.²⁶ Though significant structural differences exist relative to the all carbon cyclopentadiene derivatives, metalloles incorporating heavier group 14 elements essentially have the same electronic structure. Therefore, group 14 metalloles exhibit comparable absorption maxima in UV-vis spectra, while the cyclopentadiene analogue exhibits a much shorter absorption maximum.¹⁹

1.3. Phosphorus in Conjugated Materials

The incorporation of phosphorus(III) into conjugated polymers has garnered substantial attention due its often carbon-like reactivity²⁷ and the ability of its lone pair of electrons to participate in π -conjugation.²⁸ Heavier phosphorus analogues of polyaniline and arylamino-based π -conjugated materials were seen as desirable research targets owing to the early work devoted to polymerization of these monomers. However the field of phosphorus-containing materials was then unexplored due to the lack of suitable synthetic methods. In 1981, a discovery by Cowley and coworkers ignited

development of the field when evidence for electronic communication between the phosphorus atoms in *p*-bis(phosphino)benzene was demonstrated via ultraviolet photoelectron spectroscopy (UPE).²⁹

Commonly studied motifs include poly(*p*-phenylene)phosphine and poly(*p*-phenylene)phosphaalkene (PPP), the phosphorus analogues of polyaniline and poly(*p*-phenylene vinylene) (PPV), respectively.²⁸ However, the most prevalent class of phosphorus-containing frameworks studied as π -conjugated materials are phospholes or fused phosphole derivatives (Figure 1.4).

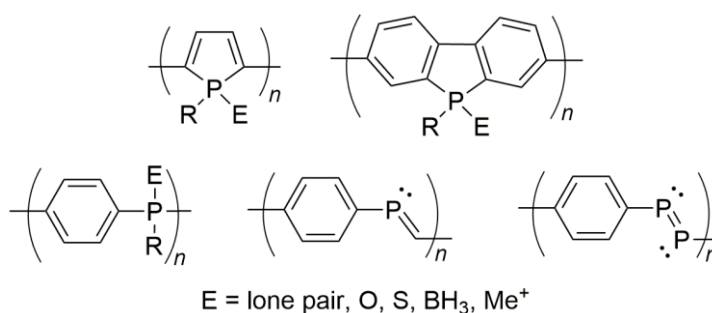


Figure 1.4 Motifs incorporating phosphorus in π -conjugated systems

Though nitrogen and phosphorus have similar π -donor capabilities, phosphorus incorporation in molecules has remarkably different effects on conjugation compared to its lighter congener.³⁰ Due to the higher inversion barrier of phosphines relative to amines, phosphines do not assume a planar sp^2 configuration for efficient conjugation of the lone pair of electrons with the aromatic system as readily as amines can.³¹ This “similar but different” aspect of these two elements prompted investigation into

phosphorus-based materials and suggested that materials based on these two elements could offer very different electronic properties.³²

In contrast to the nitrogen in pyrrole, the phosphorus atom in phosphole adopts a pyramidal geometry which results in decreased aromaticity from weak interactions between the phosphorus lone pair of electrons and the π electrons of the diene.²⁰ Furthermore, the presence of a phosphorus atom was found to increase the electron-accepting properties of these materials due to $\sigma^*-\pi^*$ orbital interactions between the phosphorus substituent and the π -conjugated diene (Figure 1.5).³³ This hyperconjugation of the P-R σ bond with the π system is responsible for most of the aromatic character of phospholes.

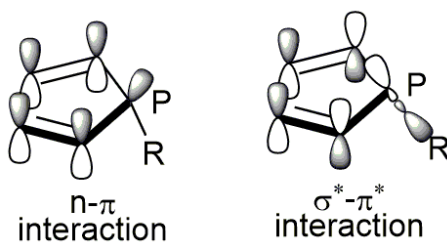
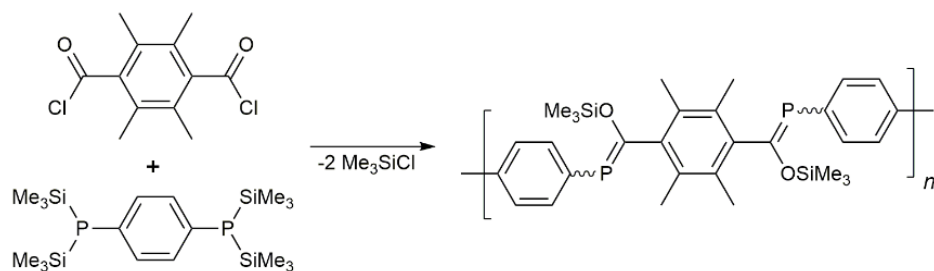


Figure 1.5 Orbital interactions in phosphole

Matano and coworkers prepared the first well-defined polyphosphole in 2010 via Stille-type palladium coupling.³⁴ Gel permeation chromatography (GPC) determined the polyphosphole had a number average molecular weight (M_n) of 13,000 with a modestly large degree of polymerization (DP) of 32. Relative to its monomer, dimer, and trimer reference compounds, the polyphosphole exhibits a narrow bandgap and displays a

strongly red-shifted UV-vis absorption band which is consistent with an increased degree of π conjugation along the polymer chain. Based on redox potentials from cyclic voltammetry (CV) studies, the polyphosphole shows significantly enhanced electron accepting character compared to polythiophene.³⁵

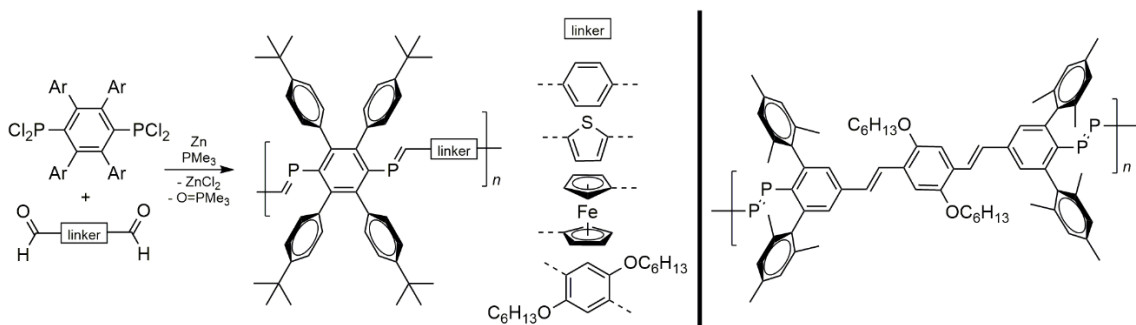
Phosphorus analogues of PPVs incorporating phosphalkene (P=C) or phosphinidine (P=P) functional groups into the polymer backbone have also been studied.³² Gates and co-workers reported the first example of a conjugated PPP polymer in 2002 which was prepared by a Becker-type condensation of a bis(trimethylsilyl)phosphine with an acid chloride (Scheme 1.1) followed by a 1,3-silatropic rearrangement.³⁶



Scheme 1.1 Synthetic route to the first poly(p-phenylene phosphalkene)

This synthetic route produced both E and Z isomers in approximately a 1:1 ratio as determined by ³¹P NMR spectroscopy. Like the polyphosphole described above, the UV-vis spectra of the PPP polymer exhibited a red shift relative to its corresponding monomer, indicating an extended π -conjugated system. In later work, Gates determined

that steric encumbrance of the phosphine moiety could stabilize the phosphalkene and promote formation of mainly the Z isomer.³⁷ An alternate approach to the preparation of conjugated PPP polymers is the use of a phospha-Wittig reaction, which Protasiewicz and co-workers utilized to prepare weakly fluorescent polymers containing (P=C) and (P=P) linkages (Scheme 1.2).



Scheme 1.2 Use of a phospha-Wittig reaction to access P=C and P=P linked polymers

The modest fluorescence of these materials was attributed to quenching via the phosphorus lone pair. Despite the fact these phospha-PPVs are only weakly emissive relative their carbon analogues, this study demonstrated this emissive property for the first time in this class of materials.

1.4. Polysilanes and σ -Conjugated Polymers

As heavier analogues of alkanes, σ -bonded catenated compounds of the group 14 elements have generated interest due to their unique physical and electronic properties, with silicon and tin garnering the most attention. Materials based on catenated silicon atoms are not recent ideas in polymer chemistry. The first example of a substituted polysilane was prepared by Kipping in the 1920s via condensation of diphenyldichlorosilane with sodium metal.³⁸ Similarly in the 1940s, Burkhard reported the synthesis of poly(dimethylsilane) using a similar protocol.³⁹ In both cases, the resulting white solids were highly crystalline and insoluble in standard organic solvents and thus were neither characterized nor understood well. For this reason, the investigation of polysilanes as materials faded until 1975 when Yajima and co-workers developed a process in which linear or cyclic polysilanes could be transformed into silicon carbide (SiC) after pyrolysis.⁴⁰ This discovery, coupled with reports of the synthesis and characterization of a variety of soluble high molecular weight polysilane homopolymers by the West and Trujillo groups indicated that high molecular weight polysilane polymers were not necessarily intractable and reinvigorated interest in polysilanes.^{41,42}

Polymers based on other group 14 elements such as germanium and tin have been less explored relative to their silane counterparts largely due to synthetic difficulties. Low yields of polymer and the tendency for germane and stannane monomers to form low molecular weight species have stunted the development of this chemistry. Despite these

complications, the first soluble, high molecular weight organogermane homopolymer and Ge–Si copolymer was developed by West and coworkers in 1985.⁴³ Soluble, high molecular weight polystannanes were not prepared until 1995 by Tilley and coworkers.⁴⁴

1.4.1. σ Electron Delocalization

The unique optical and electronic properties of polysilanes and other group 14 catenated polymers primarily result from significant delocalization of σ electron density along the polymer backbone, behavior that is markedly different than their lighter all-carbon analogues. Despite the fact that polymers of group 14 elements are held together by σ -bonds, the physical properties of these materials more closely resemble π -conjugated systems like polyacetylenes. Thus polysilanes have received considerable attention as SiC precursors,⁴⁰ photoinitiators,⁸ and electroconductors.⁴¹

The delocalization of σ electrons associated with polysilanes can be explained in terms of overlapping sp^3 orbitals, using the Sandorfy C model⁴⁵ to estimate the energy (resonance integral) between two silicon atoms.⁷ In this model, energetic states arising from Si–Si bonding along the polysilane backbone are composed of three atomic orbital interactions.⁸ The primary interaction (β_{primary}) consists of two sp^3 orbitals on adjacent silicon atoms pointing toward each other to form the Si–Si σ bond. However, these structures are only considered to be σ delocalized if additional secondary orbital interactions are also present.⁴⁶ Delocalization by σ conjugation arises from the geminal

contribution (β_{gem}) which corresponds to interactions between sp^3 orbitals on the same Si atom. The vicinal contribution (β_{vic}) results from hyperconjugation of orbitals on neighboring atoms which are not pointed at each other and is dependent on the conformation of the polysilane (Figure 1.6).⁴⁶

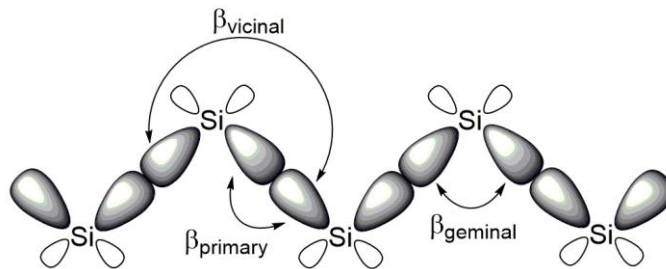


Figure 1.6 Silicon $3sp^3$ orbital interactions in a polysilane

The degree of electron delocalization is given by a ratio of $\beta_{\text{vic}}/\beta_{\text{gem}}$. When this ratio approaches 0, there is complete localization of bonding and antibonding orbitals between pairs of Si atoms. As this ratio approaches 1, perfect delocalization occurs and the chain is in the all-trans conformation.⁴⁷

Gilman and coworkers observed that the delocalization of electrons in polysilanes gave rise to strong UV absorptions.⁴⁸ In this work, they observed that polydimethylsilane and polysilane absorbed at 190–215 nm, a longer wavelength and lower energy than hydrocarbon absorption (150–190 nm).⁴⁹ As is seen in π -conjugated materials, the absorbance maximum red-shifts as length of the polysilane increases, which suggests electron delocalization along the chain. These absorptions are attributed to σ – σ^*

transitions, and though early theory suggested the involvement of empty d orbitals of Si, recent molecular orbital (MO) calculations concluded that the d orbitals have no significant role in σ electron delocalization.⁵⁰

1.4.2. Substituent and Conformational Effects

Properties of polysilanes and σ -conjugated polymers are highly dependent on the size and electronic effects of the substituents on the catenated atoms. Polysilanes can adopt a variety of stable backbone conformations including helical, trans, or gauche type conformations depending on the steric demands of the substituents (Figure 1.7).

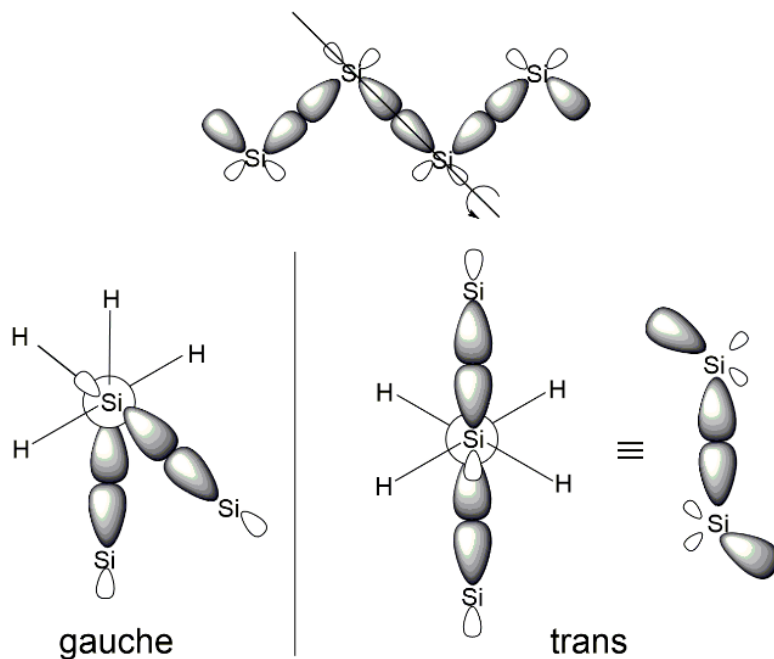


Figure 1.7 Conformations of sp^3 orbitals of an oligosilane

Research has demonstrated that trans or nearly trans segments of these polymers behave as chromophores, while the gauche and nonplanar polysilane conformations act as flexible barriers diminishing the conjugation.⁴⁵ Chain conformations influence the energy levels of the delocalized σ - σ^* orbitals and different conformations can be observed through the variance of absorption maxima in polysilane UV spectra.⁵¹

Chain conformation is strongly affected by the substituents on the silicon atoms. For example, when two bulky side groups are attached to a backbone chain, as in a poly(diarylsilane), substituents often force the backbone to adopt an all-*trans* structure.⁵² Alkyl side-groups as in poly(dihexylsilane) also affect backbone conformation through facilitation of interchain interactions that can aid crystallization.⁵³ In simple alkyl substituted polysilanes, as the steric bulk of the substituents increases, the absorbance maxima red-shifts to longer wavelengths.⁵⁴ This behavior is ascribed to conformational effects, as larger groups tend to enforce an all-*trans* conformation. Due to their ability to act as chromophores, bulky aryl substituted polysilanes exhibit more dramatic red-shifts than those imparted by alkyl substituents.⁵² Polysilanes also exhibit red shifts in absorbance maxima as their molecular weights increase or upon the incorporation of heavier group 14 elements into the polymer backbone. As an example, n-butylsilane,⁵⁵ n-butylgermane,⁴³ and n-butylstannane⁵⁶ have absorbance features of 314 nm, 333 nm, and 365 nm, respectively.

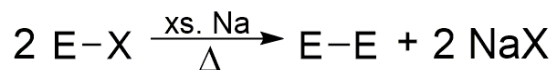
Polysilanes and other σ conjugated polymers are principally prepared in one of two ways. The first is a classic method called Würtz-type coupling and though effective,

its use in synthetic chemistry has many limitations ascribed to it.⁸ A second method of preparation which circumvents the complications of Würtz-type coupling is called dehydrogenative coupling and relies on homogeneous catalysts to effect E–E bond formation.⁵⁷

1.5. Dehydrocoupling

Relative to the field of organic polymer science, the chemistry of polymers comprised of main group elements is considerably less developed.⁵⁸ Difficulties include the preparation and stabilization of main group element (MGE) analogues of olefins and acetylenes⁵⁸ and the scarcity of synthetic methods to catalytically generate homonuclear or heteronuclear bonds between MGEs.⁵⁹ The use of transition metals as homogeneous catalysts is an attractive alternative to methods such as Würtz-type coupling or dehydrohalogenation reactions traditionally used to form bonds between MGEs.

Würtz-type coupling is an effective but harsh method of E–E bond formation where an excess of alkali metal is used to condense element-halide compounds under reflux conditions (eqn 1.1).

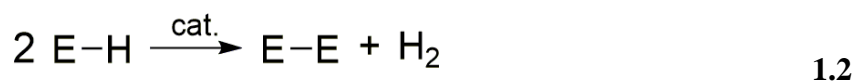


X = halogen

1.1

There are several drawbacks associated with Würtz coupling that limit the use of this methodology for MGE bond formation. This coupling requires the use of elemental sodium at elevated temperatures therefore limiting the types of functional group that can be tolerated under these conditions. Furthermore, production of stoichiometric amounts of halogenated salt byproducts, lack of product selectivity, and low isolated product yields all plague this method.⁶⁰ The lack of suitable methods to efficiently form MGE bonds has thus hampered efforts to further develop their chemistry.⁶¹

In dehydrocoupling reactions, two molecules with E–H bonds undergo a net metathesis reaction to form an E–E bond and eliminate an equivalent of H₂ gas (eqn. 1.2).



Contrary to reductive coupling methods, dehydrocoupling is selective for E–H bonds and will not cleave installed functional groups. An additional advantage over reductive coupling is the ease of product isolation after catalyst removal: dehydrocoupling catalysis is a “green” reaction in that it produces no halogenated salt byproducts and instead produces only H₂ gas.⁶⁰ In a thermodynamic study comparing the bond dissociation enthalpies of a variety of homonuclear MGE E–E compounds and their respective hydride precursors, Harrod and coworkers determined that many reactions of this type are approximately thermoneutral.⁶¹ However, the addition of organic substituents to MGE hydrides strongly influences the thermodynamics of these systems and thermoneutral reactions for unsubstituted MGE hydrides may have very different

parameters upon the addition of substituents. Thus the enthalpic and entropic benefit of H₂ formation and liberation can drive the reaction progress more so than the formation of most E–E bonds.⁶⁰

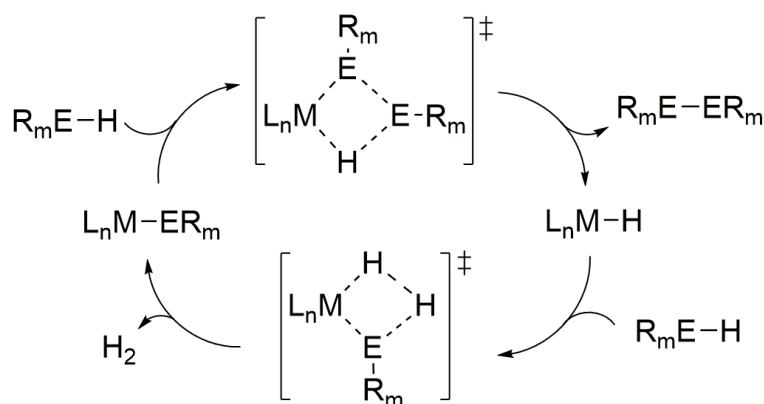
1.5.1. Mechanisms of Metal-Catalyzed Dehydrocoupling Reactions

Throughout the years dehydrocoupling has been applied to a variety of MGEs as a potential method for E–E bond formation.⁶¹ Currently many examples of both homoatomic and heteroatomic dehydrocoupling reactions from groups 13 through 15 have been demonstrated.⁶⁰ It is not surprising that for the myriad of MGEs that are readily dehydrocoupled, a variety of mechanistic pathways have been proposed. Though many viable reaction pathways exist, three key mechanistic steps, σ -bond metathesis (SBM), oxidative addition/reductive elimination, and α -elimination are most often implicated in dehydrocoupling catalysis.⁶²

The first catalytic dehydrocoupling reactions of MGEs were observed for B–B⁶³ and Si–Si⁶⁴ bond formation using late transition metal catalysts. Shortly thereafter, Harrod and coworkers reported that group 4 metallocene compounds were active catalysts for the dehydrocoupling and oligomerization of primary silanes.⁶⁵ This discovery prompted an upsurge in studies on metallocene-catalyzed silane dehydrocoupling and through mechanistic studies by Tilley, SBM was established as the operant mechanism for d⁰ metals in this catalysis.⁶⁶ A vast amount of research has been

directed towards both phosphine and silane dehydrocoupling and these efforts will be surveyed in separate sections later in this chapter.

SBM is a concerted reaction where a metal–ligand σ -bond is replaced with the σ -bond of an incoming substrate.⁶⁷ Notably, this process does not involve a change in the oxidation state of the metal. In a catalytic dehydrocoupling reaction occurring via SBM, reaction of a L_nM-ER_m compound with a MGE hydride results in a 4-centered, kite-like transition state where E–E and M–H bonds are formed simultaneously. Reaction of the newly formed M–H species with an additional equivalent of MGE hydride produces H_2 gas and regenerates the L_nM-EHR_m compound (Scheme 1.3).⁶⁷

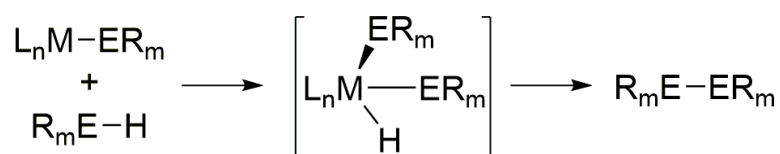


Scheme 1.3 Catalytic dehydrocoupling via a SBM-based mechanism

Researchers studying d^0 transition-metal and lanthanide compounds for dehydrocoupling activity have tried to identify factors that are indicative of SBM based mechanism. Two distinguishing pieces of evidence include the observance of a large negative entropy of activation and a considerable primary hydrogen/deuterium kinetic

isotope effect (KIE). As the transition state in SBM is a concerted $[2\sigma + 2\sigma]$ cycloaddition, negative ΔS^\ddagger values are expected for bimolecular processes and processes with highly ordered transition states. The observation of a substantial primary H/D KIE in these reactions results from the large amount of E–H bond breaking/forming activity occurring, and the nearly linear transfer of hydrogen that occurs based on the requirement of a planar transition state.

An alternate mechanism in dehydrocoupling catalysis is a classic organometallic redox mechanism by which mid to late transition metals facilitate MGE bond formation through a series of oxidative addition and reductive elimination steps (Scheme 1.4).

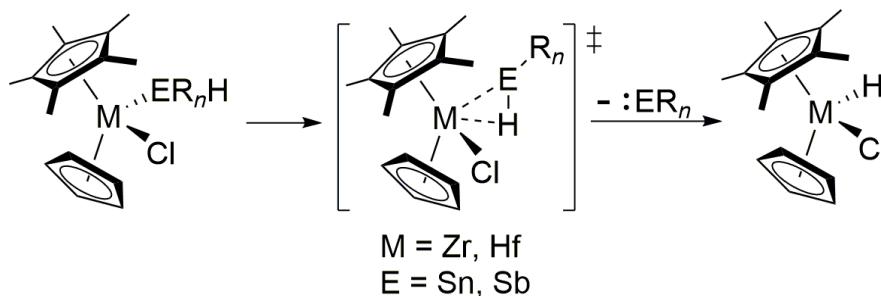


Scheme 1.4 An oxidative addition and reductive elimination dehydrocoupling mechanism

Two requirements for an oxidative addition/reductive elimination mechanism to be a viable reaction pathway include the ability of the metal center to undergo a reversible two electron oxidation, and the presence of a vacant coordination site on the metal for interaction with the incoming MGE substrate.⁶⁸ These requirements dictate that mostly mid- to late transition metals operate via this pathway, though examples of early transition metals undergoing oxidative addition with MGE substrates have also been reported.^{69,70} While productive dehydrocoupling occurs via this mechanism, competition

from off-cycle side reactions often limits the utility of late transition metals for this transformation.⁶¹ Later in Sections 1.6.2 and 1.7.2, a deeper discussion of late transition metal compounds and their uses as phosphine and silane dehydrocoupling catalysts will be presented.

The third and most recent mechanistic step common in dehydrocoupling catalysis is α elimination. α Elimination describes the migration of hydrogen or an R group from an M–EHR_n compound to produce a metal hydride and extrude a low-valent :ER_n fragment (Scheme 1.5).⁷¹ This low-valent fragment can then insert into the E–H bond of an additional equivalent of substrate (R_nEH₂) to form an E–E bond.



Scheme 1.5: α Elimination of a low-valent fragment to yield a M–H bond

This mechanism favors heavier MGEs that possess weaker element hydride bonds and can readily form low-valent species. α Elimination was first postulated by Tilley during a study on hafnium-catalyzed stannane dehydrocoupling.^{71,72} In this report, the observance of stannane dehydrocoupling products and the measurement of an unusually low KIE value suggested that the transition state was not concerted as in SBM-

based mechanisms. Later, decomposition and trapping studies on hafnium-stannyl compounds confirmed that the observed dehydrocoupling products formed via α -stannylene elimination and the subsequent insertion of $:\text{SnR}_2$ into a Sn–H bond.⁷³ Later work by Waterman and Tilley extended this chemistry to antimony,⁷⁴ and showed that this mechanistic pathway is not unique to tin dehydrocoupling. This body of work led to general parameters associated with a mechanism of α elimination. Through isotopic labeling experiments, low KIE values suggested Sn–H coordination to the Hf metal center was the rate-determining step. Negative entropies of activation are also observed in SBM mechanisms, though in α -elimination pathways these entropies have substantially smaller magnitudes^{71,73} which support claims of an ordered transition state and a one-step degradation process.

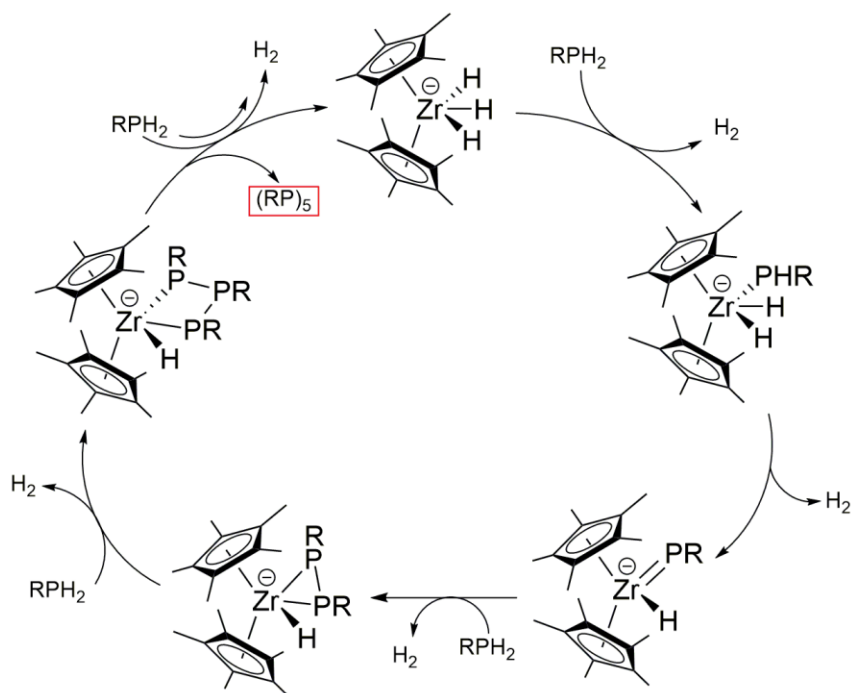
1.6. Phosphine Dehydrocoupling

Dehydrocoupling catalysis is a key transformation for MGE bond formation that avoids the inherent complications of Würtz type coupling. However, the dehydrocoupling chemistry of phosphorus is less developed than related transformations for main group substrates such as silanes and amine-boranes.⁶⁰ Catalyst design for phosphine dehydrocoupling is complicated by the fact that phosphorus can readily act as a σ -donor via its lone pair of electrons. Therefore careful choice of both the metal center

and ligand are necessary to avoid phosphine substrates acting as dative ligands and inhibiting catalysis in these reactions.

1.6.1. Early Transition-Metal Catalysts

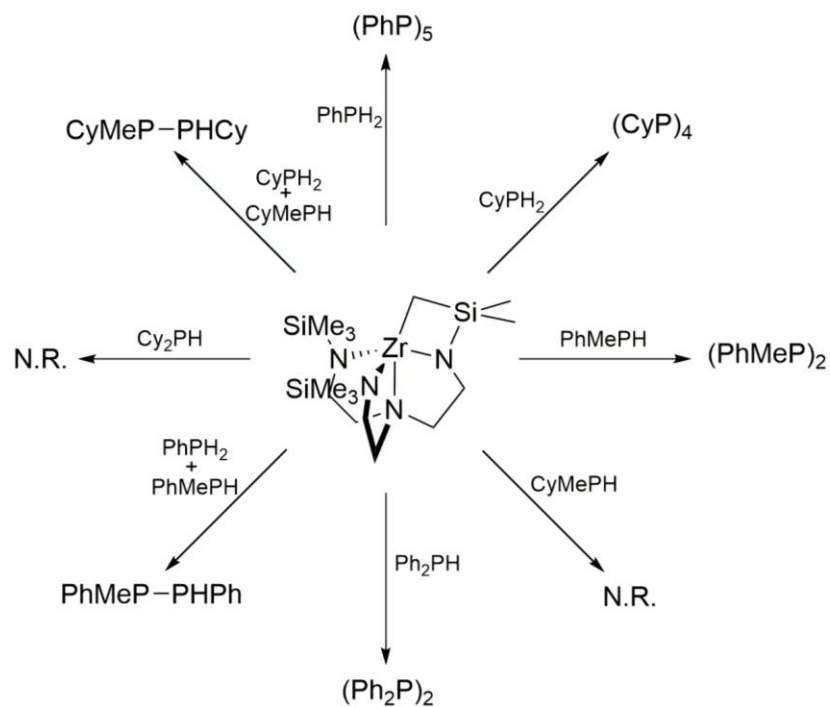
In 1995, Stephan and coworkers reported the first examples of catalytic phosphine dehydrocoupling using lithium and potassium salts of a zirconocene trihydride $[\text{Cp}^*_2\text{ZrH}_3]^-$ compound as a catalyst.⁷⁵ These salts effectively dehydrocoupled primary phosphines (RPH_2 R = Ph, Cy, Mes, Mes = 2,4,6- $\text{Me}_3\text{C}_6\text{H}_2$) to cyclic oligomers (RP_n), $n = 4$ or 5 at reflux temperatures over a reaction time of three days.⁷⁶ Despite the prevalence of SBM mechanisms in zirconocene catalyzed dehydrocoupling, the observance of an upfield resonance at $\delta = 465.8$ ppm in the ^{31}P NMR reaction spectra suggested the involvement of a terminal zirconium phosphinidene species. Furthermore, stoichiometric reaction data established the presence of the di- and tri-phosphido species $[\text{Cp}^*_2\text{ZrH}(\text{PPh})_2]^-$ and $[\text{Cp}^*_2\text{ZrH}(\text{PPh})_3]^-$ as the resting states of the catalyst in solution. These observations led Stephan to postulate a catalytic cycle based on a terminal phosphinidene engaging in 1,2-addition reactions followed by H_2 elimination, though other viable pathways exist (Scheme 1.6).



Scheme 1.6 Stephan's proposed mechanism for phosphine dehydrocoupling

In Stephan's mechanism, addition of a primary phosphine to the zirconocene trihydride initially forms a phosphido compound with elimination of H₂ gas. Elimination of a second equivalent of H₂ yields the terminal phosphinidene compound which reacts with additional equivalents of substrate to produce diphosphinato and triphosphinato compounds. Further phosphine addition results in the elimination of the cyclic oligophosphine product and regeneration of the active trihydride catalyst.

Previous work in the Waterman group utilized a triamidoamine-ligated Zr compound (N₃N)Zr, (N₃N) = [κ^5 -(Me₃SiNCH₂CH₂)₂NCH₂CH₂NSiMe₂CH₂], to dehydrocouple primary and secondary phosphines (Scheme 1.7).^{77,78}



Scheme 1.7 Reaction pinwheel summary of dehydrocoupling products obtained using $(\text{N}_3\text{N})\text{Zr}$

This catalyst exhibited temperature-dependent selectivity producing diphosphine products at lower temperatures and generating cyclic oligophosphines at higher temperatures. The proposed catalytic cycle was a SBM mechanism based on both the measurement of a positive KIE and a negative entropy of activation from an Eyring analysis.

1.6.2. Late Metal Catalysts

Dehydrocoupling catalysts utilizing late metals have been reported, though this class has been less-explored than early metal catalysts due to the propensity of

phosphorus to act as a ligand for late metals and shut down catalysis. The first example of a late metal-based phosphine dehydrocoupling catalyst $\text{Cp}^*\text{Rh}(\text{CH}_2=\text{CHSiMe}_3)_2$, was synthesized by Brookhart and coworkers in 2001 (Figure 1.8, A).⁷⁹

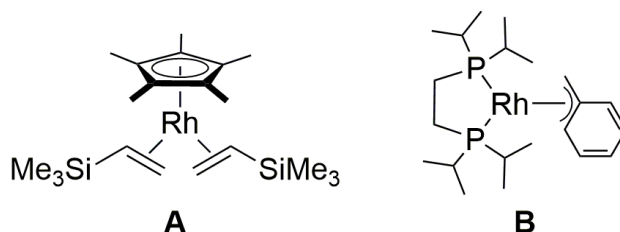


Figure 1.8 Brookhart's (A) and Tilley's (B) rhodium dehydrocoupling catalysts

Despite Brookhart's rhodium compound showing diminished reactivity towards primary phosphines, this compound was the first reported late metal to catalytically dehydrocouple secondary phosphines. The mechanism for this catalyst appears to involve an intermediate that is generated via step-wise loss of the vinylic-TMS ligands.⁷⁹ Sequential oxidative additions of P-H bonds generate a rhodium(V) center, which is then believed to reductively eliminate the diphosphine $\text{R}_2\text{P-PR}_2$, and H_2 .

An additional rhodium catalyst $(\text{dippe})\text{Rh}(\eta^2\text{-CH}_2\text{Ph})$, dippe = 1,2-bis(diisopropylphosphino)ethane was reported in 2006 by Han and Tilley (Figure 1.8, B).⁸⁰ This compound exhibited higher dehydrocoupling activity towards both primary and secondary phosphines than Brookhart's rhodium catalyst, however it only formed diphosphine products. Steric hindrance of the rhodium center prevented further dehydrocoupling of diphosphine products to cyclic oligomers, a marked difference from

Stephan's anionic zirconocene compound. Tilley proposed a mechanism based on a rhodium(I)/rhodium(III) oxidative addition/reductive elimination couple, with sequential P-H oxidative additions followed by the reductive elimination of toluene.⁸⁰

1.6.3. Main Group Catalysts

The use of transition metals as catalysts in synthesis is pervasive throughout chemistry. The unique reactivity of transition metals is ascribed to their valence d-orbitals used in the bonding that can allow metals to readily adopt multiple oxidation states and stabilize compounds with vacant coordination sites.⁸¹ Despite their wide applicability, the ever increasing price and scarcity of transition metals necessitates the need to develop catalysts based on cheaper, more earth-abundant metals. As compounds of heavier MGEs can also possess frontier orbitals with small energy separations, investigation of their use as potential replacements for transition-metals catalyst has been a rapidly developing field.

In a recent review, Power highlighted several examples of heavy MGE exhibiting reactivity similar to transition metals.⁸² A particularly relevant demonstration of this behavior was the discovery of the first main group metal phosphine dehydrocoupling catalyst reported by Wright in 2010.⁸³ Wright's catalyst $\text{Cp}^*_2\text{SnCl}_2$ was shown to be effective in catalyzing the dehydrocoupling of primary phosphines to diphosphines or cyclic oligophosphines $(\text{RP})_n$ ($\text{R} = \text{tBu, Cy, Fc,}$) $n = 4$ or 5 depending on the substrate and

reaction time used. The observance of Cp*H via ^1H NMR spectroscopy and the isolation of a tetrastannyl phosphine cage compound, $[(\text{ClSn})_4(\text{FcP-PFc})_2]$ suggested a mechanism where formation of a Sn-PHR intermediate was facilitated by loss of the Cp* ligand.

Recent collaborative work from the Waterman and Wright groups expanded the phosphine substrate scope and examined the ligand effects of other tin(IV) compounds on catalytic activity. Catalysts screened for activity included $\text{Cp}^*_2\text{SnX}_2$, ($\text{X} = \text{Cl}, \text{Me}, \text{Ph}$) and Ph_2SnCl_2 . Sterically demanding substrates showed diminished conversions for all catalysts used, which discounted an α elimination mechanism and supported Wright's mechanistic conclusions. Furthermore $\text{Cp}^*_2\text{SnCl}_2$ was an effective hydrophosphination catalyst, exhibiting moderate selectivity for the mono-hydrophosphinated products over bis-hydrophosphinated products with primary phosphine substrates. Clearly MGEs deserve additional attention as potential replacements for transition metals in catalytic reactions. Current efforts are focused on improving both the reactivity and selectivity of MGE based catalysts to levels that rival their transition-metal counterparts.

1.7. Silane Dehydrocoupling

Though the efforts described in the development of phosphorus dehydrocoupling catalysts are impressive, the field of dehydrocoupling catalysis in general was born in the

1980's largely from seminal work on the dehydropolymerization of silanes by the groups of Harrod,⁶¹ Corey,⁵⁷ and Tilley.⁸⁴

The gross majority of transition metal catalysts for silane dehydrocoupling can be grouped into two general categories: early metal metallocene compounds of the type $\text{Cp}'_x\text{MR}_y$ [$\text{Cp}' = \text{Cp}$ or Cp^* , ($x = 1-2$); $\text{M} = \text{Ti}, \text{Zr}, \text{Hf}$; $\text{R} = \text{Me}, \text{H}, \text{Cl}, \text{SiMe}_3$ ($y = 0-2$)] and late metal catalysts of the type L_nM . ($\text{L}_n =$ anionic/dative ligands, $\text{M} =$ late transition metal). With these structural motifs in mind, trends in the field and factors that impact the catalytic activity and selectivity of these compounds will be discussed below.

1.7.1. Early Transition Metal Catalysts

Unquestionably, the most studied transition metals for Si dehydrocoupling are metallocene compounds of the group 4 metals.⁵⁷ Copious research has been devoted to metallocene compounds, so much so that within the general $\text{Cp}'_x\text{MR}_y$ motif (vide supra), three general subclasses are recognized. Historically the first class is the type Cp_2MR_2 ($\text{M} = \text{Ti}, \text{Zr}$ $\text{R} = \text{Me}, \text{Bz}$) reported by Harrod in the 1980's.^{65,85} These metallocene compounds dehydrocoupled RSiH_3 ($\text{R} = \text{Ph}, \text{Hex}$) at ambient temperature yielding polysilanes with low molecular weights in the range of 900–1400 amu as determined by vapor pressure osmometry. It was noted that while both Ti and Zr catalysts produced polymers with identical molecular weight and product distributions, activity of the Zr analogue was roughly ten times faster than the Ti derivative.⁸⁵ Extension of this catalysis

to secondary silanes resulted in both low conversions and reduced dehydrocoupling activity presumably arising from steric congestion during the bond forming step. When PhMeSiH₂ was used as a substrate after two weeks reaction time, only 50% conversion was achieved where oligosilane products had an average degree of polymerization (DP) of four.

Shortly thereafter, Tilley introduced the second class of catalysts including mixed-metallocenes of the type CpCp**M*(SiR₃)X (*M* = Zr, Hf; R = Me, SiMe₃; X = Cl or Me).⁸⁶ In reactions with primary silanes, substitution of one Cp* ligand for one Cp ligand afforded higher molecular weight polysilanes and demonstrated an increased selectivity for linear over cyclic products.⁸⁴ The steric bulk of the Cp* ligand also precludes formation of catalytically inactive hydride-bridged dimers which were observed with reactions using Cp₂ZrMe₂.⁸⁵ An additional benefit of this class of compounds is faster entry into the catalytic cycle due to the facile removal of the silyl ligand relative to the organic substituents that were present in Harrod's catalysts. Tilley's early efforts were mostly focused on elucidation of the mechanism of silane dehydrocoupling.⁸⁷ Based on detailed work using the slower Hf based compound Cp*CpHf[Si(SiMe₃)₃]Cl, he proposed a mechanism of SBM, which is widely accepted as the operant mechanism for group four metallocene catalyzed silane dehydrocoupling.

Corey introduced the final class of metallocene compounds which used commercially available reagents and relied on *in situ* generation of the active catalyst from Cp₂MCl₂.⁸⁸ This strategy generated the fragment [Cp₂M] which was effective in the oligomerization of secondary silanes. For reactions with PhMeSiH₂, Corey's method

produced oligosilanes up to the octasilane while the previous two classes of compounds could only oligomerize PhMeSiH₂ to the tri- and tetrasilane. Later, this chemistry was extended to reactions using primary silanes as substrates where this method produced polysilanes with molecular weights in the range of 1500 – 4000 amu.⁸⁹

Further developments of each of these metallocene classes stemmed from the need to improve the molecular weights of the polysilane products and the selectivity of these catalysts for high molecular weight linear polysilanes over small cyclic oligomers. Ideas for structural modification of these classes of compounds were based on the same design motifs that were successful for metallocene olefin polymerization catalysis.⁵⁷ Structurally modified Cp rings,⁹⁰ ansa-bridged metallocenes,^{91,92} and more reactive cationic analogues^{90,93,94} are design considerations that have been studied to promote more effective silane dehydrocoupling. These approaches have been successful with the highest polysilane molecular weights approaching 35,000 amu.⁹⁵ However, the polysilanes produced by current group 4 metallocene catalysts are too polydisperse and their molecular weights are still not large enough for material applications.

1.7.2. Late Transition-Metal Catalysts

Despite the fact that the first publication on silane dehydrocoupling in 1973 used a late transition metal,⁶⁴ this class of compounds has received considerably less attention than group 4 metallocene compounds. In that report, Ojima and coworkers reported

Wilkinson's catalyst (Ph_3P)RhCl, dehydrocoupled the secondary silanes PhMeSiH_2 and Ph_2SiH_2 to di- and trisilane products.⁶⁴ Notably in addition to the dehydrocoupling products present, the authors observed significant amounts of products from a competing reaction of silane redistribution in these reaction mixtures.

Most successful silane dehydrocoupling catalysts based on late metals are also competent catalysts for hydrosilation, which is defined as addition of Si-H across an unsaturated bond.⁹⁶ In 1987 during a study on hydrosilation, Brown-Wensley observed disilane product formation when using platinum group metal catalysts.⁹⁷ She reported a comparative study examining the selectivity of several platinum group compounds for disilane vs hydrosilation product formation and showed that silane dehydrocoupling occurred at rates competitive with hydrosilation (Table 1.2). The secondary silane Et_2SiH_2 was used in this work, as the author noted extensive silane redistribution occurred when the arylsilane PhMeSiH_2 was used in these reactions.

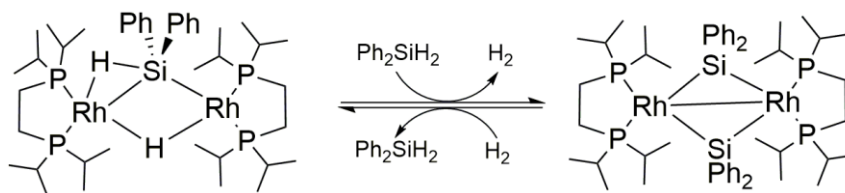
Table 1.2 Relative rates of dehydrocoupling and hydrosilation reactions catalyzed by platinum group metals⁹⁷

Catalyst	Si-Si bond formation	Hydrosilation
$(\text{Ph}_3\text{P})_2\text{Pt}(\text{C}_2\text{H}_4)$	1.0	0.8
H_2PtCl_6	0.1	6
$(\text{Ph}_3\text{P})_2\text{PtCl}_2$	0.1	0.1
$(\text{COD})\text{PtCl}_2$	0.7	70
$(\text{Ph}_3\text{P})_3\text{RhCl}$	31	400
$[\text{Rh}(\text{CO})_2\text{Cl}]_2$	5	60
$\text{CpRh}(\text{C}_2\text{H}_4)$	0.2	0.7
RhCl_3	0.3	3
$[(\text{COD})\text{IrCl}]_2$	1	25
$[(\text{COD})\text{RhCl}]_2$	0.2	3
$[(\text{allyl})\text{PdCl}]_2$	12	100

In addition to silane redistribution, catalysis of yet another reaction type occurred upon exposure of these reaction mixtures to O₂ or H₂O. Catalytic Si–O bond formation occurred at measured rates of 10 to 100 times that of hydrosilation and yielded siloxane products.

Of all compounds screened, Wilkinson's catalyst (Ph₃P)RhCl was found to have the highest activity. Therefore it is not surprising that further research has utilized it for silane dehydrocoupling studies which will be highlighted in the introduction to Chapter 3.

A bimetallic rhodium compound [(dippe)Rh(μ -H)]₂ was studied by Fryzuk and coworkers for silane dehydrocoupling activity. In an initial report, catalytic amounts of rhodium dimer reacted with Ph₂SiH₂ and generated the disilane product [Ph₂SiH]₂.⁹⁸ Reaction of the dimer with a single equivalent of Ph₂SiH₂ yielded [(dippe)Rh]₂(μ -H)(μ - η^2 -HSiPh₂) featuring bridging silyl and hydride ligands. Addition of a second equivalent of silane yielded the bis(silylene) compound [(dippe)Rh(μ -SiPh₂)]₂ (Scheme 1.8). Interconversion of these two species could be accomplished by further addition of H₂ or Ph₂SiH₂, and suggested the possibility that a catalytic cycle could be developed using this compound.



Scheme 1.8 Reversible interconversion of rhodium silyl compounds

In a second report, Fryzuk and coworkers focused on catalytic reactions of this bimetallic Rh compound with primary silanes.⁹⁹ Treatment of *p*-tolylsilane with 1 mol % of catalyst resulted in the formation of the dehydrocoupling product $[(p\text{-Tol})\text{SiH}_2]_2$ and the silane redistribution products $(p\text{-Tol})_2\text{SiH}_2$ and $(p\text{-Tol})_3\text{SiH}$ with 36% conversion of the starting material. Use of the alkylsilane substrate *n*-butylsilane in these reactions resulted in oligomerization of the starting material up to linear pentasilane products with no evidence of silane redistribution. Thus Si dehydrocoupling catalyzed by late transition metals can occur, though silane redistribution side reactions must be suppressed.

The late metal compounds discussed to this point have demonstrated lower activity than the group 4 metallocene catalyzed reactions as demonstrated by their lower molecular weight polysilane products. In silane dehydrocoupling, nickel-based catalysts have garnered special attention because of their higher activity. Zagarian has reported a variety of nickel based compounds that exhibit dehydrocoupling activity comparable to metallocene catalysts.¹⁰⁰⁻¹⁰² However, one of the most active nickel-based silane dehydrocoupling catalysts is $[(\text{dippe})\text{Ni}(\mu\text{-H})]_2$ reported in 2010 by Abu Omar and coworkers.¹⁰³ This binuclear compound was used to dehydrocouple PhSiH_3 and showed

both activity and polysilane molecular weights comparable to those of metallocene compounds (Table 1.3).

Table 1.3 Comparison of PhSiH₃ dehydrocoupling using zirconium and nickel catalysts¹⁰³

Compound	Solvent	Time (h)	M _w range	PDI
Cp ₂ ZrMe ₂	neat	1	2390–580	-
Ind ₂ ZrMe ₂	neat	24	3200–1530	1.09
CpCp*Zr[Si(SiMe ₃) ₃]Me	neat	0.25	3100	1.8
Cp ₂ ZrCl ₂ / 2 <i>n</i> BuLi	toluene	240	2450	1.18
[(dippe)Ni(μ-H)] ₂	toluene	1.5	3200-549	1.44

In addition to dehydrocoupling, silane redistribution and oxygenation are two competitive side reactions that late transition metals catalyze. Therefore, it is neither the cost nor activity of late metal catalysts that stunted their development for dehydrocoupling, rather the lack of product selectivity and need for specific reaction conditions to avoid side reactions that renders this class underutilized compared to group 4 metallocene compounds. In Chapter 3, efforts toward studying the interplay between redistribution and dehydrocoupling using iridium pincer compounds will be presented.

1.8. Pincer Compounds

The chemistry of pincer-ligated transition metals has developed considerably since these types of compounds were first prepared in the 1970s.¹⁰⁴ The term pincer compound has no precise definition, but generally these chelating ligands consist of two dative bonds and one anionic central atom bonded to metal in a meridional coordination mode with all bonding elements in the same plane. These three coordinating atoms provide the nomenclature for how pincer compounds are named (e.g.: PCP or NCN).¹⁰⁵ Pincer ligands are popular in catalysis because of their rigid frameworks, which most often contain an aryl backbone and confer a high degree of thermal stability to their compounds. The tridentate coordination mode of these ligands allows for precise control of steric and electronic properties (Figure 1.9).¹⁰⁶

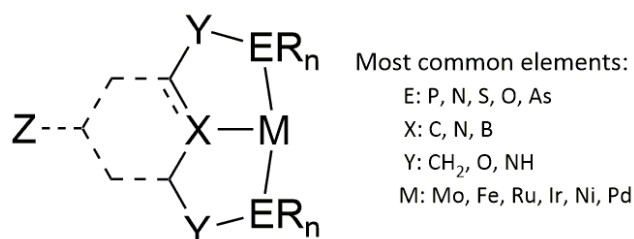


Figure 1.9 Various substitution modes in a pincer ligand

Pincer ligands can be tuned in many ways to impart desired effects in catalysis. Heteroatom substitution of the ER_n group can drastically influence steric crowding near the metal center. Variation of the substituents *para* to the metal at Z can tune the electronics

of the ligand without affecting the coordination sphere of the metal or be used to install a tether for attachment to solid supports.¹⁰⁷ Subtle electronic modulation can be imparted through substitution at position Y while stronger electronic control can be achieved at the X position, which influences the reactivity of the system through trans effects.¹⁰⁵

1.8.1. Catalysis with Iridium Pincer Compounds

Iridium pincer compounds have been shown to be active as dehydrogenation catalysts for alkanes¹⁰⁸ and other isoelectronic substrates.¹⁰⁵ Besides this high activity, catalysts of this type have also been studied for small molecule activation¹⁰⁶ and exhibit high product selectivity in reactions.

The high activity of these compounds is demonstrated in catalytic reactions with amine-boranes. Using Brookhart's iridium(III) pincer compound,¹⁰⁹ (POCOP)Ir(H)₂ (POCOP = [κ^3 -1,3-(OP^tBu)₂C₆H₃]), Goldberg reported vigorous dehydrocoupling of ammonia borane (NH₃BH₃). This catalyst was highly active with 0.5 mol % loading producing one equivalent of H₂ within 15 minutes of reaction time at ambient temperature.¹¹⁰ The product was an insoluble white powder of the form [H₂N·BH₂]_n as determined by solid-state ¹¹B NMR spectroscopy. Insolubility prevented absolute product characterization, though the authors used data from IR spectroscopy and powder X-ray diffraction to propose the cyclic pentamer, [H₂N·BH₂]₅ as the main product.

Later, Manners and co-workers revisited this dehydrocoupling reaction and found that linear high molecular weight poly(aminoboranes) could also be solicited via this catalyst.¹¹¹ The product insolubility that plagued Goldberg's study was overcome simply through the use of a more soluble amine–borane, MeHNBH₂. Using this substrate poly(methylamino)boranes with GPC-determined molecular weights of 160,000 and 156,000 amu were isolated.

As dehydrocoupling can be thought of as a type of dehydrogenation reaction, the high activity and selectivity of these pincer compounds demanded further investigation into their use as potential dehydrocoupling catalysts. In Chapter 3, POCOP Ir compounds were investigated for Si dehydrocoupling activity. A study modulating the steric and electronic effects of the POCOP ligand and how these parameters effect product selectivity will be presented.

1.9. References

- (1) Williams, J. W. *J. Phys. Chem.* **1931**, *36*, 437.
- (2) Shirakawa, H.; Louis, E. J.; MacDiarmid, A. G.; Chiang, C. K.; Heeger, A. J. *J. Chem. Soc., Chem. Commun.* **1977**, 578.
- (3) 2014 ed.; Nobel Media AB: Nobelprize.org.
- (4) Heeger, A. J. *J. Phys. Chem. B* **2001**, *105*, 8475.
- (5) Günes, S.; Neugebauer, H.; Sariciftci, N. S. *Chem. Rev.* **2007**, *107*, 1324.

- (6) van Mullekom, H. A. M.; Vekemans, J. A. J. M.; Havinga, E. E.; Meijer, E. W. *Mater. Sci. Eng., R* **2001**, *32*, 1.
- (7) Balaji, V.; Michl, J. *Polyhedron* **1991**, *10*, 1265.
- (8) Miller, R. D.; Michl, J. *Chem. Rev.* **1989**, *89*, 1359.
- (9) Facchetti, A. *Chem. Mater.* **2011**, *23*, 733.
- (10) Kraft, A.; Grimsdale, A. C.; Holmes, A. B. *Angew. Chem. Int. Ed* **1998**, *37*, 402.
- (11) Torsi, L.; Dodabalapur, A.; Rothberg, L. J.; Fung, A. W. P.; Katz, H. E. *Science* **1996**, *272*, 1462.
- (12) Hide, F.; Díaz-García, M. A.; Schwartz, B. J.; Andersson, M. R.; Pei, Q.; Heeger, A. J. *Science* **1996**, *273*, 1833.
- (13) Guo, X.; Baumgarten, M.; Müllen, K. *Prog. Polym. Sci.* **2013**, *38*, 1832.
- (14) McCullough, R. D.; Lowe, R. D.; Jayaraman, M.; Anderson, D. L. *J. Org. Chem.* **1993**, *58*, 904.
- (15) Hoeben, F. J. M.; Jonkheijm, P.; Meijer, E. W.; Schenning, A. P. H. J. *Chem. Rev.* **2005**, *105*, 1491.
- (16) Son, H. J.; He, F.; Carsten, B.; Yu, L. *J. Mater. Chem.* **2011**, *21*, 18934.
- (17) Roncali, J. *Macromol. Rapid Commun.* **2007**, *28*, 1761.
- (18) Fukazawa, A.; Yamaguchi, S. *Chem. Asian J.* **2009**, *4*, 1386.
- (19) Hissler, M.; Dyer, P. W.; Réau, R. *Coord. Chem. Rev.* **2003**, *244*, 1.
- (20) He, X.; Baumgartner, T. *RSC Adv.* **2013**, *3*, 11334.

- (21) Katritzky, A. R.; Ramsden, C. A.; Joule, J. A.; Zhdankin, V. V. In *Handbook of Heterocyclic Chemistry*; Elsevier Science: Amsterdam, 2010, p 87.
- (22) Gidron, O.; Varsano, N.; Shimon, L. J. W.; Leitun, G.; Bendikov, M. *Chem. Commun.* **2013**, *49*, 6256.
- (23) Patra, A.; Bendikov, M. *J. Mater. Chem.* **2010**, *20*, 422.
- (24) Jeffries-El, M.; Kobilka, B. M.; Hale, B. J. *Macromolecules* **2014**, *47*, 7253.
- (25) Bird, C. W. *Tetrahedron* **1985**, *41*, 1409.
- (26) Yamaguchi, S.; Itami, Y.; Tamao, K. *Organometallics* **1998**, *17*, 4910.
- (27) Dillon, K. B. *Phosphorus : the carbon copy : from organophosphorus to phospho-organic chemistry*; John Wiley: New York, 1998.
- (28) Baumgartner, T.; Réau, R. *Chem. Rev.* **2006**, *106*, 4681.
- (29) Cabelli, D. E.; Cowley, A. H.; Dewar, M. J. S. *J. Am. Chem. Soc.* **1981**, *103*, 3286.
- (30) Kapp, J.; Schade, C.; El-Nahasa, A. M.; von Ragué Schleyer, P. *Angew. Chem. Int. Ed.* **1996**, *35*, 2236.
- (31) Giordan, J. C.; Moore, J. H.; Tossell, J. A.; Kaim, W. *J. Am. Chem. Soc.* **1985**, *107*, 5600.
- (32) Gates, D. P. *Top. Curr. Chem.* **2005**, *250*, 107.
- (33) Saito, A.; Miyajima, T.; Nakashima, M.; Fukushima, T.; Kaji, H.; Matano, Y.; Imahori, H. *Chem. Eur. J.* **2009**, *15*, 10000.
- (34) Saito, A.; Matano, Y.; Imahori, H. *Org. Lett.* **2010**, *12*, 2675.

- (35) Izumi, T.; Kobashi, S.; Takimiya, K.; Aso, Y.; Otsubo, T. *J. Am. Chem. Soc.* **2003**, *125*, 5286.
- (36) Wright, V. A.; Gates, D. P. *Angew. Chem. Int. Ed* **2002**, *41*, 2389.
- (37) Wright, V. A.; Patrick, B. O.; Schneider, C.; Gates, D. P. *J. Am. Chem. Soc.* **2006**, *128*, 8836.
- (38) Kipping, F. S. *J. Chem. Soc. Trans.* **1924**, *125*, 2291.
- (39) Burkhard, C. A. *J. Am. Chem. Soc.* **1949**, *71*, 963.
- (40) Yajima, S.; Hayashi, J.; Omori, M. *Chem. Lett.* **1975**, *4*, 931.
- (41) West, R.; David, L. D.; Djurovich, P. I.; Stearley, K. L.; Srinivasan, K. S. V.; Yu, H. *J. Am. Chem. Soc.* **1981**, *103*, 7352.
- (42) Trujillo, R. E. *J. Organomet. Chem.* **1980**, *198*, C27.
- (43) Trefonas, P.; West, R. *J. Polym. Sci. Polym. Chem. Ed.* **1985**, *23*, 2099.
- (44) Imori, T.; Lu, V.; Cai, H.; Tilley, T. D. *J. Am. Chem. Soc.* **1995**, *117*, 9931.
- (45) Sandorfy, C. *Can. J. Chem.* **1955**, *33*, 1337.
- (46) Bande, A.; Michl, J. *Chem. Eur. J.* **2009**, *15*, 8504.
- (47) Nešpůrek, S. *Mater. Sci. Eng., C* **1999**, *8–9*, 319.
- (48) Gilman, H.; Atwell, W. H.; Schwebke, G. L. *J. Organomet. Chem.* **1964**, *2*, 369.
- (49) Gilman, H.; Chapman, D. R. *J. Organomet. Chem.* **1966**, *5*, 392.
- (50) Halevi, E. A.; Winkelhofer, G.; Meisl, M.; Janoschek, R. *J. Organomet. Chem.* **1985**, *294*, 151.

- (51) Harrah, L. A.; Zeigler, J. M. *Macromolecules* **1987**, *20*, 601.
- (52) Miller, R. D.; Sooriyakumaran, R. *Macromolecules* **1988**, *21*, 3120.
- (53) Damewood, J. R.; West, R. *Macromolecules* **1985**, *18*, 159.
- (54) Zhang, X.-H.; West, R. *J. Polym. Sci. B Polym. Lett. Ed.* **1985**, *23*, 479.
- (55) Trefonas, P.; West, R.; Miller, R. D. *J. Am. Chem. Soc.* **1985**, *107*, 2737.
- (56) Kozima, S.; Kobayashi, K.; Kawanisi, M. *Bull. Chem. Soc. Jpn.* **1976**, *49*, 2837.
- (57) Corey, J. Y. *Adv. Organomet. Chem.* **2004**, *51*, 1.
- (58) Manners, I. *Angew. Chem. Int. Ed.* **1996**, *27*, 1602.
- (59) Manners, I. *J. Polym. Sci., Part A: Polym. Chem.* **2002**, *40*, 179.
- (60) Waterman, R. *Cur. Org. Chem.* **2008**, *12*, 1322.
- (61) Gauvin, F.; Harrod, J. F.; Woo, H. G. *Adv. Organomet. Chem.* **1998**, *42*, 363.
- (62) Waterman, R. *Chem. Soc. Rev.* **2013**, *42*, 5629.
- (63) Corcoran, E. W.; Sneddon, L. G. *J. Am. Chem. Soc.* **1984**, *106*, 7793.
- (64) Ojima, I.; Inaba, S.-I.; Kogure, T.; Nagai, Y. *J. Organomet. Chem.* **1973**, *55*, C7.
- (65) Aitken, C.; Harrod, J. F.; Samuel, E. *J. Organomet. Chem.* **1985**, *279*, C11.
- (66) Woo, H. G.; Walzer, J. F.; Tilley, T. D. *J. Am. Chem. Soc.* **1992**, *114*, 7047.
- (67) Waterman, R. *Organometallics* **2013**, *32*, 7249.

- (68) Crabtree, R. H. *The Organometallic Chemistry of the Transition Metals*; 5th ed.; John Wiley & Sons, 2009.
- (69) Sloan, M. E.; Staubitz, A.; Clark, T. J.; Russell, C. A.; Lloyd-Jones, G. C.; Manners, I. *J. Am. Chem. Soc.* **2010**, *132*, 3831.
- (70) Hillhouse, G. L.; Bercaw, J. E. *J. Am. Chem. Soc.* **1984**, *106*, 5472.
- (71) Neale, N. R.; Tilley, T. D. *J. Am. Chem. Soc.* **2002**, *124*, 3802.
- (72) Woo, H. G.; Freeman, W. P.; Tilley, T. D. *Organometallics* **1992**, *11*, 2198.
- (73) Neale, N. R.; Tilley, T. D. *J. Am. Chem. Soc.* **2005**, *127*, 14745.
- (74) Waterman, R.; Tilley, T. D. *Angew. Chem. Int. Ed* **2006**, *45*, 2926.
- (75) Fermin, M. C.; Stephan, D. W. *J. Am. Chem. Soc.* **1995**, *117*, 12645.
- (76) Etkin, N.; Hoskin, A. J.; Stephan, D. W. *J. Am. Chem. Soc.* **1997**, *119*, 11420.
- (77) Waterman, R. *Organometallics* **2007**, *26*, 2492.
- (78) Ghebreab, M. B. Ph.D. Thesis, University of Vermont, 2013.
- (79) Böhm, V. P. W.; Brookhart, M. *Angew. Chem. Int. Ed* **2001**, *40*, 4694.
- (80) Han, L.-B.; Tilley, T. D. *J. Am. Chem. Soc.* **2006**, *128*, 13698.
- (81) Less, R. J.; Melen, R. L.; Wright, D. S. *RSC Adv.* **2012**, *2*, 2191.
- (82) Power, P. P. *Nature* **2010**, *463*, 171.
- (83) Naseri, V.; Less, R. J.; Mulvey, R. E.; McPartlin, M.; Wright, D. S. *Chem. Commun.* **2010**, *46*, 5000.
- (84) Tilley, T. D. *Acc. Chem. Res.* **1993**, *26*, 22.

- (85) Mu, Y.; Aitken, C.; Cote, B.; Harrod, J. F.; Samuel, E. *Can. J. Chem.* **1991**, *69*, 264.
- (86) Woo, H. G.; Tilley, T. D. *J. Am. Chem. Soc.* **1989**, *111*, 3757.
- (87) Woo, H. G.; Tilley, T. D. *J. Am. Chem. Soc.* **1989**, *111*, 8043.
- (88) Corey, J. Y.; Zhu, X. H.; Bedard, T. C.; Lange, L. D. *Organometallics* **1991**, *10*, 924.
- (89) Grimmond, B. J.; Corey, J. Y. *Organometallics* **1999**, *18*, 2223.
- (90) Imori, T.; Tilley, T. D. *Polyhedron* **1994**, *13*, 2231.
- (91) Aitken, C.; Barry, J. P.; Gauvin, F.; Harrod, J. F.; Malek, A.; Rousseau, D. *Organometallics* **1989**, *8*, 1732.
- (92) Choi, N.; Onozawa, S.-y.; Sakakura, T.; Tanaka, M. *Organometallics* **1997**, *16*, 2765.
- (93) Dioumaev, V. K.; Rahimian, K.; Gauvin, F.; Harrod, J. F. *Organometallics* **1999**, *18*, 2249.
- (94) Dioumaev, V. K.; Harrod, J. F. *J. Organomet. Chem.* **1996**, *521*, 133.
- (95) Corriu, R. J. P.; Enders, M.; Huille, S.; Moreau, J. J. E. *Chem. Mater.* **1994**, *6*, 15.
- (96) Nakajima, Y.; Shimada, S. *RSC Adv.* **2015**, *5*, 20603.
- (97) Brown-Wensley, K. A. *Organometallics* **1987**, *6*, 1590.
- (98) Fryzuk, M. D.; Rosenberg, L.; Rettig, S. J. *Organometallics* **1991**, *10*, 2537.

- (99) Fryzuk, M. D.; Rosenberg, L.; Rettig, S. J. *Inorg. Chim. Acta* **1994**, 222, 345.
- (100) Fontaine, F.-G.; Kadkhodazadeh, T.; Zargarian, D. *Chem. Commun.* **1998**, 1253.
- (101) Fontaine, F.-G.; Zargarian, D. *Organometallics* **2002**, 21, 401.
- (102) Fontaine, F.-G.; Zargarian, D. *J. Am. Chem. Soc.* **2004**, 126, 8786.
- (103) Smith, E. E.; Du, G.; Fanwick, P. E.; Abu-Omar, M. M. *Organometallics* **2010**, 29, 6527.
- (104) Moulton, C. J.; Shaw, B. L. *J. Chem. Soc., Dalton Trans.* **1976**, 1020.
- (105) Choi, J.; MacArthur, A. H. R.; Brookhart, M.; Goldman, A. S. *Chem. Rev.* **2011**, 111, 1761.
- (106) Benito-Garagorri, D.; Kirchner, K. *Acc. Chem. Res.* **2008**, 41, 201.
- (107) Huang, Z.; Rolfe, E.; Carson, E. C.; Brookhart, M.; Goldman, A. S.; El-Khalafy, S. H.; MacArthur, A. H. R. *Adv. Synth. Catal.* **2010**, 352, 125.
- (108) Gupta, M.; Hagen, C.; Flesher, R. J.; Kaska, W. C.; Jensen, C. M. *Chem. Commun.* **1996**, 2083.
- (109) Göttker-Schnetmann, I.; White, P.; Brookhart, M. *J. Am. Chem. Soc.* **2004**, 126, 1804.
- (110) Denney, M. C.; Pons, V.; Hebden, T. J.; Heinekey, D. M.; Goldberg, K. *J. Am. Chem. Soc.* **2006**, 128, 12048.

(111) Staubitz, A.; Sloan, M. E.; Robertson, A. P. M.; Friedrich, A.; Schneider, S.; Gates, P. J.; Günne, J. r. S. a. d.; Manners, I. *J. Am. Chem. Soc.* **2010**, *132*, 13332.

CHAPTER 2: ZIRCONIUM-CATALYZED PHOSPHINE DEHYDROCOUPLING: EFFORTS TOWARD SOLUBLE POLYPHOSPHINES

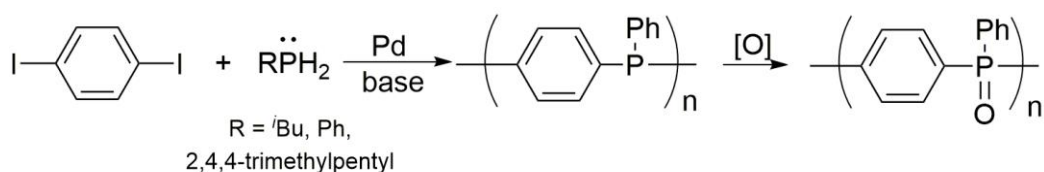
2.1. Introduction

Heteroatom substitution in the main chain of π -conjugated materials is a powerful method used to diversify and tailor their properties.¹ The incorporation of phosphorus(III) into conjugated polymers has garnered substantial attention due its often carbon-like reactivity² and the ability of its lone pair of electrons to participate in π -conjugation.¹

Effects of conjugation resulting from phosphorus incorporation into aromatic systems were studied in 1981 through a comparison study of several aryl phosphines with their lighter nitrogen analogues.³ Using ultraviolet photoelectron spectroscopy (UPE), it was demonstrated that communication existed between the phosphorus atoms in 1,4-bisphosphinobenzene. Based on this observation, efforts to extend different types of nitrogen based π -conjugated systems to phosphorus and other group 15 elements began.

The first well defined poly(*para*-phenylenephosphine)s were reported by Lucht in 2000.⁴ These polyphosphine materials were of modest molecular weights and fairly monodisperse based on their narrow PDIs (Scheme 2.1). UV-vis spectra of these polyphosphines exhibited one absorption attributed to π - π^* transitions. As the number

of arylsubstituted phosphines increased, red shifts were observed in absorption spectra and suggested extended π -delocalization involving the lone pair of electrons on phosphorus. Oxidation of the phosphorus to its higher oxidation state of P(V) resulted in blue shifted π - π^* absorption bands in the UV-vis spectra attributed to reduced conjugation.



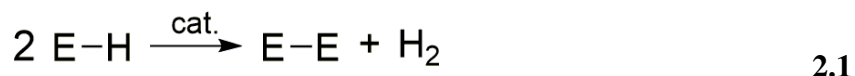
R	M_n	PDI	$\lambda_{\max}(\pi-\pi^*)$
<i>i</i> Bu	1700	1.3	278
2,4,4-trimethylpentyl	3100	1.5	276
Ph	1300	1.4	291

Scheme 2.1 The first well-defined poly(phenylphosphine)

Lucht's polymers were prepared by a palladium-catalyzed condensation reaction which necessarily resulted in the concomitant elimination of hydrogen iodide as a byproduct. This acid formation requires that this catalysis be performed in the presence of stoichiometric amounts of base.⁵ This additional reagent does not affect the polymeric properties of the material, however it does place additional constraints on functional group tolerance as well as increase the overall cost of the process.⁶

Relative to organic polymer science, the chemistry of main group polymers is considerably less developed.⁷ Difficulties include the preparation and stabilization of the

main group element (MGE) analogues of olefins and acetylenes⁷ and the scarcity of synthetic methods to catalytically generate homonuclear or heteronuclear bonds between MGE.⁸ The use of transition metals as dehydrocoupling catalysts is an attractive alternative to methods such as Würtz-type coupling or dehydrohalogenation reactions traditionally used to form bonds between MGEs. In dehydrocoupling reactions, two molecules with E–H bonds undergo a net metathesis reaction to form an E–E bond and eliminate an equivalent of H₂ gas (eqn. 2.1).



Several catalysts have demonstrated the ability to mediate P–P bond formation, each with specific selectivity and applications (Section 1.6).⁹ Stephan and Fermin published the first example of zirconium catalyzed phosphine dehydrocoupling in 1995, utilizing an anionic zirconocene trihydride compound [Cp*₂ZrH₃]⁻Li to catalyze cyclic oligophosphine (PR)_n (n = 4, 5) formation from primary phosphine substrates.¹⁰

Though the exact mechanism of the reaction has not been verified, isolation of several products resulting from stoichiometric reactions supported a mechanism involving a terminal phosphinidene intermediate (Scheme 1.6).¹¹ In this mechanism, the P–P bond forming step can be envisioned as occurring via a nucleophilic attack of RPH₂ on the phosphinidene phosphorus.¹²

Previous efforts on zirconium-catalyzed dehydrocoupling of group 15 elements by the Waterman group have been dedicated to the study of a triamidoamine-ligated

zirconium compound $(N_3N)Zr$, **1**, $(N_3N) = [\kappa^5-$
 $(Me_3SiNCH_2CH_2)_2NCH_2CH_2NSiMe_2CH_2]$ (Figure 2.1). Compound **1** demonstrates
 reactivity akin to the zirconium hydride compound $(N_3N)ZrH$ and is best described as a
 “hydride surrogate”.¹³

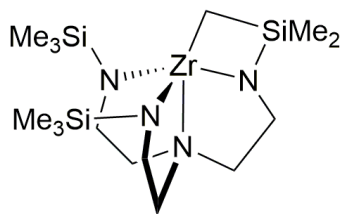
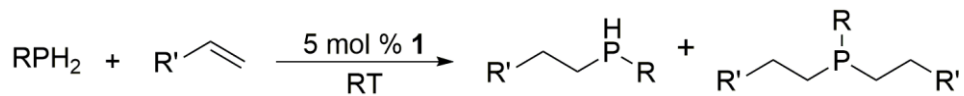


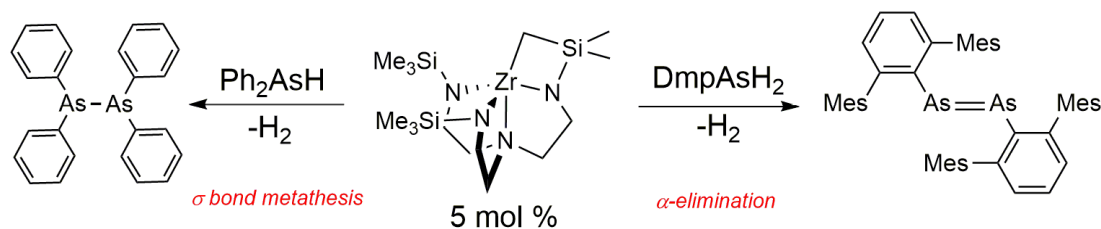
Figure 2.1 Triamidoamine ligated zirconium $(N_3N)Zr$, **1** studied by the Waterman group

Compound **1** is a versatile scaffold that has been utilized as a precursor to prepare a variety of compounds of the type $(N_3N)ZrX$ ($X =$ anionic ligand) and to stabilize low valent fragments.¹⁴ It has been demonstrated that small polar substrates, isonitriles, and alkynes readily insert into the $Zr-P$ bond of phosphido compounds prepared from stoichiometric reactions of **1** and primary or secondary phosphines.¹⁵ Based on these observations, it was hypothesized and further confirmed that **1** could act as a rare Group 4 metal hydrophosphination catalyst for alkene and alkyne substrates (Scheme 2.2).¹⁶



Scheme 2.2 Hydrophosphination of an alkene

Compound **1** is a phosphine and arsine dehydrocoupling catalyst that has demonstrated the ability to operate under multiple mechanisms depending on the steric constraints of the MGE substrate.¹⁷ For phosphine dehydrocoupling reactions, kinetic isotope effects and the measurement of a negative entropy of activation suggested a catalytic cycle based on σ -bond metathesis.¹³ In a related arsine dehydrocoupling study, reaction of 5 mol % of **1** with Ph_2AsH yielded the product $(\text{Ph}_2\text{As})_2$, the product expected from a SBM pathway. Use of the more sterically demanding arsine dmpAsH_2 ($\text{dmp} = 1,3$ -dimesitylphenyl) in these reactions resulted in α arsinidine elimination and yielded the diarsine product $\text{dmpAs}=\text{Asdmp}$ arising from condensation of two low valent dmpAs : fragments (Scheme 2.3).¹⁷



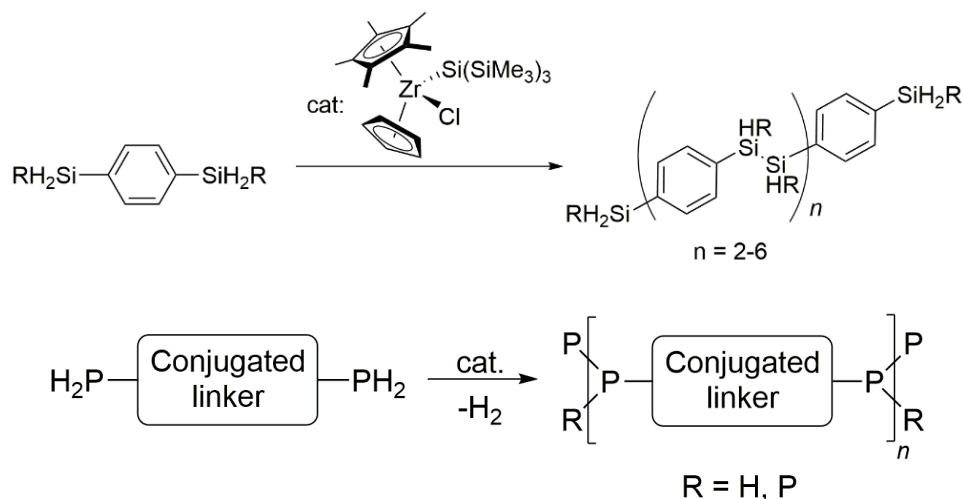
Scheme 2.3 Mechanistic variety in arsine dehydrocoupling using **1**

The goal of my research was to support previous Waterman group efforts in the utilization of **1** in catalytic dehydrocoupling reactions of bisphosphine substrates towards the formation of P–P linked π -conjugated dimers, oligomers and polymers. The synthesis of new bisphosphine substrates incorporating solubilizing alkoxy substituents would allow for the characterization of polyphosphine products by solution-based spectroscopic

and analytical methods. To this effect, it is worth noting that most conjugated materials incorporating phosphorus consist of P–C, P=C and P=P linkages, though comparatively very little is reported on P–P linked materials (Section 1.3).^{1,18}

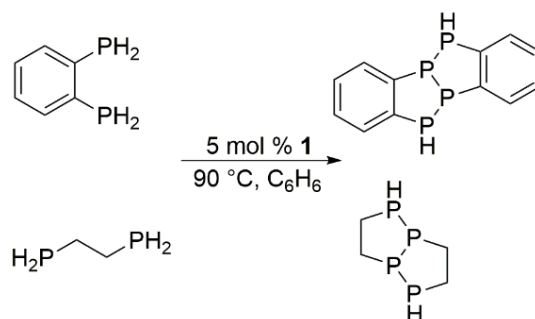
Research by Dr. Michael Ghebreab, formerly of the Waterman group, also focused on this topic. Mike explored phosphine heterodehydrocoupling reactions catalyzed by **1** and determined that the steric demands of the phosphine substituents play a large role in product formation using this catalyst (Scheme 1.7). In general, the less bulky phosphines PhPH₂, CyPH₂, and PhMePH demonstrated higher conversions and activity than the larger substrates CyMePH, Ph₂PH, and Cy₂PH which either exhibited low activity or did not yield heterodehydrocoupling products.

In addition to phosphine heterodehydrocoupling reactions, Mike also studied reactions of **1** with bisphosphine linker substrates with the goal of forming π -conjugated dimers, oligomers, and polymers. This strategy was analogous to that used in earlier work by Tilley on zirconocene catalyzed silane dehydrocoupling (Scheme 2.4).¹⁹



Scheme 2.4 Tilley's strategy for linear oligosilane formation (top) Our extension of this idea to phosphorus substrates (bottom)

Stephan had reported similar catalysis where treatment of *o*-bisphosphinobenzene with 5 mol % of $[\text{Cp}^*_2\text{ZrH}_3]\text{Li}$ (**2**) completely consumed the substrate and resulted in the formation of the 16-membered phosphorus macrocycle $[(\text{C}_6\text{H}_4)\text{P}_2]_8$.²⁰ For comparison, Mike examined the reaction of **1** with *o*-bisphosphinobenzene and the related alkyl derivative 1,2-bisphosphinoethane. Treatment of these substrates with 5 mol % of **1** resulted in diphosphine products as determined via ^{31}P NMR spectroscopy with no evidence of further dehydrocoupling activity (Scheme 2.5).²¹



Scheme 2.5 Oligomerization of bisphosphine substrates catalyzed by compound **1**

The observation of further dehydrocoupling of the diphosphine $[(\text{C}_6\text{H}_4)\text{PHP}]_2$ to the macrocycle $[(\text{C}_6\text{H}_4)\text{P}_2]_8$ by **2** lends credence to the argument that **2** is a more active phosphine dehydrocoupling catalyst than **1**, though initial efforts for this project were focused on using **1**, the compound our group developed.

Additional bisphosphine linker molecules including 2,5-bis(phosphino)furan, (**3**) 1,4-bis(phosphino)benzene, 1,1'-bis(phosphino)ferrocene and 1,4-bis(phosphino)-2,3,5,6-tetrafluorobenzene were prepared by members of the Waterman group and initially screened for dehydrocoupling activity by Mike. However, use of these substrates resulted in either dimeric phosphine products or insoluble hyperbranched polyphosphine materials (Figure 2.2).

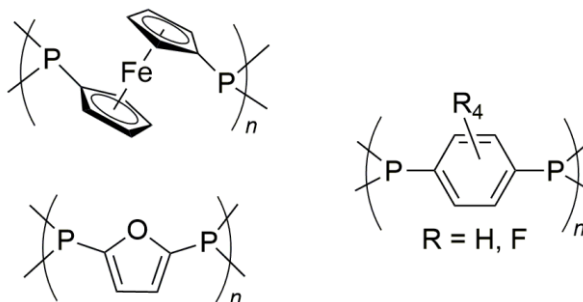


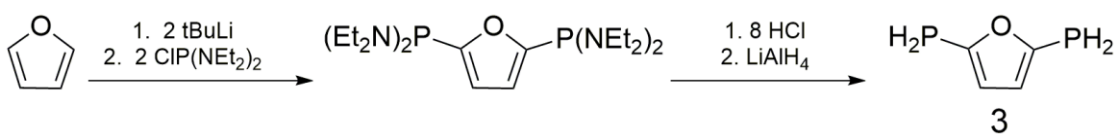
Figure 2.2 Insoluble hyperbranched polyphosphine products from dehydrocoupling reactions with **1**

2.2. Results

Coming into this project, the goal of my work was to expand Mike's previous research by attempting further characterization of these insoluble hyperbranched polyphosphine materials. The second aspect of this project was the design and synthesis of "second generation" linker molecules incorporating alkyl or alkoxy side chain substituents to engender solubility. These new substrates would produce soluble polyphosphine products once dehydrocoupled that could be characterized by solution-based spectroscopic and analytical methods.

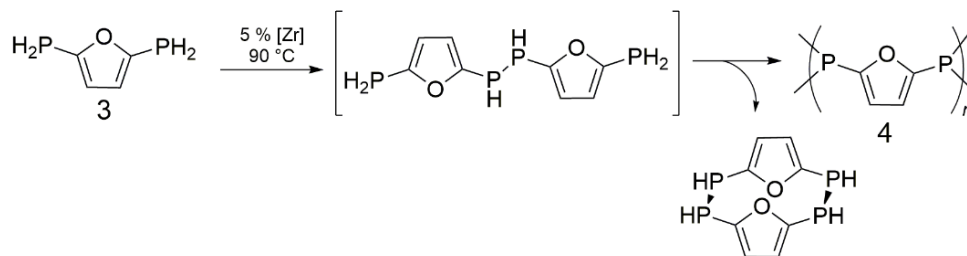
The first bisphosphine linker molecule I synthesized and studied was 2,5-bis(phosphino)furan, **3**. The motivation for initial study of this substrate was primarily due to the small relative size of the molecule and the presence of a reactive heteroatom. The initial synthesis and dehydrocoupling of this molecule was completed by Michael Ghebreab, but full characterization of the dehydrocoupling products needed to be

completed when I joined the Waterman group. Synthesis of this substrate was straightforward and was accomplished by the dilithiation of furan with $t\text{BuLi}$, followed by the installation of bis(diethylamino)phosphino substituents. These ethylamino groups were removed through chlorination with HCl , then lithium aluminum hydride was used to reduce the PCl_2 groups yielding the desired substrate as a highly air- and moisture-sensitive colorless liquid (Scheme 2.6).²²



Scheme 2.6 Synthesis of 2,5-bis(phosphino)furan, **3**

Treatment of **3** with 5 mol % of **1** in benzene solution resulted in conversion first to diphosphine products, then eventual conversion to the hyperbranched material **4** (Scheme 2.7). Running this reaction for a shorter time period resulted in conversion only to diphosphine products. After five days of continual heating at $80\text{ }^\circ\text{C}$ and periodic removal of byproduct H_2 gas, chunky bright orange precipitate was observed in the reaction vessel. The reaction was cooled and the polymer was isolated via filtration as a chalky yellow solid.



Scheme 2.7 Formation of insoluble hyperbranched polymer, **4**

Solution phase characterization of **4** has been hampered by its extreme insolubility in common laboratory solvents due to polymeric hyperbranching of P–P linkages, and/or π – π stacking of the furan moieties. Preliminary efforts were undertaken to functionalize **3** with a hexyl sidechain, however the synthetic protocol to prepare this variant was deemed too demanding and alternate solutions were explored instead.

Despite the insolubility of **4**, some structural and molecular mass information could be ascertained from solid state methods. Compound **4** was analyzed by elemental analysis (EA) and its composition was determined as 2.5% nitrogen, 34.5% carbon, and 5.02% hydrogen. Due to the detection of nitrogen via EA, this result indicated the presence of residual **1** embedded in the material from the N_3N ligand. From this data and the monomer's EA composition, it can be crudely inferred based on ratios of percent nitrogen present that there are approximately 14 phosphinyl furan moieties per molecule of **1** present.

Thermogravimetric analysis (TGA) data was obtained for **4** over a temperature range of 100–800 °C (Figure 2.3, compound **4**). Compound **4** is thermally stable at 100 °C with 97.3% remaining after holding at the initial analysis temperature. As **4** is heated,

its weight percent slowly increases to a maximum of 111.9%, observed at 271.6 °C. This increase of 14.6% by weight indicates slow oxidation of **4** during heating. For comparison, the theoretical increase in mass resulting from oxidation of the furan monomer **3**, to its phosphorus(V) analogue is 24.2%. The observed lower percentage is attributed to thermal degradation of lighter molecular weight fractions of **4** at increasing temperature. After this increase, slow degradation was observed with increasing temperature until 47.4% of the initial mass remained post analysis.

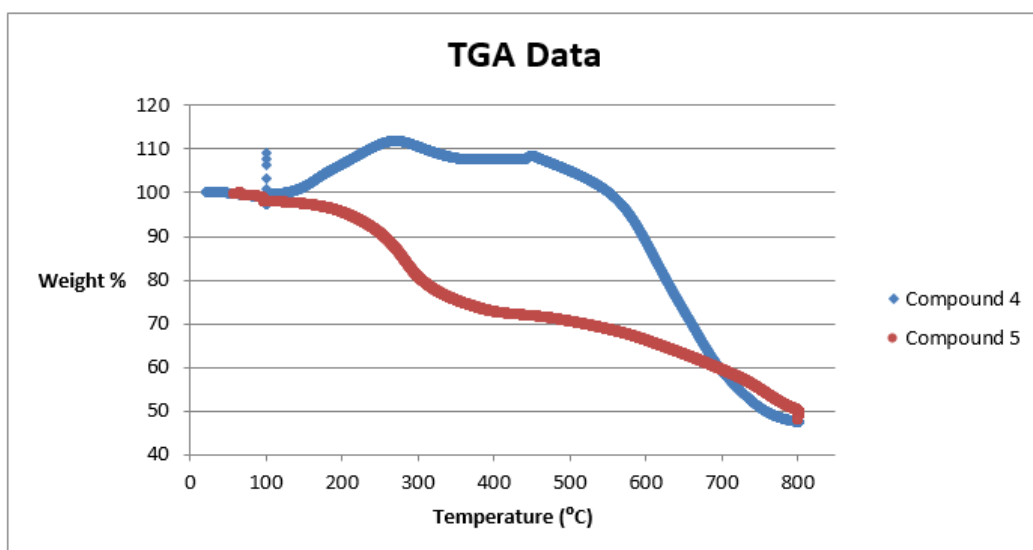


Figure 2.3 TGA data for polymers **4** and **5**

To compare the TGA profile of **4** to its phosphorus(V) analogue **5**, oxidized materials were prepared by rinsing **4** with hydrogen peroxide. Upon oxidation, the color of **4** was bleached chalky white. In contrast to the curve for **4**, the TGA curve of **5** indicated no increase in mass at any temperature (Figure 3, Compound **5**). Gradual

degradation was observed for the duration of the temperature range and 47.8% mass remained post analysis. Both the phosphorus(III) and phosphorus(V) materials have ~47% of their mass remaining at the end of their respective analyses which likely corresponds to residual phosphorus. This assumption was made based on the fact that the furan monomer **3** is 46.9% phosphorus prior to dehydrocoupling.

At this point my project diverged from Mike's with his focus on development of additional bisphosphine substrates and secondary phosphines linker molecules designed to prevent hyperbranching.²³ The contents of the rest of this chapter describe the design and synthesis of linker molecules incorporating alkyl or alkoxy side chain substituents to engender solubility and their use in catalytic reactions with both **1** and **2**.

2.2.1. Synthesis of Linker Molecules Incorporating Long-Chain Alkoxy Groups

The insolubility of the hyperbranched polyphosphine products prevented determination of their molecular weights and structure. Therefore the synthesis of primary phosphine linker molecules functionalized with solubilizing long-chain alkoxy groups was investigated. The initial target molecule was a PPV derivative, **6** that was largely inspired by a report by Protasiewicz and coworkers (Figure 2.4).²⁴

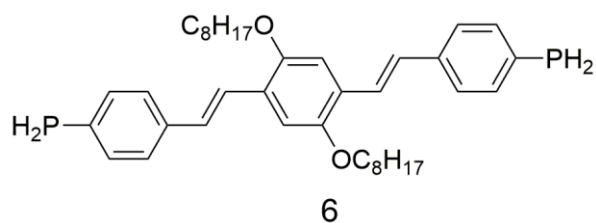
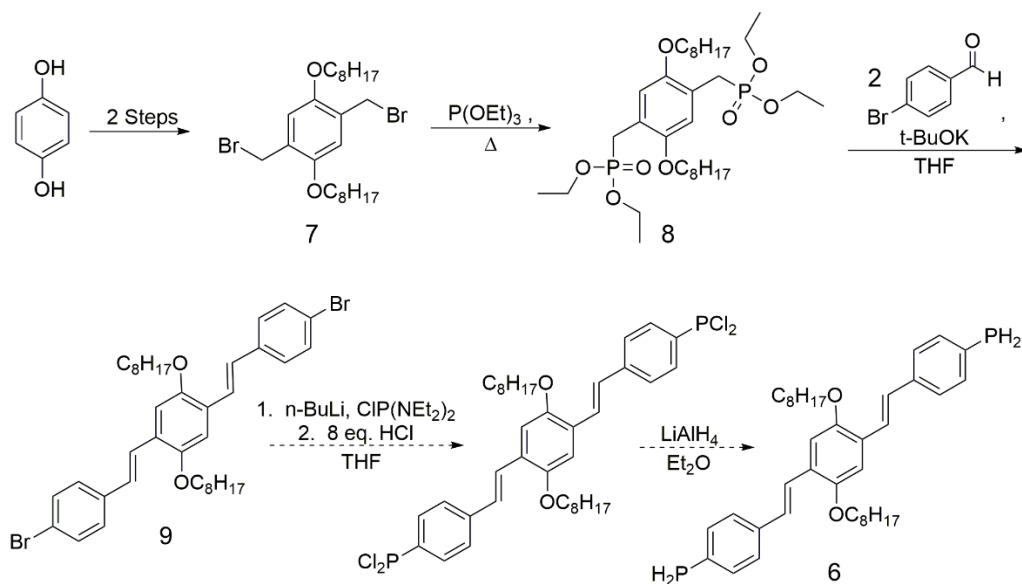


Figure 2.4 PPV-based synthetic target **6** for phosphine dehydrocoupling

In addition to the incorporation of alkoxy side chain substituents, the most desirable design aspect of **6** is its extended π system. This linker was expected to provide a planar and rigid backbone potentially preventing dimerization and promoting long chain products. The starting material for the synthesis of **6** was hydroquinone (Scheme 2.8).



Scheme 2.8 Proposed synthesis of compound **6**

Following a modified literature protocol,²⁵ hydroquinone was first converted to *p*-octyloxybenzene via the Williamson ether synthesis with KOH and octylbromide. This long-chain functionalized benzene molecule was then bromomethylated in an acidic medium yielding 2,5-di-*n*-octyloxy-1,4-bis(bromomethyl)benzene, **7**. An Arbuzov reaction of triethoxyphosphite and **7** furnished 2,5-di-*n*-octyloxy-1,4-xylylene-bis(diethylphosphonate)-ester, **8**. Compound **8** was utilized in a Horner-Wadsworth-Emmons reaction with *p*-bromobenzaldehyde to yield the brominated polyphenylvinylene **9**.²⁶

Installation of the phosphorus substituents to **9** via lithiation was problematic due to the cold temperature (−78 °C) necessary for complete formation of the dilithiated intermediate. At reduced temperatures **9** was not appreciably soluble in THF solution, which prevented complete dilithio- species formation and yielded complex mixtures of phosphorus-containing products. Attempts to use **9** as a Grignard reagent were also unsuccessful due to the inability to cleanly install and isolate the desired bis(*N*-diethylamino)phosphine product. Poor solubility at reduced temperatures for **9** suggested that eventual dehydrocoupling products resulting from **6** would encounter similar solubility issues as observed for the previous bisphosphine substrates.

Despite the degree of conjugation present and the solubilizing effect imparted by the incorporation of alkoxy side chains, the rigidness of **6** precluded its eventual use as a substrate in phosphine dehydrocoupling catalysis. With this rationale in mind, synthetic efforts focused on the smaller, less planar substrates 1,4-bisphosphino-2,5-

bis(octyloxy)benzene, **10** and 1,4-bis(phosphinomethyl)-2,5-bis(octyloxy)benzene **11** (Figure 2.5).

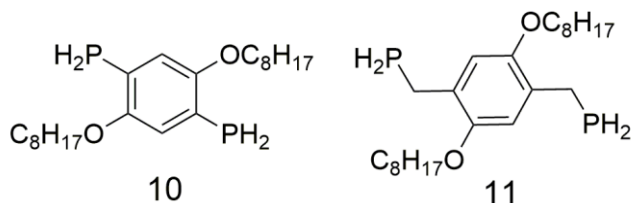
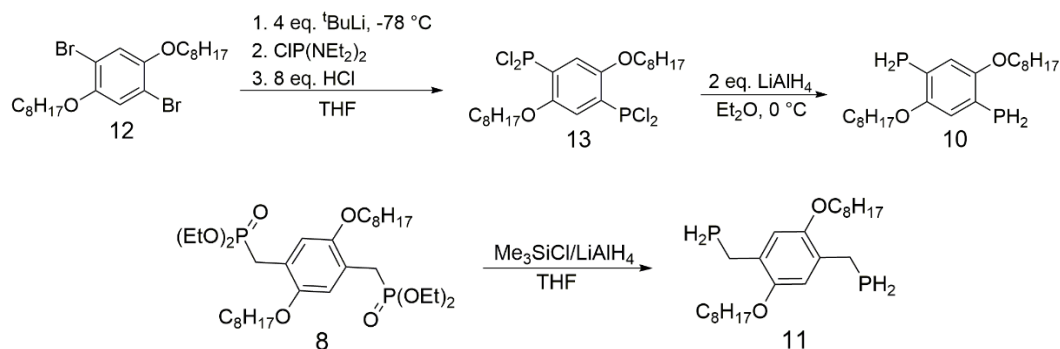


Figure 2.5 Small molecule synthetic targets for phosphine dehydrocoupling

Compounds **10** and **11** were chosen as synthetic targets because each substrate could be accessed via short synthetic routes from readily available precursors synthesized for the failed PPV molecule **6**. Initial routes to **10** utilizing *n*-BuLi as the lithium source led to considerable amounts of mono-phosphorylated products resulting from the limited solubility of the polar starting material **12** at $-78\text{ }^\circ\text{C}$.

Synthesis of **10** proved difficult because of tenacious impurities produced along the synthetic route and the need to remain under Schlenk conditions. Alternate routes based on phosphorus(V) reagents obviated the need for exclusion of air and potentially allowed for purification of products via column chromatography. To this end palladium catalyzed cross coupling, UV photo irradiation, and a nickel catalyzed Arbuzov reaction variant were attempted. All were unsuccessful in facilitating clean C–P bond formation and isolation of bisphosphine products. The presence of the octyloxy- functional groups

complicated the isolation of pure **10** as impurities were both nonvolatile and highly soluble in alkane solvents rendering sublimation and recrystallization futile.



Scheme 2.9 Final synthetic conditions for the preparation of bisphosphines **10** and **11**

The clean installation of two diethylamino phosphine groups to **12** was accomplished via lithiation using four equivalents of $t\text{BuLi}$ in THF solution. Solubility of **12** at reduced temperatures was not a concern using this source of lithium as the two additional equivalents of $t\text{BuLi}$ acted to deprotonate the two equivalents of $t\text{BuBr}$ formed *in situ*. This second lithium halogen exchange yields *tert*-butylene and LiBr as impurities, which are facile to remove. Quenching of this dilithio species with $\text{CIP}(\text{NEt}_2)_2$ as an electrophile yielded a hexane soluble intermediate. Chlorination using excess HCl in Et_2O cleanly yielded 1,4-bis(dichlorophosphino)-2,5-(bis(octyloxy)benzene, **13**. Reduction of **13** with lithium aluminum hydride yielded the desired product **10** as determined by ^1H and ^{31}P NMR spectroscopy. In stark contrast to **10**, preparation of the methylene spaced analogue **11** was straightforward and followed a modified literature

preparation using a potent reduction mixture consisting of a 1:1 molar ratio of trimethylsilyl chloride/lithium aluminum hydride (Scheme 2.9).²⁷

2.2.2. Dehydrocoupling Reactions of Second Generation Bisphosphine Substrates

Compounds **10** and **11** were used as substrates in dehydrocoupling reactions utilizing both **1** and **2** as catalysts. Treatment of **10** with 5 mol % of **1** in toluene solution resulted in a slight color change from clear to pale yellow. Refluxing this reaction for 48 hours under an N₂ atmosphere resulted in minimal (< 3%) conversion to the singly dehydrocoupled diphosphine product **14** ($\delta = d, -86.6, -89.2$ PH, -138.7 PH₂) as determined by distinct AA'BB' splitting pattern observed in proton-coupled ³¹P spectra and comparison to known diphosphine products (Figure 2.6). A second unidentified product was observable via ³¹P NMR at $\delta -59.7$, and is speculated to be the phosphido compound (N₃N)Zr-PHR based on an AB splitting pattern observed in proton-coupled ³¹P spectra.

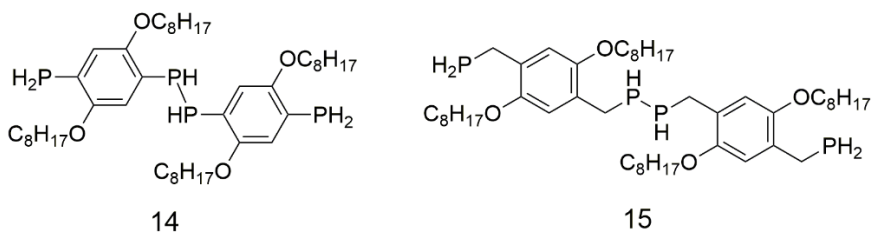


Figure 2.6 Diphosphine products produced in reactions catalyzed by **1** and **2**

Activity towards substrate **10** was not impacted in reactions catalyzed by the more active zirconocene catalyst **2** and suggested steric demands of the substrate may dominate the system. Treatment of **10** with 5 mol % of **2** in toluene solution at 90 °C resulted in H₂ evolution and a color change from clear to orange. Refluxing this reaction for 48 hours under an N₂ atmosphere resulted in minimal conversion to the diphosphine product, with no additional products present. No internal standard was used in these dehydrocoupling reactions, so exact comparisons of catalyst activity between **1** and **2** cannot be made for this substrate. Based on crude integration of ³¹P NMR resonances, reactions using bisphosphine **10** as a substrate had close to 95% starting material remaining post reaction.

To this point, all primary phosphine linkers have had phosphorus conjugated to an aromatic system. Compound **11** was the first departure from this paradigm, however the decreased steric bulk around phosphorus due to the presence of the methylene carbon in **11** encouraged activity. Treatment of **11** with 5 mol % of **1** in toluene solution resulted in immediate H₂ evolution and a color change from clear to orange. Heating this sealed reaction for one week at 90 °C with daily evacuation of the headspace resulted in the formation of new phosphine compounds. Products present in this reaction included the diphosphine, **15** (³¹P δ = d, -92.2, -95.2 PH, -127.2 PH₂) as determined by distinct AA'BB' splitting pattern observed in proton-coupled ³¹P spectra. The other predominant product after one week of reaction is currently unknown (³¹P δ = s, -60.9) but is coupled to one proton on phosphorus, and a working hypothesis for this product is the dimeric species **16** (Figure 2.7).

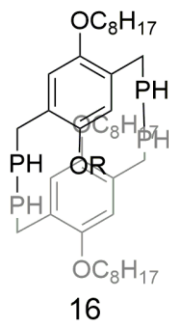


Figure 2.7 Proposed major product for unknown ^{31}P $\delta = -60.9$ s, observed in dehydrocoupling reactions catalyzed by **11**.

Other products of this reaction account for less than 1% of the total distribution, with an estimated overall conversion of 23% as determined by ^{31}P NMR spectroscopy. Due to low conversions to diphosphine products after a week of reaction time, future work utilized catalyst **2**.

Compared to the reaction catalyzed by **1**, **2** yielded a higher overall conversion over a shorter time period of 5 days with both catalysts yielding the same phosphine products (Figure 2.8). No ^{31}P NMR internal standard was added though integration of all resonances corresponded to an estimated substrate conversion of 55%.

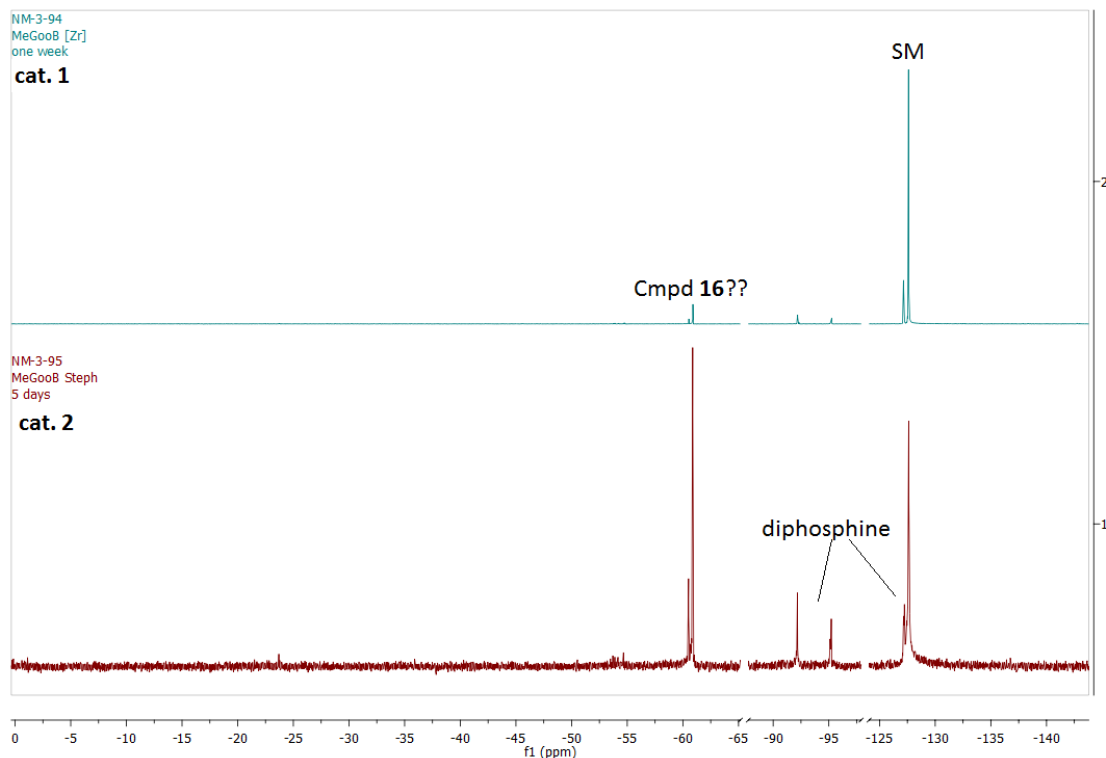


Figure 2.8 Comparison of product distributions in NMR-scale reactions highlighting the higher activity of **2** (SM= starting material)

Dehydrocoupling activity of these bulky phosphines is predominantly governed by steric considerations and these reactions are not as sensitive to efficient gaseous byproduct removal like the iridium compounds discussed in the next chapter. To facilitate substrate conversion, reactions using higher catalyst loadings of 10 mol % of **2** with **11** were run open to an N₂ manifold. Gratifyingly, after 4 days of reflux in toluene solution at 90 °C a viscous orange liquid had formed in the reaction vessel (Figure 2.9, left). Precipitation from hexanes yielded a sparingly soluble yellow powder, **17** (Figure 2.9, right).

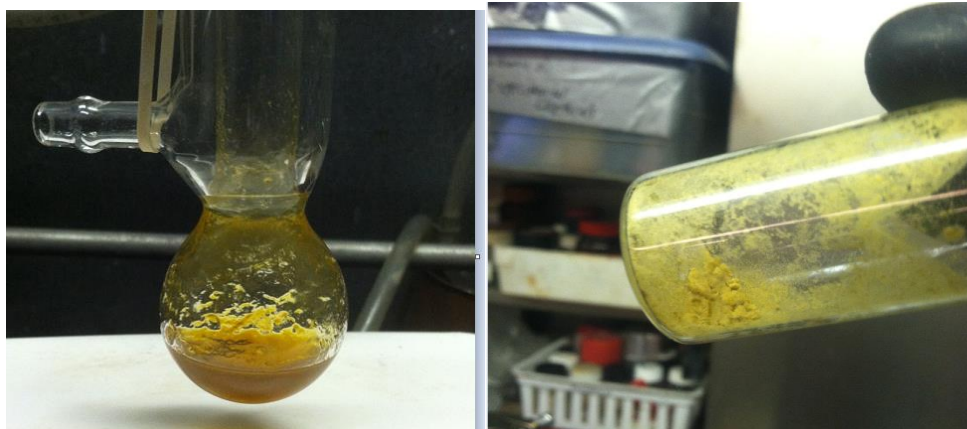


Figure 2.9 Polyphosphine material **17** in toluene solution (left) and after precipitation from hexanes (right)

Isolated, fractionated **17** was only sparingly soluble in benzene- d_6 and other laboratory solvents. The soluble portion of the sample was analyzed by ^{31}P NMR spectroscopy and revealed formation of an unknown new product (^{31}P $\delta = \text{d}, -53.7, -54.2 \text{ PH}$) in addition to the diphosphine **15**, and minor amounts of unreacted **11**. GPC was utilized to obtain molecular weight information on the benzene soluble portion of this material. Relative to polystyrene standards, two signals corresponding to modest molecular weights of 880 and 503 amu were observed. These signals likely refer to the diphosphine **15** and unreacted **11**, respectively. It is expected that the insoluble hyperbranched material **17** is of higher molecular weight than the soluble portions analyzed by solution methods.

Solid state magic angle spinning (MAS) ^{31}P NMR data was acquired for insoluble **17** to determine if signals from any additional phosphorus environments were present

(Figure 2.10). Spectral analysis shows three narrow signals with high intensity spinning sidebands $\delta = -54.4$ -60.4 , and -126.8 that correlate closely to the resonances observed in the solution phase ^{31}P NMR spectrum of **17** ($\delta = \text{d } -53.9$, $\text{d } -60.7$, and $\text{s } -127.6$). An additional broad symmetrical signal is centered at $\delta 32.2$ that presumably corresponds to the resonance of hyperbranched material. In related titanocene-catalyzed phosphine dehydrocoupling work, Harrod observed ^{31}P NMR signals in the region of $\delta 17$ – 22 and assigned these resonances to higher order oligophosphines products with P–H end groups.²⁸

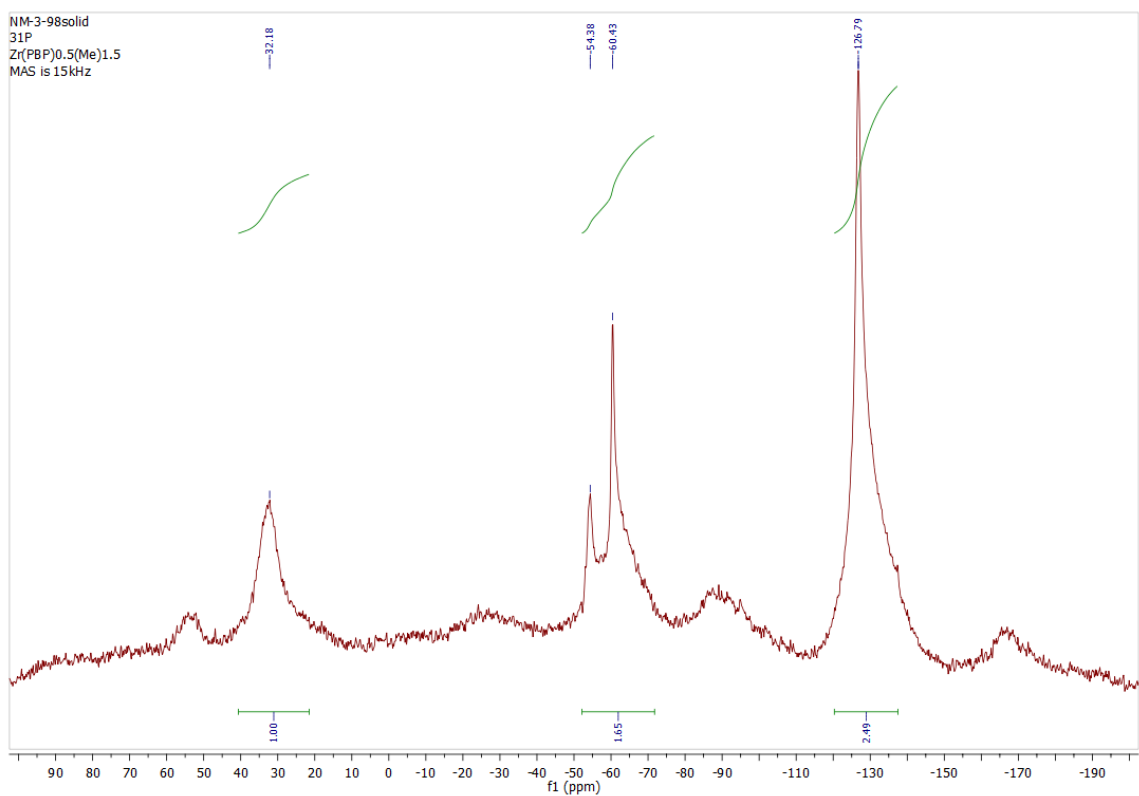


Figure 2.10 Solid-state MAS ^{31}P NMR spectrum of **17**

2.3. Conclusions

In conclusion, zirconium catalysts **1** and **2** were shown to dehydrocouple first generation primary bisphosphine substrates yielding diphosphines, oligophosphines and insoluble hyperbranched materials. Characterization efforts of these hyperbranched materials has been stunted due to the lack of effective polymer characterization methods available to solid state materials. The use of these insoluble materials as potential heavy metal ion scavengers in aqueous solutions need to be explored.

Solution based methods are necessary for molecular weight determination via GPC. The rational design of new bisphosphine linker molecules incorporating long chain alkoxy substituents to engender solubility in phosphine substrates has been accomplished. Use of the bisphosphine substrate **10** in reactions with both **1** and **2** led to poor conversions of starting material and yielded the diphosphine dehydrocoupling product **14** presumably due to steric congestion during the bond forming step in catalysis.

To diminish the steric constraints around the phosphine moiety, the bisphosphine substrate **11** containing a methylene carbon between the aryl ring and the phosphine substituent was synthesized. Catalysts **1** and **2** exhibited higher activity in reactions with **11** and converted 23% and 55% of starting material to phosphine products, respectively.

Despite the incorporation of alkoxy sidechain functional groups, the polymer resulting from **11** was still insoluble and therefore further substrate design is necessary.

The synthesis of substrates incorporating longchain alkyl or alkoxy groups remote from the phosphine substituents will be necessary for efficient dehydrocoupling activity using catalysts **1** and **2**. The work in this chapter demonstrates that through appropriate substrate design and reaction conditions, dehydrocoupling catalysis can be utilized to prepare polyphosphine materials.

2.4. Experimental Methods

General Considerations. All manipulations, unless otherwise stated, were performed under an atmosphere of dry nitrogen using Schlenk or in a M. Braun glovebox. Dry, oxygen-free solvents were employed throughout. NMR spectra were recorded on a Bruker AXR 500 MHz spectrometer where ^1H and ^{13}C NMR spectra were referenced to residual solvent resonances. ^{31}P NMR spectra were referenced to external 85% H_3PO_4 standards. Benzene- d_6 was degassed and dried over NaK alloy. Thermogravimetric analysis was performed on a Perkin-Elmer Pyris 1 DSC-TGA. Scans were performed between 25 and 800 °C at 5 °C/min. Elemental analyses were performed using an Elementar VarioMicro cube. The catalysts $(\text{N}_3\text{N})\text{Zr}$ (**1**),²⁹ and $[\text{Cp}^*\text{ZrH}_3]\text{Li}$ (**2**),³⁰ and the compounds $\text{CIP}(\text{NEt}_2)_2$,³¹ **3**,²² **8**,²⁵ and **9**²⁶ were prepared as described in the literature. GPC data was collected using a Hewlett-Packard 1100 series HPLC equipped with a refractive index detector. Samples were eluted through a Waters μ Styragel 103 Å (7.8×300 mm) column using tetrahydrofuran at a flow rate of 1 mL min^{-1} . The average

molecular weights of the polysilane samples were determined relative to five polystyrene standards obtained from Waters with molecular weights ranging from 489 to 6480 amu.

(1) Typical Procedure for NMR-scale dehydrocoupling reactions.

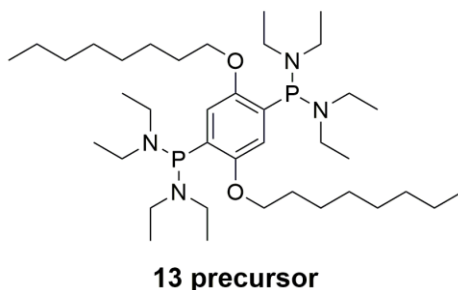
A PTFE-valved NMR tube was charged with phosphine (104.2 mg, 0.244 mmol), catalyst (12.2 μmol), and approximately 0.5 mL of benzene- d^6 . After two freeze-pump-thaw cycles, an initial ^1H NMR spectrum was collected. The yellow or orange solution was then heated for 16 hours at 90 $^\circ\text{C}$, which resulted in the solution darkening to a deep red color. After heating, ^{31}P NMR spectra were collected. Products could not be isolated due to the presence of large amounts of unreacted substrate and the low yields of mixtures of dehydrocoupling products. Final products were identified by comparison of spectral data with known products.

(2) Typical Procedure for reflux Schlenk dehydrocoupling reactions.

A Schlenk flask with an attached condenser was charged with catalyst (0.072 mmol), and (0.733 mmol, 10 equiv) **11**, where upon a color change from clear to light orange occurred. After an initial aliquot of the reaction mixture was analyzed by ^{31}P NMR, the reagents were diluted in ~2 mL toluene, and then refluxed for 16 hours under an N_2

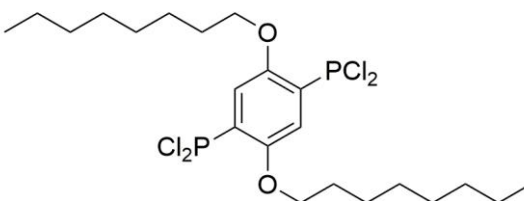
atmosphere. After cooling the reaction mixture to ambient temperature, the solution was dried under reduced pressure to afford the product as a viscous orange gel. This residue was brought up in hexane, then dried again under reduced pressure to ensure all toluene was removed. The resulting orange powder was then quickly washed with cold (-30 °C) hexanes then filtered to give a yellow-orange powder. An aliquot of this powder which was sparingly soluble in benzene-*d*₆ was then analyzed by ³¹P NMR spectroscopy.

(2) Synthesis of Second Generation Primary Phosphine Substrates



1,4-bis(diethylaminophosphino)-2,5-bis(octyloxy)benzene, precursor to 13. To a stirred solution of 1,4-dibromo-2,5-bis(octyloxy)benzene (2.41 g, 4.90 mmol) in THF (150 mL) was added ^tBuLi (12.6 mL, 1.6 M, 20.1 mmol) at -78° C over a period of 10 minutes. The reaction mixture was stirred for one hour at this temperature then was added dropwise to a stirred solution of chlorobis(diethylamino)phosphine (2.26 g, 10.7 mmol) in Et₂O (100 mL) at -78 °C. Subsequently, the reaction mixture was allowed to warm slowly to room temperature and stirred for 3 hours. The solvent was removed *in vacuo*,

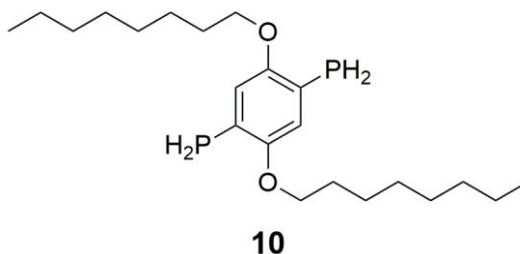
the product was extracted into hexanes (2 x 100 mL) and filtered, and the hexanes was removed in vacuo affording a white solid. Yield = 2.16 g (82.3 %). ^1H NMR (500 MHz, 25 °C, C_6D_6): δ 7.20 (t, $J = 4.6$ Hz, 2 H, Ar), 4.01 (t, $J_{\text{HH}} = 6.5$ Hz, 4 H, OCH_2), 3.23–3.10 (m, 16 H, $\text{N}[\text{CH}_2(\text{CH}_3)]_2$), 1.81 (p, 4 H, OCH_2CH_2), 1.49 (m, 4 H, CH_2), 1.32–1.26 (m, 16 H, $[\text{CH}_2]_4$), 1.15 (t, $J_{\text{HH}} = 7.1$ Hz, 24 H, CH_3), 0.90 (t, 6 H, CH_3). ^{13}C NMR (125.8 MHz, C_6D_6): δ 154.1 (d, $J_{\text{PC}} = 16.3$ Hz C_{ArOR}); 130.7 (d, $J_{\text{PC}} = 11.4$ Hz C_{Ar}); 115.5 (t, $J_{\text{PC}} = 3.5$ Hz C_{ArP}); 68.5 (s, OCR); 43.9 (d, $J_{\text{PC}} = 19.1$ Hz PNCH_2); 31.9 (s, CH_2); 29.9 (s, CH_2); 29.5 (s, CH_2); 29.4 (s, CH_2); 26.3 (s, CH_2); 22.7 (s, CH_2); 15.0 (s, PNCH_2CH_3); 14.0 (s, CH_2). ^{31}P NMR (202.5 MHz): δ 93.0 (s).



13

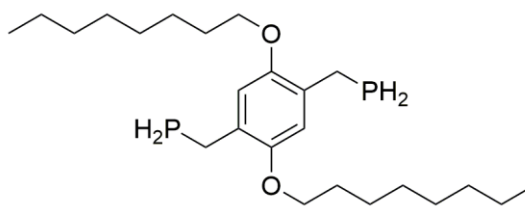
1,4-bis(dichlorophosphino)-2,5-bis(octyloxy)benzene, 13. To a stirred solution of 1,4-bis(diethylaminophosphino)-2,5-bis(octyloxy)benzene (3.71 g, 5.43 mmol) in Et_2O (100 mL) at 0 °C was slowly added a solution of 2N HCl in Et_2O (22 mL, 44 mmol). The reaction mixture was allowed to warm slowly to room temperature and stirred for 4 hours. The solvent was removed in vacuo, the product was extracted with hexanes (2 x 100 mL) then filtered, and the hexanes was removed *in vacuo* to afford a light yellow oil. Yield =

2.59 g (88.9 %). ^1H NMR (500 MHz, 25 °C, C_6D_6): δ 7.43 (t, $^3J_{\text{PH}} = 4.1$ Hz, 2 H, *Ar*), 3.59 (t, $J_{\text{HH}} = 6.3$ Hz, 4 H, OCH_2), 1.53 (p, 4 H, OCH_2CH_2), 1.32–1.24 (m, 20 H, $[\text{CH}_2]_5$), 0.93 (t, $J_{\text{HH}} = 7.0$ Hz, 6 H, CH_3). ^{13}C NMR (125.8 MHz, C_6D_6): ^{13}C NMR (125.8 MHz, C_6D_6): δ 154.5 (d, $J_{\text{PC}} = 21.1$ Hz C_{ArOR}); 133.1 (dd, $J_{\text{PC}} = 63.0$ Hz, $J_{\text{PH}} = 2.3$ Hz C_{Ar}); 113.4 (d, $J_{\text{PC}} = 3.3$ Hz C_{ArP}); 69.5 (s, OCR); 31.8 (s, CH_2); 29.2 (s, $2 \times \text{CH}_2$); 28.9 (s, CH_2); 25.9 (s, CH_2); 22.7 (s, CH_2); 14.0 (s, CH_3). ^{31}P NMR (202.5 MHz): δ 157.3 (s).



1,4-bis(phosphino)-2,5-bis(octyloxy)benzene, 10. To a cooled (-78 °C) suspension of LiAlH_4 (0.4 g, 10.5 mmol) in Et_2O (100 mL) was added dropwise a solution of **13** (1.24 g, 2.31 mmol) in Et_2O (60 mL). After the addition was complete, the reaction was allowed to warm to room temperature and stirred overnight. Degassed water (ca. 50 mL) was added to quench excess LiAlH_4 . The Et_2O layer was separated and the aqueous layer was extracted with a further 100 mL of Et_2O . The organic layers were combined, dried with MgSO_4 , filtered, then the ether was removed *in vacuo* to afford a powdery white solid. Yield = 0.83 g (90.2 %). ^1H NMR (500 MHz, 25 °C, C_6D_6): δ 6.84 (dd, $J_{\text{PH}} = 7.0$ Hz, $J_{\text{PH}} = 3.4$ Hz 2 H, *Ar*), 3.98 (d, $J_{\text{PH}} = 202.2$ Hz, 4 H, PH_2), 3.58 (t, $J_{\text{HH}} = 6.4$ Hz, 4 H,

OCH₂), 1.62 (p, 4 H, OCH₂CH₂), 1.39 (m, 4 H, CH₂), 1.31–1.24 (m, 16 H, [CH₂]₄), 0.92 (t, $J_{\text{HH}} = 7.1$ Hz 6 H, CH₃). ¹³C NMR (125.8 MHz, C₆D₆): δ 154.2 (dd, $J_{\text{PC}} = 7.2$ Hz, $J_{\text{CH}} = 4.6$ Hz C_{Ar}OR); 118.0 (d, $J_{\text{PC}} = 11.9$ Hz C_{Ar}); 115.4 (s, C_{Ar}P); 68.7 (s, OCR); 31.9 (s, CH₂); 29.3 (s, 3 \times CH₂); 26.1 (s, CH₂); 22.7 (s, CH₂); 14.0 (s, CH₃). ³¹P NMR (202.5 MHz): δ -139.0 (s).



11

1,4-bis(methylenephosphino)-2,5-bis(octyloxy)benzene, 11. Trimethylsilyl chloride (3.85 g, 35.4 mmol) was added to a stirred solution of lithium aluminum hydride (1.36 g, 35.8 mmol) in THF (100 mL) at -78 °C. The resulting mixture was allowed to warm to room temperature and stirred for 2 h. The reducing mixture was re-cooled to -78 °C, then a solution of **8** (3.55 g, 5.6 mmol) in THF (60 mL) was added. The resulting mixture was allowed to warm to room temperature and stirred for 36 h. THF was removed *in vacuo* and Et₂O was added to re-dissolve the pale suspension. Degassed water (ca. 50 mL) was added to quench excess reductants. The Et₂O layer was separated and the aqueous layer was extracted with a further 100 mL of Et₂O. The organic layers were combined, dried with MgSO₄, filtered, then the ether was removed *in vacuo* to afford a

powdery white solid. Yield = 1.98 g (83.2 %). ^1H NMR (500 MHz, 25 °C, C_6D_6): δ 6.56 (s, 2 H, Ar), 3.68 (t, $J_{\text{HH}} = 6.4$ Hz, 4 H, OCH_2), 3.07 (dt, $J_{\text{PH}} = 214.7$ Hz, $J_{\text{HH}} = 6.9$ Hz 4 H, PH_2), 2.90–2.83 (m, 4 H, PCH_2Ar), 1.67 (p, 4 H, CH_2), 1.41 (m, 4 H, CH_2), 1.32–1.28 (m, 16 H, $[\text{CH}_2]_4$), 0.92 (t, $J_{\text{HH}} = 6.9$ Hz 6 H, CH_3). ^{13}C NMR (125.8 MHz, C_6D_6): δ 150.2 (s, C_{ArOR}); 129.7 (s, C_{Ar}); 113.2 (s, C_{ArMeP}); 68.7 (s, OCR); 32.2 (s, CH_2); 30.0 (s, CH_2); 29.8 (s, $2 \times \text{CH}_2$) 26.7 (s, CH_2); 23.1 (s, CH_2); 15.7 (d, $J_{\text{PC}} = 11.0$ Hz $\text{PH}_2\text{CH}_2\text{Ar}$); 14.4 (s, CH_3). ^{31}P NMR (202.5 MHz): δ -127.6(s).

2.5. References

- (1) Baumgartner, T.; Réau, R. *Chem. Rev.* **2006**, *106*, 4681.
- (2) Dillon, K. B. *Phosphorus : the carbon copy : from organophosphorus to phospho-organic chemistry*; John Wiley: New York, 1998.
- (3) Cabelli, D. E.; Cowley, A. H.; Dewar, M. J. S. *J. Am. Chem. Soc.* **1981**, *103*, 3286.
- (4) Lucht, B. L.; St. Onge, N. O. *Chem. Commun.* **2000**, 2097.
- (5) Kanbara, T.; Takase, S.; Izumi, K.; Kagaya, S.; Hasegawa, K. *Macromolecules* **2000**, *33*, 657.
- (6) Gauvin, F.; Harrod, J. F.; Woo, H. G. *Adv. Organomet. Chem.* **1998**, *42*, 363.
- (7) Manners, I. *Angew. Chem. Int. Ed.* **1996**, *27*, 1602.

- (8) Manners, I. J. *Polym. Sci., Part A: Polym. Chem.* **2002**, *40*, 179.
- (9) Waterman, R. *Cur. Org. Chem.* **2008**, *12*, 1322.
- (10) Fermin, M. C.; Stephan, D. W. *J. Am. Chem. Soc.* **1995**, *117*, 12645.
- (11) Masuda, J. D.; Hoskin, A. J.; Graham, T. W.; Beddie, C.; Fermin, M. C.; Etkin, N.; Stephan, D. W. *Chem. Eur. J.* **2006**, *12*, 8696.
- (12) Greenberg, S.; Stephan, D. W. *Chem. Soc. Rev.* **2008**, *37*, 1482.
- (13) Waterman, R. *Organometallics* **2007**, *26*, 2492.
- (14) Roering, A. J.; Maddox, A. F.; Elrod, L. T.; Chan, S. M.; Ghebreab, M. B.; Donovan, K. L.; Davidson, J. J.; Hughes, R. P.; Shalumova, T.; MacMillan, S. N.; Tanski, J. M.; Waterman, R. *Organometallics* **2008**, *28*, 573.
- (15) Roering, A. J.; Leshinski, S. E.; Chan, S. M.; Shalumova, T.; MacMillan, S. N.; Tanski, J. M.; Waterman, R. *Organometallics* **2010**, *29*, 2557.
- (16) Ghebreab, M. B.; Bange, C. A.; Waterman, R. *J. Am. Chem. Soc.* **2014**, *136*, 9240.
- (17) Roering, A. J.; Davidson, J. J.; MacMillan, S. N.; Tanski, J. M.; Waterman, R. *Dalton Trans.* **2008**, 4488.
- (18) McWilliams, A.; Dorn, H.; Manners, I. *Top. Curr. Chem.* **2002**, *220*, 141.
- (19) Imori, T.; Woo, H. G.; Walzer, J. F.; Tilley, T. D. *Chem. Mater.* **1993**, *5*, 1487.
- (20) Etkin, N.; Fermin, M. C.; Stephan, D. W. *J. Am. Chem. Soc.* **1997**, *119*, 2954.

- (21) Ghebreab, M. B.; Shalumova, T.; Tanski, J. M.; Waterman, R. *Polyhedron* **2010**, *29*, 42.
- (22) Reiter, S. A.; Nogai, S. D.; Schmidbaur, H. *Dalton Trans.* **2005**, 247.
- (23) Ghebreab, M. B. Ph.D. Thesis, University of Vermont, 2013.
- (24) Smith, R. C.; Protasiewicz, J. D. *J. Am. Chem. Soc.* **2004**, *126*, 2268.
- (25) Drury, A.; Maier, S.; Ruther, M.; Blau, W. J. *J. Mater. Chem.* **2003**, *13*, 485.
- (26) Jiu, T.; Li, Y.; Liu, H.; Ye, J.; Liu, X.; Jiang, L.; Yuan, M.; Li, J.; Li, C.; Wang, S.; Zhu, D. *Tetrahedron* **2007**, *63*, 3168.
- (27) Kyba, E. P.; Liu, S. T.; Harris, R. L. *Organometallics* **1983**, *2*, 1877.
- (28) Xin, S.; Woo, H. G.; Harrod, J. F.; Samuel, E.; Lebuis, A.-M. *J. Am. Chem. Soc.* **1997**, *119*, 5307.
- (29) Roering, A. J.; Maddox, A. F.; Elrod, L. T.; Chan, S. M.; Ghebreab, M. B.; Donovan, K. L.; Davidson, J. J.; Hughes, R. P.; Shalumova, T.; MacMillan, S. N.; Tanski, J. M.; Waterman, R. *Organometallics* **2009**, *28*, 573.
- (30) Etkin, N.; Hoskin, A. J.; Stephan, D. W. *J. Am. Chem. Soc.* **1997**, *119*, 11420.
- (31) Gillon, B. H.; Noonan, K. J. T.; Feldscher, B.; Wissensz, J. M.; Kam, Z. M.; Hsieh, T.; Kingsley, J. J.; Bates, J. I.; Gates, D. P. *Can. J. Chem.* **2007**, *85*, 1045.

CHAPTER 3: IRIIDIUM–CATALYZED SILANE DEHYDROCOUPLING: LIGAND EFFECTS ON PRODUCT SELECTIVITY

3.1. Introduction

Polysilanes have received considerable attention for material applications owing to their electronic properties, which primarily result from σ electron conjugation. In industry, their preparation still relies on Würtz-type coupling methods because high molecular weight polysilanes can be produced by this method. Despite this coupling ability, the harsh reaction conditions and difficulties associated with product isolation limit the substrates that can undergo this process.¹⁻³

Dehydrocoupling is an attractive alternative method where a metal reacts with two E–H bonds catalyzing E–E bond formation with concomitant elimination of H₂ gas (Section 1.5).⁴ Group 4 metallocene compounds are well studied and have shown the most promise for this process, but the polysilanes that these catalysts yield are too low molecular weight to be useful in material applications. Hence after nearly forty years of study, polysilanes are still not primarily prepared via dehydrocoupling catalysis.

The development of late transition-metal catalysts for Si dehydrocoupling has lagged behind that of early metals because of the initial observance of low activity and the side reactions that they also catalyze. Platinum group metals have been the most

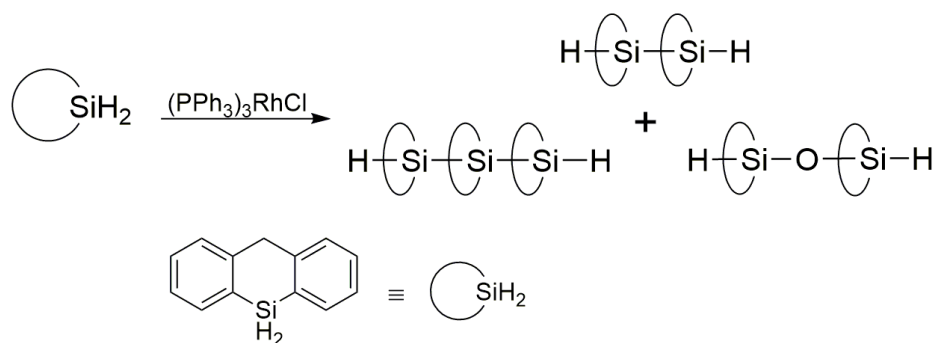
commonly studied for silane dehydrocoupling catalysis though these metals can also catalyze the competing side reactions of silane redistribution and oxidation of Si-Si bonds depending on reaction conditions.^{4,5}

Redistribution at silicon and Si-O cross dehydrocoupling (catalytic siloxane formation) are two of the most problematic side reactions that are commonly observed in late-metal catalyzed reactions. These side reactions have not been observed with group 4 metallocenes.⁴ The high activities exhibited by platinum group metals, specifically iridium and rhodium, towards facilitating these side reactions underlines a main challenge in organometallic catalysis: namely, what parameters facilitate or mitigate these side reactions and can appropriate ligands or metal choice selectively deactivate these alternate pathways?

Brown-Wensely's work has shown that Wilkinson's catalyst is an active late metal compound for silane dehydrocoupling (Section 1.7.2).⁶ In addition to dehydrocoupling, products from resulting from silane disproportionation and the oxidation of Si-Si bonds have also been reported using this catalyst.^{7,8} Silane coupling and redistribution activity are highly dependent on the steric demands of the substrate. In reactions of Wilkinson's catalyst with secondary silanes, the use of PhMeSiH₂ yielded trisilane while Ph₂SiH₂ only formed disilane products, in addition to redistribution products present for both substrates.⁷

Researchers have attempted to minimize undesirable side reactions using a variety of clever techniques. Corey and coworkers designed a clever substrate that prevented redistribution through the fusion of the two phenyl groups of Ph₂SiH₂ together

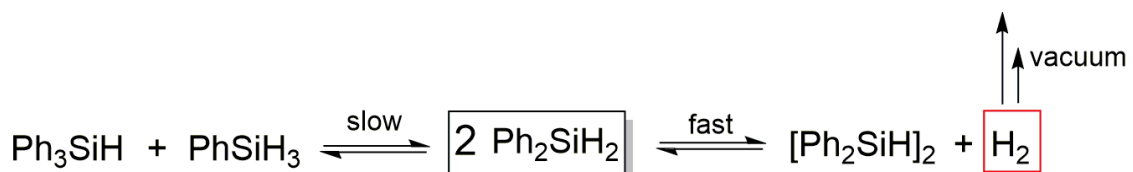
ortho to silicon.^{9,10} Treatment of this silanthracene substrate 9,10-dihydro-9-silanthracene, yielded high substrate conversions to a mixture of di- and trisilane products (Scheme 3.1). Catalyst removal required the use of silica gel and during this purification process the authors observed siloxane formation resulting from residual catalyst reacting with oligosilane products during column chromatography. Therefore, thorough substrate design can solicit dehydrocoupling products over redistribution and a purification process with rigorous exclusion of moisture and air are necessary to avoid siloxane product formation.



Scheme 3.1 Dehydrocoupling of a silanthracene

Rosenberg and coworkers have also studied Wilkinson's catalyst for silane dehydrocoupling.^{11,12} In a preliminary 2001 communication, they described results indicating that Wilkinson's catalyst is highly active for silane dehydrocoupling, though not thermodynamically favored. Rosenberg reported catalytic redistribution of the Ph groups in Ph_2SiH_2 which was not observed in reactions where efficient H_2 removal

occurred. Under dynamic vacuum, treatment of Ph_2SiH_2 with 0.2 mol % of catalyst instead resulted in quantitative conversion to the disilane product $[\text{Ph}_2\text{SiH}]_2$ in two hours reaction time at ambient temperature (Scheme 3.2).



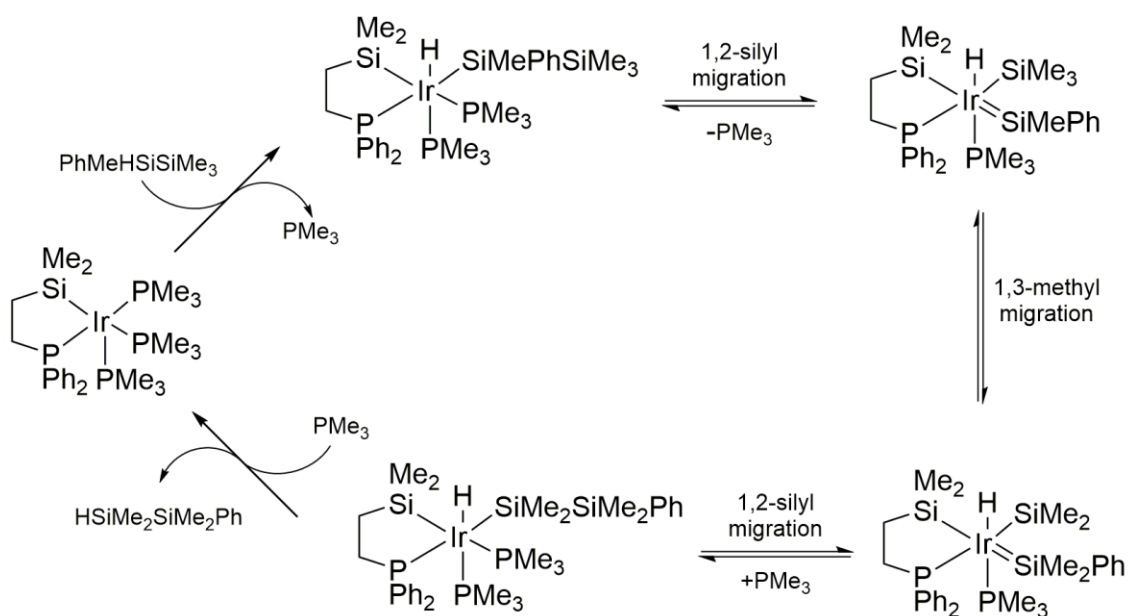
Scheme 3.2 The use of dynamic vacuum to selectively yield dehydrocoupling products

This catalysis represented a dramatic improvement in activity with a measured turnover frequency (TOF) of 240 h^{-1} , compared to a TOF of $\sim 3 \text{ h}^{-1}$ in a titanocene-catalyzed process using the same substrate.¹³ Rosenberg and coworkers have also used this strategy to effectively dehydrocouple alkylsilanes.¹² Using *n*-octyl SiH_3 ($\text{C}_8\text{H}_{17}\text{SiH}_3$) and *n*-dodecyl SiH_3 ($\text{C}_{12}\text{H}_{25}\text{SiH}_3$) this method produced polysilanes with GPC-determined molecular weights in the range of 97–2184 amu and 318–3435 amu, respectively.¹²

Rosenberg has also conducted mechanistic studies on this rhodium-catalyzed dehydrocoupling reaction. Using *in situ* electrospray ionization mass spectrometry (ESI-MS), trace amounts ($\leq 1 \%$) of a rhodium-silylene species $(\text{Ph}_3\text{P})_2\text{Rh}(\text{H})=\text{SiPh}_2$ was detected. In Rosenberg's proposed mechanism, this compound could liberate a low-valent “ $\cdot\text{SiPh}_2$ ” fragment which could condense with other silanes present resulting in Si–Si bond formation.

Iridium silylene compounds of the type $L_nIr=SiR_2$ have long been implicated as intermediates in silane redistribution reactions.^{5,14-16} The major basis for this claim lies in the fact that several platinum group base-free silylene compounds have been characterized and isolated.^{17,18}

Ogino reported that a silyl iridium(I) compound $Ir[\eta^2-Me_2Si(CH_2)_2](PMe_3)_3$ catalyzed the redistribution of methyl groups in $HPhMeSi-SiMe_3$, yielding a 2:3 ratio of the starting disilane and $HMe_2Si-SiMe_2Ph$, respectively. Ogino proposed this product distribution could arise from a mechanism consisting of reversible formation of an iridium silylene intermediate, 1,2-silyl shifts, and migratory 1,3-methyl shifts (Scheme 3.3).



Scheme 3.3 Ogino's proposed redistribution mechanism based on silylene formation

Iridium pincer compounds are powerful dehydrogenation catalysts.¹⁹ As dehydrocoupling is a type of dehydrogenation reaction, the Waterman group sought to explore these pincer compounds for potential silane dehydrocoupling activity.

Preliminary results obtained by Dr. Anthony Wetherby, a former researcher in the Waterman group, indicated that reaction of PhSiH₃ with 0.8 mol % of the iridium(III) compound *t*Bu(POCOP)IrHCl *t*Bu(POCOP) = 2,6-(^tBu₂PO)₂C₆H₃ completely consumed the substrate and yielded predominantly one product. The initial product was proposed as the cyclodecasilane (PhSiH)₁₀ based on ¹H NMR spectroscopy data consistent with a cyclic silane and GPC data which suggested a molecular weight of 972 amu relative to polystyrene standards.

Thus, the initial goal of my research was to determine what parameters determined the observed high selectivity for ring formation in reactions catalyzed by this iridium pincer compound. However, what ultimately became of this project and presented in this chapter is a deeper general discussion on iridium-catalyzed silane dehydrocoupling. Iridium pincer compounds can be used as effective silane dehydrocoupling catalysts provided that reaction conditions and ligand design are carefully selected. Reaction parameters and design considerations that enhance catalyst selectivity for dehydrocoupling over redistribution products are described.

3.2. Results

The goal of this study was to determine what factors determine product selectivity in silane dehydrocoupling reactions using POCOP iridium compounds. Both steric and electronic effects of the ligand could potentially modulate the activity and selectivity in catalytic reactions with silanes. Therefore, the following $p\text{-X}^R(\text{POCOP})\text{IrHCl}$ (POCOP) = 2,6-(R₂PO)₂C₆H₃ R = *i*Pr, X = H (**18**); R = *t*Bu, X = COOMe (**19**); = H (**20**); = NMe₂ (**21**) compounds were chosen for this study. Steric factors of the POCOP ligand could be evaluated through comparison of reactions of compounds **18** and **20** while electronic effects could be studied through comparison of reactions of compounds **19** and **21** (Figure 3.1).

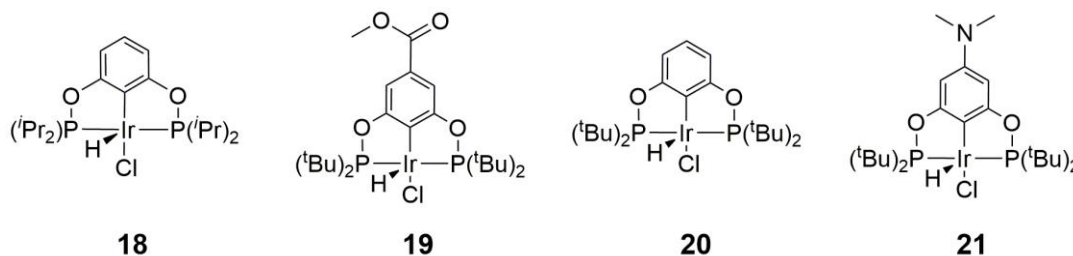


Figure 3.1 The four pincer compounds chosen for silane dehydrocoupling studies

3.2.1. Synthesis and Characterization of Pincer Compounds

The synthesis of **20** has been previously reported by Brookhart.²⁰ The remaining $p\text{-X}^{tBu}(\text{POCOP})\text{IrHCl}$ compounds **19** and **21** were readily prepared by heating the

appropriate ligand with $[(\text{COD})\text{IrCl}]_2$ (COD = 1,5-cyclooctadiene) in toluene at reflux under an inert atmosphere. The apical hydride ligand on these pincer compounds results from the insertion of iridium into the sp^2 C–H bond of the ligand backbone. After washing with cold pentane and subsequent filtration, compounds **19** and **21** were isolated in 88 % and 81 % yields. The slightly lower isolated yield of **21** relative to **19** is attributed to the greater solubility of **21** in pentane.

By analogy to **19-21**, efforts to prepare the ^iPr analogue **18** via Brookhart's method were unsuccessful. A literature preparation²¹ for **18** using an iridium source with more labile ligands $[(\text{COE})_2\text{IrCl}]_2$ (COE = *cis*-cyclooctene) was also unsuccessful and instead yielded a mixture of products including **18** in low yield (ca. 10 %, ^{31}P δ = 173.0). The major product of this reaction was tentatively proposed as the chloro-bridged dimer, $[\text{}^i\text{Pr}(\text{POCOP})\text{IrH}(\mu\text{-Cl})]_2$ (Figure 3.2). A closely related chloro-bridging compound ${}^i\text{Pr}(\text{POCOP})\text{IrH}(\mu\text{-Cl})_2\text{Ir}(\text{COE})_2$ ²² has diagnostic NMR resonances (^{31}P δ = 153.4; Ir–H δ = -24.0) that mirror those of the major product of the reaction (^{31}P δ = 153.0; Ir–H δ = -25.1).

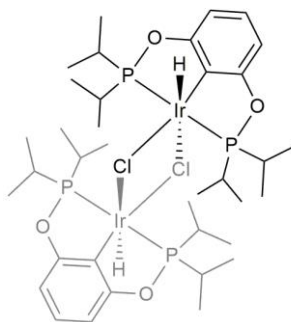


Figure 3.2 Proposed chloro-bridged dimeric compound from initial attempts at preparing ${}^i\text{Pr}(\text{POCOP})\text{IrHCl}$, **18**

Successful preparation of analytically pure **18** was accomplished by refluxing a toluene solution of [(COE)₂IrCl]₂ and ^{iPr}(POCOP) ligand for 16 hours under an H₂ atmosphere. Compounds **18**, **19**, and **21** were characterized by multinuclear NMR, combustion analysis, and single crystal X-ray diffraction.

Like related POCOP nickel compounds with substituted pincer aryl backbones,²³ the values of ³¹P NMR resonances for **18–21** fall into a narrow range. There is no apparent correlation between the identity of the substituent para to iridium and the ³¹P NMR chemical shifts values observed for **18–21**. The hydride chemical shift of compounds **19–21** are in a narrow range with **19** displaying the most downfield shift and **21** the most upfield shift (Table 3.1). For compound **18**, the hydride resonance is broadened to a singlet and shifted downfield to δ –36.7. This difference in chemical shift is consistent with the ligand environment of **18**, which possesses the less electron rich ^{iPr} phosphine ligand relative to the ^tBu phosphine substituents employed in **19** and **21**. These diagnostic resonances compare favorably to *p*-H^{tBu}(POCOP)IrHCl (**20**), reported by Brookhart and coworkers (Table 3.1).²⁴

Table 3.1 Diagnostic NMR data (δ) for compounds **18–21** in benzene-*d*₆ solution.

Compound	Ir–H ¹ H NMR	³¹ P NMR
^{iPr} [Ir], 18	-36.7	173.0
<i>p</i> -COOMe ^{tBu} [Ir], 19	-40.1, ² J _{PH} = 12.9	176.5
<i>p</i> -H ^{tBu} [Ir], 20	-40.7, ² J _{PH} = 13.1	175.3
<i>p</i> -NMe ₂ ^{tBu} [Ir], 21	-41.1, ² J _{PH} = 13.3	176.3

[Ir] = (POCOP)IrHCl

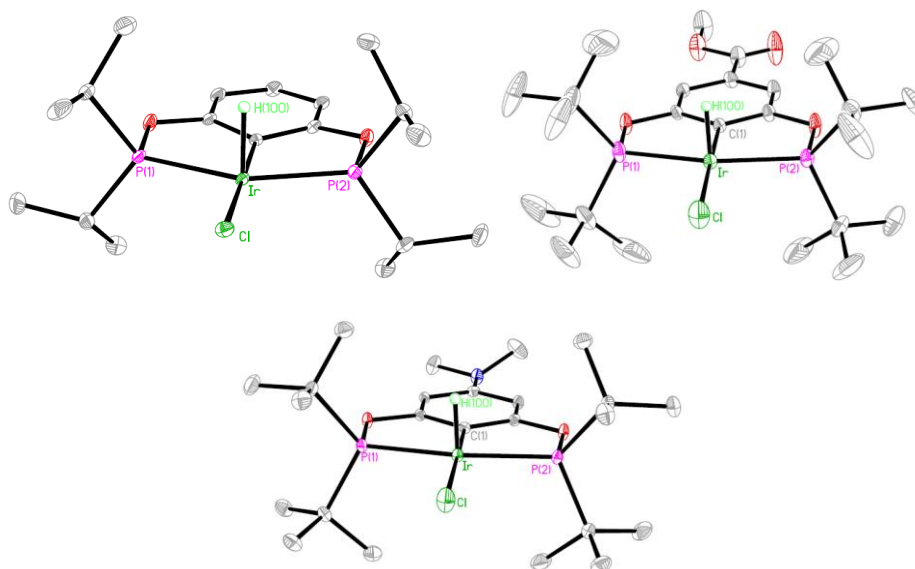


Figure 3.3 Molecular structure of **18**, **19**, and **21** (clockwise from top left) with thermal ellipsoids drawn at the 30% probability level. Hydrogen atoms, except the hydride located on iridium, are omitted for clarity

Crystals were grown for compounds **18**, **19**, and **21** and subjected to single crystal X-ray diffraction studies (Figure 3.3). To quantitatively describe the geometries of **18**–**21** the parameter τ was utilized, where a perfect trigonal bipyramid displays a value of 1.00 and a perfect square pyramid displays a value of 0.00.²⁵ The compounds are square-based pyramidal at iridium as demonstrated by calculated τ values of 0.10, 0.02, and 0.08 for **18**, **19**, and **21**, respectively. The hydride ligand was located for all three compounds from the Fourier difference map. Additional evidence for the location of this ligand comes from the less than linear P(1)–Ir–P(2) and C(1)–Ir–Cl angles, which suggest the presence of an apical ligand with small steric requirements (Table 3.2).²⁶ There is no apparent structural difference between compounds **19**, **20**, and **21** to suggest a significant

trend based on the para substitution. Compound **18** is isostructural with the *tert*-butyl analogs, though it has a substantially longer Ir–Cl bond (Table 3.2).

Table 3.2 Select bond lengths (Å) and angles (deg) for compounds **18–21**

	<i>ipr</i> [Ir], 18	<i>p</i> -COOMe ^{<i>t</i>Bu} [Ir], 19	<i>p</i> -H ^{<i>t</i>Bu} [Ir] ²⁷ , 20	<i>p</i> -NMe ₂ ^{<i>t</i>Bu} [Ir], 21
Ir–C(1)	2.033(5)	1.992(4)	2.000(3)	1.996(3)
Ir–P(1)	2.2994(14)	2.2871(13)	2.2897(10)	2.2890(8)
Ir–P(2)	2.2977(14)	2.2864(13)	2.2925(11)	2.2940(8)
Ir–Cl	2.5501(13)	2.3933(13)	2.3947(12)	2.3954(8)
P(1)–Ir–P(2)	156.79(5)	160.37(4)	159.90(4)	159.79(3)
C(1)–Ir–Cl(1)	176.26(13)	177.69(14)	179.50(11)	176.33(9)

[Ir] = (POCOP)IrHCl. Data for **20** is reproduced from Wendt and coworkers.²⁷

3.2.2. Sealed NMR-Scale Reactions with PhSiH₃ and Catalytic Siloxane Formation

To determine the effect of the POCOP ligand substituents on the activity and product distributions of these reactions, PhSiH₃ was used as a model substrate. In initial screening, PhSiH₃ was treated with 2 mol % of each catalyst **18–21** with C₆D₆ as solvent in J-young NMR tube scale reactions. These solutions were degassed via one freeze-pump-thaw cycle, heated overnight at 120 °C then analyzed via ¹H NMR. Trace amounts of PhSiH₂Cl (¹H NMR δ = 5.05) were observed by ¹H NMR spectroscopy. It is therefore presumed that **18–21** undergo ligand exchange to the respective iridium dihydride species, (POCOP)Ir(H)₂, of which *p*-H^{*t*Bu}(POCOP)Ir(H)₂ is known.²⁸

Results from these reactions appeared to support the initial observations by Dr. Wetherby. Using this higher catalyst loading of 2 mol %, not only was the dominant “cyclosilane” product at $\delta = 5.08$ present, but additional dehydrocoupling products were also observed as determined by ^1H NMR spectroscopy. In reactions with ^tBu -substituted **19–21**, silane dehydrocoupling is favored and evident by the presence of 1,2-diphenyldisilane (PhSiH_2)₂, H_2 , linear oligosilanes with ^1H NMR resonances in the range $\delta = 4.3\text{--}4.8$, and cyclic oligomers with resonances in the range $\delta = 5.2\text{--}5.5$. However in addition to dehydrocoupling products, signals due to Ph_2SiH_2 and SiH_4 are also present in the ^1H NMR spectra, demonstrating competitive silane redistribution.

The observance of silane redistribution as a competitive side reaction was confirmed in reactions with ^iPr -substituted **18**. Compound **18** favored redistribution of PhSiH_3 over dehydrocoupling and yielded Ph_2SiH_2 (73%) as the main product of the reaction with Ph_3SiH (4%) present as well. It is worthwhile to note that these product percentages are based on normalized integration of Si–H resonances post reaction and only reflect the post-reaction product distributions of these reactions. Trace amounts of dehydrocoupling products including, $(\text{PhSiH}_2)_2$, $(\text{Ph}_2\text{SiH})_2$, and $\text{PhSiH}_2\text{--SiPh}_3$, were detected and suggest that **18** may engage in dehydrocoupling catalysis under alternate reaction conditions

To confirm the identities of these silane products, DEPT ^{29}Si NMR ($\theta = 90^\circ$, 135°) spectroscopy was utilized to determine the number of hydrogen atoms per silicon atom.^{29,30} The use of this technique had shown the resonance (^1H $\delta = 5.08$, ^{29}Si $\delta = -33.6$) we previously assigned as $(\text{PhSiH})_{10}$ corresponded to a molecule that had two protons on

the silicon atom. Furthermore, the ^1H NMR shift we attributed to the decasilane corresponded instead to the Si–H shift of the redistribution product Ph_2SiH_2 . The resonance for the silyl protons ($\delta = 5.08$) is a singlet and falls within the range usually seen for cyclic silane products, which when coupled with GPC data suggesting a molecular weight of 972 amu, supported the assignment of the product as $(\text{PhSiH})_{10}$.

The initial cyclosilane product assignment was incorrect, but the question remained as to why the GPC data obtained repeatedly suggested a MW of ~ 950 amu for these silane products. To determine whether any post injection modifications to the silane products had occurred on-column, several replicate GPC injections were made and the post-column eluent was collected. Analysis of the post-column eluent via ^1H NMR showed several new resonances in the region of $\delta = 5.0\text{--}5.6$ due to siloxane formation.

Catalyst removal from these reactions was accomplished by passing the reaction products down a florisil column eluted with toluene. Further work centered on effective catalyst removal using different column eluents was performed. By subjecting both toluene and pentane eluted components of the same silane products to GPC analysis, it was determined that the use of toluene as the sole eluent did not remove all of the catalyst from the reaction mixture. It is hypothesized that this Si–O catalysis arose through the reaction of residual amounts of catalyst **20** in GPC samples with adventitious water present in the THF mobile phase used for chromatographic analysis.

To confirm this hypothesis, reactions were done using **20** as a potential catalyst for Si–O bond formation. Immediately upon addition of H_2O to a solution of 2 mol % of **20** and PhSiH_3 in THF, vigorous evolution of H_2 gas was observed. Refluxing this

solution overnight yielded a clear oil. Product analysis via ^1H NMR spectroscopy showed the dominant Si–H containing product was the siloxane $(\text{Ph}_2\text{SiH})_2\text{O}$. Additional unidentified products with signals in a relatively narrow region from $\delta = 5.2$ – 5.9 were also present (Figure 3.4).

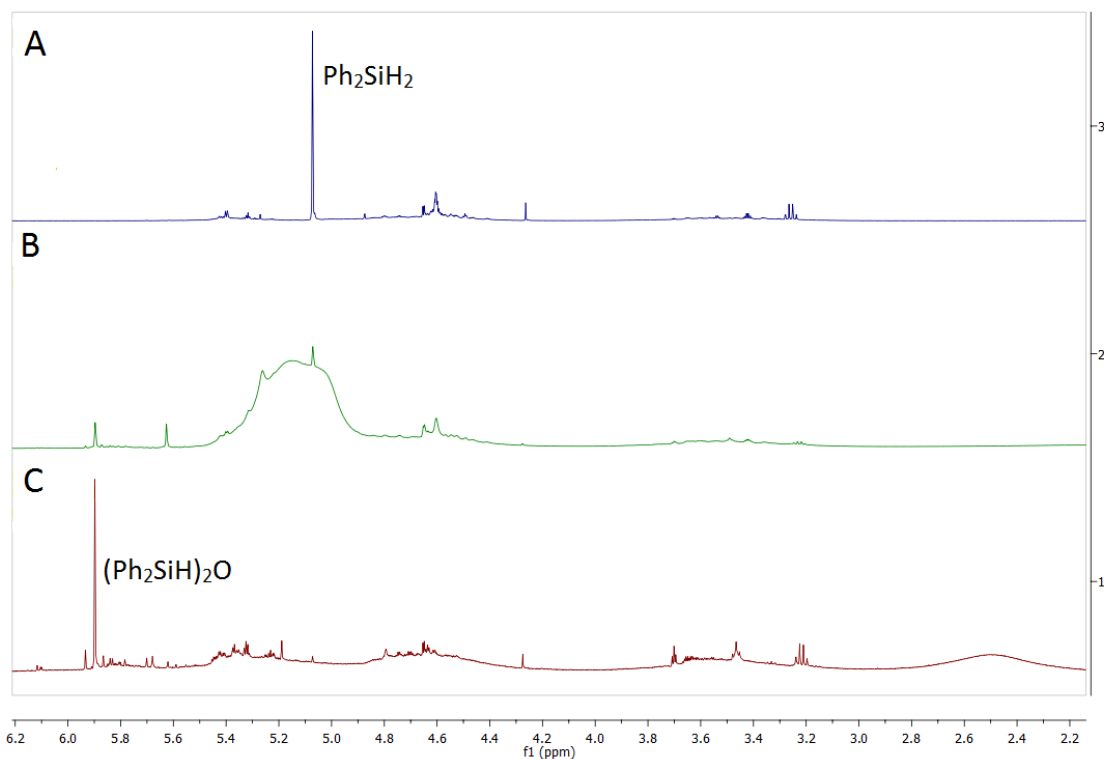


Figure 3.4 ^1H NMR spectra in benzene- d_6 solution of 16 hour reactions of **20** with PhSiH_3 at ambient temperature: (A) No added H_2O (B) One hour after H_2O addition (C) 16 hours after H_2O addition

Analysis of these siloxanes via GPC showed the presence of products with a narrow molecular weight distribution of 722–926 amu relative to polystyrene standards.

bulkier ^tBu derivatives are less active and require >12 hours of reaction time to reach completion, but these compounds favor dehydrocoupling products over redistribution (Table 3.3).

Table 3.3 Product distributions of NMR tube scale reactions of PhSiH₃ with catalytic **18–21**

Compound.	Conversion ^a (%)	Products ^a	
		Redistribution	Dehydrocoupling
<i>ipr</i> [Ir], 18 ^b	97	83	13
<i>p</i> -COOMe ^{<i>t</i>Bu} [Ir], 19	75	5	70
<i>p</i> -H ^{<i>t</i>Bu} [Ir], 20	83	18	65
<i>p</i> -NMe ₂ ^{<i>t</i>Bu} [Ir], 21	86	37	49

Reaction conditions: 2 mol% [Ir], 120 °C, 16 hours. ^a Measured by ¹H NMR spectroscopy with respect to an internal standard of C₆Me₆. ^b Trace (Ph₂SiH)O (≤1%) was observed in this reaction

Among the series of compounds screened, the relative amount of dehydrocoupling versus redistribution in the product distribution was affected by the substituents para to iridium more than the conversion. Each of the three ^tBu phosphine compounds (**19–21**) converted 70–80% of the starting material to products after heating for 16 hours. Compound **19** afforded the lowest conversion, but it displayed the highest selectivity for dehydrocoupling products over redistribution products. Conversely, **21** had the highest conversion of starting material and also gave the greatest amount of secondary silane and SiH₄ relative to dehydrocoupling products (Table 3.3).

The observed product distributions for **18–21** can best be explained by considering their relative steric environments. Iridium-catalyzed silane redistribution is

proposed to occur via silylene intermediates.⁵ Both a vacant coordination site on the metal and subsequent Si–H/R activation are necessary to form silylene compounds from organosilanes.¹⁷ Thus, the heightened reactivity of **18** for redistribution is a likely consequence of the more open metal coordination sphere, which can accommodate both the silylene ligand and an incoming silane substrate. For compounds **19–21**, reductive elimination to form Si–Si bonds must be accelerated under steric pressure from the *tert*-butyl substituents.

The more subtle electronic effect observed in reactions with **19–21** could be a function of the less electron-rich *p*-COOMe ligated system favoring reductive elimination to the lower iridium oxidation state. An alternate possibility is that the more electron rich *p*-NMe₂ ligated system stabilizes the higher iridium oxidation state thus allowing silylene intermediates to form. As the reactivity of **19** is lower and the selectivity for dehydrocoupling is greater than that of **20** and **21**, Si–H bond activation could be less favorable for the more electron deficient analogue, which supports the former hypothesis.

3.2.3. Reactions of PhSiH₃ Open to N₂ Atmosphere

To facilitate conversion of substrates, reactions were run in reflux Schlenk flasks that were open to a N₂ manifold. Rapidly stirred reactions on this scale allowed for any evolved gases to be readily dissipated. Under these conditions, the reaction of PhSiH₃

spiked with an internal standard of C₆Me₆ with 2 mol % of **18** at reflux in toluene solution for 16 hours resulted in the complete conversion of PhSiH₃ to primarily silane redistribution products. Compared to the same reaction run in an NMR tube (*vide supra*), reaction of **18** and PhSiH₃ open to N₂ showed increased activity with a measured turnover frequency of (TOF) = 219 h⁻¹, based on the extent of redistribution products present (Figure 3.6).

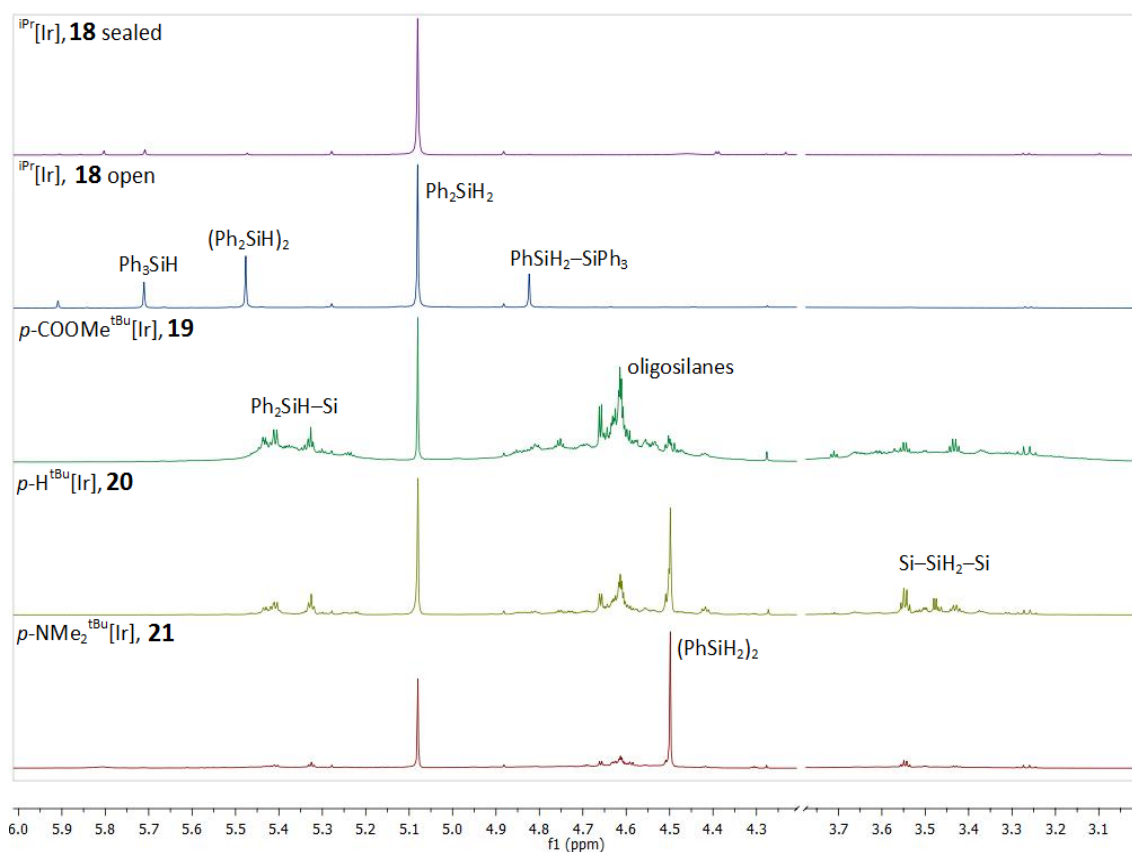


Figure 3.6 ¹H NMR spectra in benzene-*d*₆ solution of reactions of **18** with PhSiH₃ both sealed and open to a N₂ atmosphere and reactions of **19–21** open to a N₂ atmosphere after 16 hours. Redistribution products are seen with **18**, while dehydrocoupling products are primarily seen with **19**, **20**, and **21**.

In addition to Ph₂SiH₂ which is the dominant product under both sets of reaction conditions, Ph₃SiH, (Ph₂SiH)₂, and PhSiH₂-SiPh₃, are also present as determined by ¹H and ²⁹Si NMR spectroscopy. These products were minimal (< 4%) in the sealed variant of this same reaction (Table 3.4). Under these conditions, H₂ and SiH₄ cannot be detected though it is presumed that the open manifold facilitates dissipation of these gases and drives conversion of the substrate. The presence of disilane products continues to demonstrate that **18** can act as a dehydrocoupling catalyst. However, redistribution is still favored under these conditions, and observation of (Ph₂SiH)₂ and PhSiH₂-SiPh₃ suggests that dehydrocoupling may occur after redistribution. Trace quantities of the oxidation product (Ph₂SiH)₂O were observed in the product mixture of this reaction, most likely due to oxidation from O₂ or the Florisil used to remove the catalysts from these reactions.¹⁰

Table 3.4 Product distributions for reaction of PhSiH₃ with catalytic **18–21** under N₂

Compound.	TOF ^{a,b} (h ⁻¹)	Products ^a (%)				
		Ph ₂ SiH ₂	Ph ₃ SiH	SiH ₂ Ph-SiPh ₃	(Ph ₂ SiH) ₂	Oligosilanes
^{iPr} [Ir], c 18	219	54	12	14	20	-
<i>p</i> -COOMe ^{tBu} [Ir], 19	19	3	-	-	-	97
<i>p</i> -H ^{tBu} [Ir], 20	39	11	-	-	-	89
<i>p</i> -NMe ₂ ^{tBu} [Ir], 21	53	15	-	-	6	79

Reaction conditions: 2 mol % of [Ir], 120 °C, 16 h. ^a Measured by ¹H NMR spectroscopy (Si-H region) ^b Measured at 0.25 hour reaction time with respect to an internal standard of C₆Me₆. ^c Trace (Ph₂SiH)₂O (≤ 3%) was observed in this reaction.

Treatment of PhSiH_3 with 2 mol % of compounds **19–21** spiked with an internal standard of C_6Me_6 in toluene solution at reflux for 16 hours resulted in complete consumption of the substrate and yielded a mixture of dehydrocoupling and redistribution products. When these reactions were stopped after 2 hours, the disilane $(\text{PhSiH}_2)_2$ was the dominant product of these reactions with conversions ranging from 30–75%. Extending the reaction time to 16 hours yields a mixture of oligosilanes with terminal $-\text{SiH}_2$ groups having apparently undergone redistribution. This observation demonstrates that redistribution occurs slower than dehydrocoupling for these compounds, which is consistent with work using Wilkinson's catalyst.¹¹

Compared to the sealed NMR tube reactions, reactions open to N_2 yielded a higher percentage of oligosilanes relative to redistribution products as measured by ^1H and ^{29}Si NMR spectroscopy (Figure 3.6). The product distributions of **19**, **20**, and **21** were consistent with the NMR-scale reactions, though greater activity was observed under N_2 with TOFs = 19, 39, and 53 h^{-1} respectively, based on sampling after 15 min reaction time.

Though the gaseous products H_2 and SiH_4 cannot be detected under these conditions, a key redistribution product, Ph_2SiH_2 , is still present in considerable amounts (3–15%). The relative selectivity of **19**, **20**, or **21** for dehydrocoupling over redistribution is unchanged from the NMR scale, where **19** demonstrated the highest selectivity for dehydrocoupling and **21** produced the greatest amount of secondary silane (Table 3.4).

Further analysis of the products by ^1H NMR spectroscopy reveals complex, overlapping signals in the region of $\delta = 3.0\text{--}6.0$. To gain more information about the

structure of these oligosilane products, DEPT ^{29}Si NMR ($\theta = 90^\circ, 135^\circ$) spectroscopy was utilized to determine the number of hydrogen atoms per silicon atom.^{29,30} The extent of oligomerization in these reactions is low based on the number of ^{29}Si resonances present, with signals seen in three distinct regions of the DEPT ^{29}Si NMR spectra (Figure 3.7).

The most downfield signals of the silane products are located from $\delta = -25$ to -35 and correlate to proton resonances in the range of $\delta = 5.2$ – 5.5 as determined by ^1H – ^{29}Si HSQC NMR spectroscopy. Other than the ^{29}Si resonance for Ph_2SiH_2 , all of the signals present in this region correspond to Ph_2SiH – groups that most likely formed from redistribution of a terminal $-\text{PhSiH}_2$ unit. The broad massif of overlapping resonances from $\delta = -30$ to -32 likely corresponds to products containing more than one $-\text{PhSiH}$ – unit in a cyclosilane that consists of mostly Ph_2Si – units (e.g., $\text{Ph}_8\text{Si}_5\text{H}_2$).^{32,33}

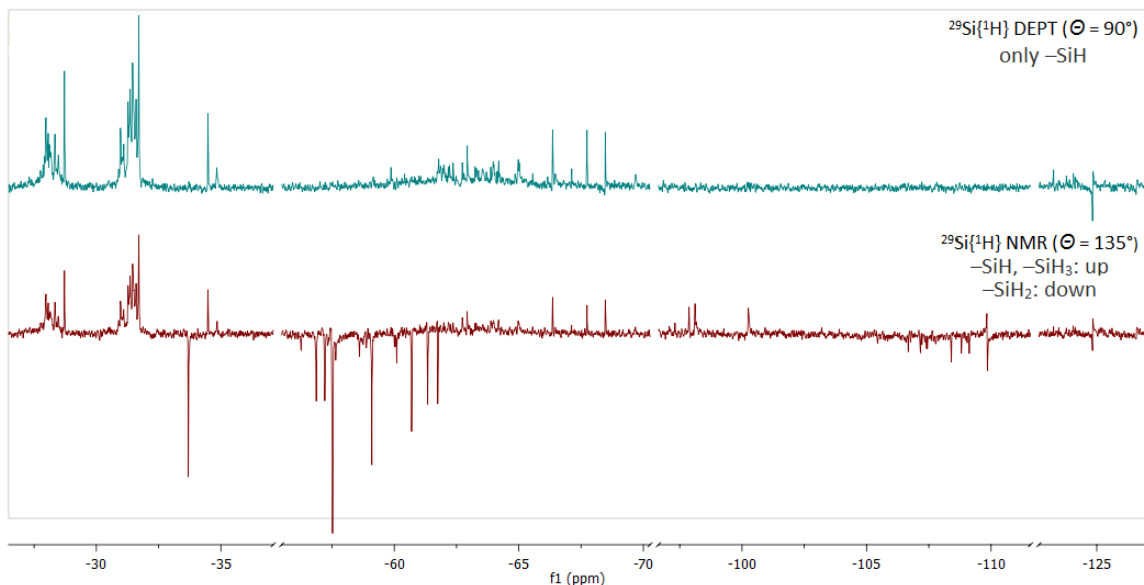


Figure 3.7 $^{29}\text{Si}\{^1\text{H}\}$ DEPT ($\Theta = 90^\circ, 135^\circ$) NMR spectra in benzene- d_6 solution of reaction of **19** with PhSiH_3 open to a N_2 atmosphere after 16 hours of reaction time. Three distinct regions are visible and correspond to the number of H and Ph groups present.

The second region of silane products in the DEPT ^{29}Si NMR spectra are in the range of $\delta = -55$ to -70 and correspond to proton resonances in the range of $\delta = 4.4$ – 4.8 as determined by ^1H – ^{29}Si HSQC NMR spectroscopy. The signals from $\delta = -56$ to -60 are due to terminal PhSiH_2 – groups. Resonances in the $\delta = -60$ to -70 range, with the exception of that of $(\text{PhSiH}_2)_2$, correspond to internal $-\text{PhSiH}-$ groups of linear oligosilanes.³⁴ From these spectra no information regarding the polymer microstructure is evident, other than to suggest an atactic structure based on the number of signals present.³⁵ In addition to the linear di- through tetrasilanes $-(\text{PhSiH})_n-$ $n = 2$ – 4 present, the products of these reactions are disilanes such as $\text{Ph}_2\text{SiH}-\text{SiH}_2\text{Ph}$ or oligosilanes that differ in the number of phenyl substituents due to redistribution.

The most upfield ^{29}Si NMR resonances occurred in the region of $\delta = -100$ to -130 and correspond to proton resonances in the range of δ 3.3–3.7 as determined by ^1H – ^{29}Si HSQC NMR spectroscopy. Resonances in this range are typical of internal silane atoms lacking organic substituents of the type $\text{H}_2\text{Si}(\text{SiH}_2\text{Ph})_2$ ($\delta = -110.6$) or $\text{HSi}(\text{SiH}_3)_3$ ($\delta = -131.5$),³⁶ which could have resulted from the incorporation of SiH_4 into the backbone³⁷ or the redistribution of a substituted oligosilane. Products of this type that can be conclusively identified from these reaction mixtures include $\text{Ph}_2\text{SiH-SiH}_3$ and $\text{Ph}_2\text{SiH-SiH}_2\text{-SiH}_2\text{Ph}$, though other unidentified products of this type are also present in this region.³⁸

Due to the complexity and overlapping of the peaks seen in the Si–H region in the ^1H and ^{29}Si NMR spectra for these reactions, complete assignment of Si–H signals to specific products cannot be accomplished. Therefore, gel permeation chromatography (GPC) was used to obtain approximate molecular weight information for silane products produced by compounds **19**, **20**, and **21**. Relative to polystyrene standards (M_w 489–2780 amu), GPC traces for the oligosilanes analyzed were broad, corresponding to multiple low molecular weight products ($M_w = 190$ –720 amu), in agreement with the ^{29}Si NMR data.

3.2.4. Reactions of Primary Silanes Open to N₂ Atmosphere

To probe steric effects of the silane substrate on catalytic activity and product distributions, primary arylsilanes including, *o*-tol- (*o*-tol = *o*-tolyl), naphthyl- and mesitylsilane were used in reactions with **18–21**. In these reactions, more sterically encumbered primary arylsilanes tempered the extent of both dehydrocoupling and redistribution for **18–21**, but the relative activity and type of products (dehydrocoupling vs. redistribution) generated were not affected. Using (*o*-tol)SiH₃ as the substrate, reaction with **18** exclusively yielded the redistribution product (*o*-tol)₂SiH₂ (Table 3.5).

Table 3.5 Product distributions of preparative scale reactions of (*o*-tol)SiH₃ with catalytic **18–21** under N₂.

Compound.	Conversion ^a (%)	[(<i>o</i> -tol)SiH ₂] ₂	Products (%)	
			(<i>o</i> -tol) ₂ SiH ₂	Redistributed Oligomers
<i>ipr</i> [Ir] 18	100	-	100	-
<i>p</i> -COOMe ^{<i>t</i>Bu} [Ir] 19	100	66	7	27
<i>p</i> -H ^{<i>t</i>Bu} [Ir] 20	100	79	4	17
<i>p</i> -NMe ₂ ^{<i>t</i>Bu} [Ir] 21	99	26	8	66

Reaction conditions: 2 mol % of [Ir], 120 °C, 16 h. ^a Measured by ¹H NMR spectroscopy with respect to an internal standard of C₆Me₆

Reactions of (*o*-tol)SiH₃ using **19–21** produced the same types of redistributed oligosilanes by comparison to reactions with PhSiH₃, though each catalyst yielded a different distribution of products (Table 3.5). Compared to reactions with PhSiH₃,

oligosilane product formation with (*o*-tol)SiH₃ was decreased and [(*o*-tol)SiH₂]₂ was the major product observed upon reaction for all ^tBu compounds. The electron rich compound **21**, again was the most active towards further dehydrocoupling/redistribution of the dominant disilane product producing the linear trisilane and other redistributed oligosilane products such as (*o*-tol)SiH₂-SiH₂-(*o*-tol)₂SiH. These products were only present in trace amounts in reactions using **19** and **20** as detected by ¹H and ²⁹Si NMR spectroscopy and GCMS.

Reactions of **19–21** with naphthylsilane and mesitylsilane did not reach completion and reinforce the notion that product selectivity for silane dehydrocoupling is governed by steric factors. As with the other substrates, reaction of NapSiH₃ (Nap = naphthyl) with 2 mol % of **18** exclusively gave the redistribution product Nap₂SiH₂. In comparison, treatment of NapSiH₃ with 2 mol % of **19–21** in toluene solution at reflux for 16 hours yielded partial conversion to the disilane (NapSiH₂)₂, as the major product. The secondary silane Nap₂SiH₂ (≤ 6%) was present in all reactions and trace amounts of trisilane (≤ 4%) was also observed in the ²⁹Si NMR spectra for the reactions with **20** and **21**.³⁹ Compound **19** converted only 25% of the starting material to products under these conditions, while reaction of this substrate with **20** and **21** converted 72% and 62% of NapSiH₃ to the disilane, respectively (Table 3.6).

Table 3.6 Product distributions of preparative scale reactions of NapSiH₃ with catalytic **18–21** under N₂.

Compound	Conversion ^a (%)	Nap ₂ SiH ₂	Products (%)	
			(NapSiH ₂) ₂	Dehydrocoupling
<i>ipr</i> [Ir] 18	100	99	-	1-
<i>p</i> -COOMe ^{<i>t</i>Bu} [Ir] 19	25	1	20	27
<i>p</i> -H ^{<i>t</i>Bu} [Ir] 20	71	6	55	17
<i>p</i> -NMe ₂ ^{<i>t</i>Bu} [Ir] 21	56	5	30	66

Reaction conditions: 2 mol % of [Ir], 120 °C, 16 h. ^a Measured by ¹H NMR spectroscopy with respect to an internal standard of C₆Me₆

For all of the previous substrates discussed, the ^{*i*}Pr phosphine compound **18** yielded redistribution products while the ^{*t*}Bu compounds **19–21** primarily yielded dehydrocoupling products. This pattern of reactivity breaks upon treatment of MesSiH₃ (Mes = mesityl) with 2 mol % of **18** at reflux for 16 hours in toluene solution, which yields oligosilane *dehydrocoupling* products with minimal redistribution (Table 3.7). Based on ²⁹Si NMR spectroscopy and GPC data, linear products up to the tetrasilane H(MesSiH)₄H were present. The few remaining unassigned peaks (ca. 5% by ¹H NMR) are presumably due to cyclic oligomers.

Table 3.7 Product distributions of preparative scale reactions of MesSiH₃ with catalytic **18–21** under N₂.

Compound	Conversion ^a (%)	Products (%)		
		(MesSiH ₂) ₂	Mes ₂ SiH ₂	Oligomers
<i>ipr</i> [Ir] 18	97	37	8	52
<i>p</i> -COOMe ^{<i>t</i>Bu} [Ir] 19	20	18	1	-
<i>p</i> -H ^{<i>t</i>Bu} [Ir] 20	25	24	1	1
<i>p</i> -NMe ₂ ^{<i>t</i>Bu} [Ir] 21	58	56	2	-

Reaction conditions: 2 mol % of [Ir], 120 °C, 16 h. ^a Measured via ¹H NMR spectroscopy with respect to an internal standard of C₆Me₆

Rosenberg has shown that the selectivity of Wilkinson's catalyst for dehydrocoupling over redistribution of secondary silanes could be enhanced through the efficient removal of produced hydrogen gas.¹¹ In this iridium system, the chemoselectivity of **18–21** for dehydrocoupling over redistribution is steric in nature. Therefore, it was hypothesized that rigorous removal of hydrogen could further influence the product selectivity of these catalysts for non-volatile substrates.

Ambient temperature reactions of neat MesSiH₃ and 0.2 mol % of each catalyst **18–21** were conducted under reduced pressure. Catalysts were used at a lower loading in these reactions to ensure solubility in neat silane. After 4 hours under these conditions, **18** completely consumed the starting material and yielded only the dehydrocoupling product, (MesSiH₂)₂. No redistribution to Mes₂SiH₂ or further dehydrocoupling of the disilane to the trisilane or higher oligomers was evident under these conditions, as further oligomerization presumably requires thermal energy to overcome steric constraints of the catalyst. Thus, not only selectivity for dehydrocoupling was achieved, greater product

selectivity was also seen. Under these conditions, no reaction occurred with **19**, **20**, or **21**.

Given the greater preference for aryl redistribution relative to alkyl groups,⁴⁰ *n*-octylsilane (*n*-oct = *n*-octyl) was also screened. Treatment of (*n*-oct)SiH₃ with 2 mol % of **18** at reflux for 16 hours in toluene solution gave complete consumption of the substrate and yielded the redistribution product (*n*-oct)₂SiH₂ as determined by ¹H and ²⁹Si NMR spectroscopy. No redistribution to the tertiary silane product (*n*-oct)₃SiH was observed. Under the same conditions, reactions of (*n*-oct)SiH₃ with **19**, **20**, or **21** yielded oligosilane dehydrocoupling products and a small amount ($\leq 11\%$) of (*n*-oct)₂SiH₂.

Analysis of the product mixtures of each reaction via ¹H NMR spectroscopy showed that the disilane [(*n*-oct)SiH₂]₂ is the predominant single product for each catalyst in this series. Reactions of para-substituted **19** and **21** with *n*-octSiH₃ generated trace amounts of oligosilanes, while the reaction of **20** with (*n*-oct)SiH₃ showed a majority of the [(*n*-oct)SiH₂]₂ was converted to higher order oligosilane products (Figure 4). Similar to reactions with PhSiH₃, products with upfield²⁹Si NMR resonances in the region of $\delta = -110$ to -130 were produced and are indicative of internal silane centers of the type H₂Si(SiH₂R)₂ or HSi(SiH₃)₃.³⁶ Products of catalysis with **20** were analyzed by GPC to obtain molecular weight information. Traces for the samples analyzed contained broad peaks that corresponded to a distribution of low molecular weight products ($M_w = 300$ – 930).³¹ In these systems, the degree of oligomerization increases as substrate conversion increases, which suggests a step growth mechanism.

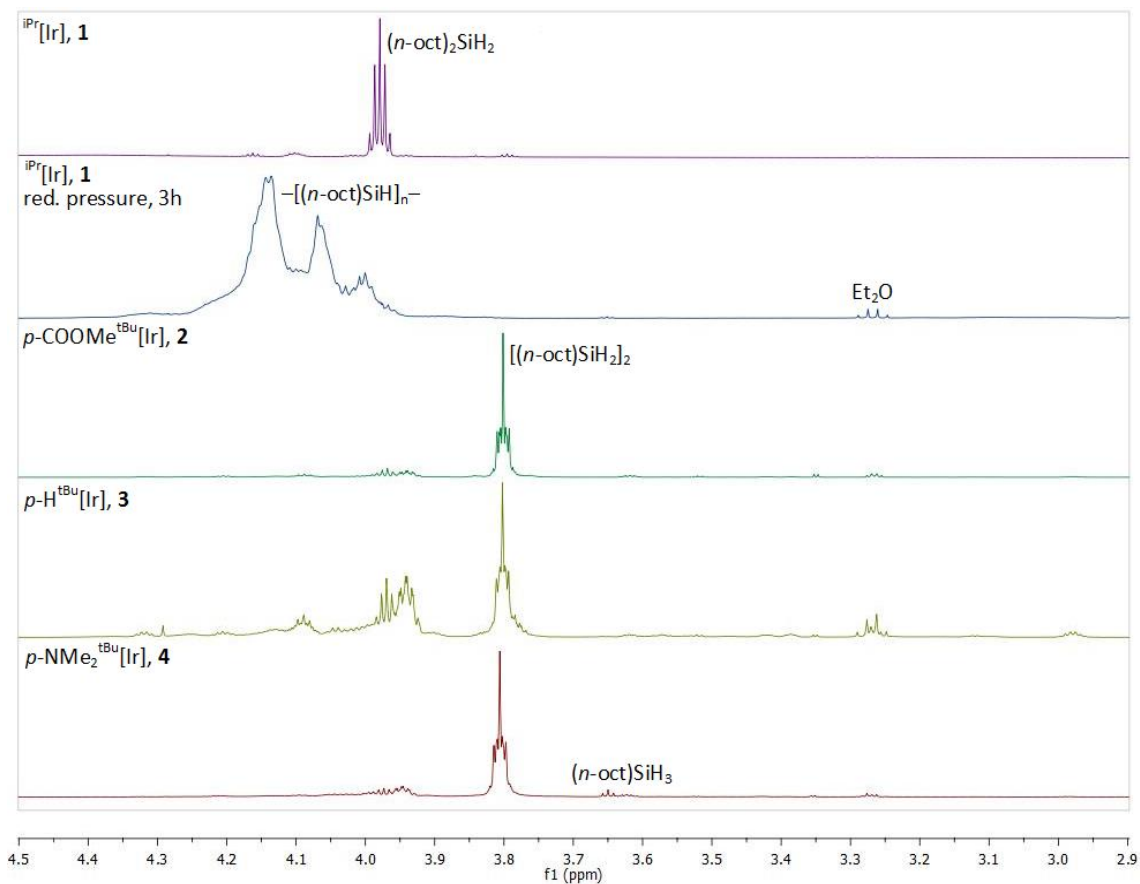


Figure 3.8 Reactions of **18** with $(n\text{-oct})\text{SiH}_3$ under both N_2 and reduced pressure conditions and reactions of **19–21** under N_2 .

For $(n\text{-oct})\text{SiH}_3$, product selectivity for dehydrocoupling vs redistribution using **18** can be enhanced by controlling the concentration of H_2 gas produced. Under dynamic vacuum, 0.2 mol % of **18** completely consumed the $n\text{-oct}\text{SiH}_3$ within 3 hours and yielded oligooctylsilane and < 1 % $(n\text{-oct})_2\text{SiH}_2$ (Figure 3.8). Product analysis via GPC shows two broad overlapping peaks corresponding to molecular weights of 2910 and 1100, respectively. Again, a concert of steric factors and H_2 management lead to substantial improvement in the selectivity of this catalysis.

3.2.5. Reactions of Secondary Silanes

The secondary silanes PhMeSiH₂ and Ph₂SiH₂ were used as substrates to probe dehydrocoupling activity in a system potentially less prone to redistribution. However, treatment of neat PhMeSiH₂ with 2 mol % of **18** for 16 hours at reflux facilitated extensive redistribution of the substrate to the tertiary silanes Ph₂MeSiH, PhMe₂SiH, and trace amounts of Ph₃SiH as seen by ¹H and ²⁹Si NMR spectroscopy (Table 3.8).

Table 3.8 Product distributions of preparative scale reactions of **18–21** with PhMeSiH₂ open to a N₂ atmosphere.

Compound.	Conversion ^a (%)	Products (%)						
		Unknown	Ph ₃ SiH	Ph ₂ MeSiH	Ph ₂ SiH ₂	PhMe ₂ SiH	Me ₂ SiH ₂	Dehydrocoupling
<i>ipr</i> [Ir] 18	100	-	2	71	-	27	-	-
<i>p</i> -COOMe ^{<i>t</i>Bu} [Ir] 19	24	4	-	3	7	-	3	7
<i>p</i> -H ^{<i>t</i>Bu} [Ir] 20	74	6	-	5	38	-	5	20
<i>p</i> -NMe ₂ ^{<i>t</i>Bu} [Ir] 21	65	9	-	9	8	16	3	20

Reaction conditions: 2 mol % of [Ir], 120 °C, 16 h. ^a Measured via ¹H NMR spectroscopy with respect to an internal standard of C₆Me₆

To gain insight into complete set of redistribution products produced, a sealed NMR-scale reaction of PhMeSiH₂ and 2 mol % of **18** was heated for 50 mins at 120 °C, and the products were analyzed by ¹H NMR spectroscopy. In addition to the tertiary silane products seen in the 16 hour reaction, Ph₂SiH₂, Me₂SiH₂, MeSiH₃, and trace amounts of PhSiH₃ were present in the 50 min reaction mixture (Figure 3.9). None of

these primary or secondary silane products were observed after 16 hours of reaction with **18**, which implies these volatile intermediate products (e.g., Me_2SiH_2 and MeSiH_3) escape through the open manifold.

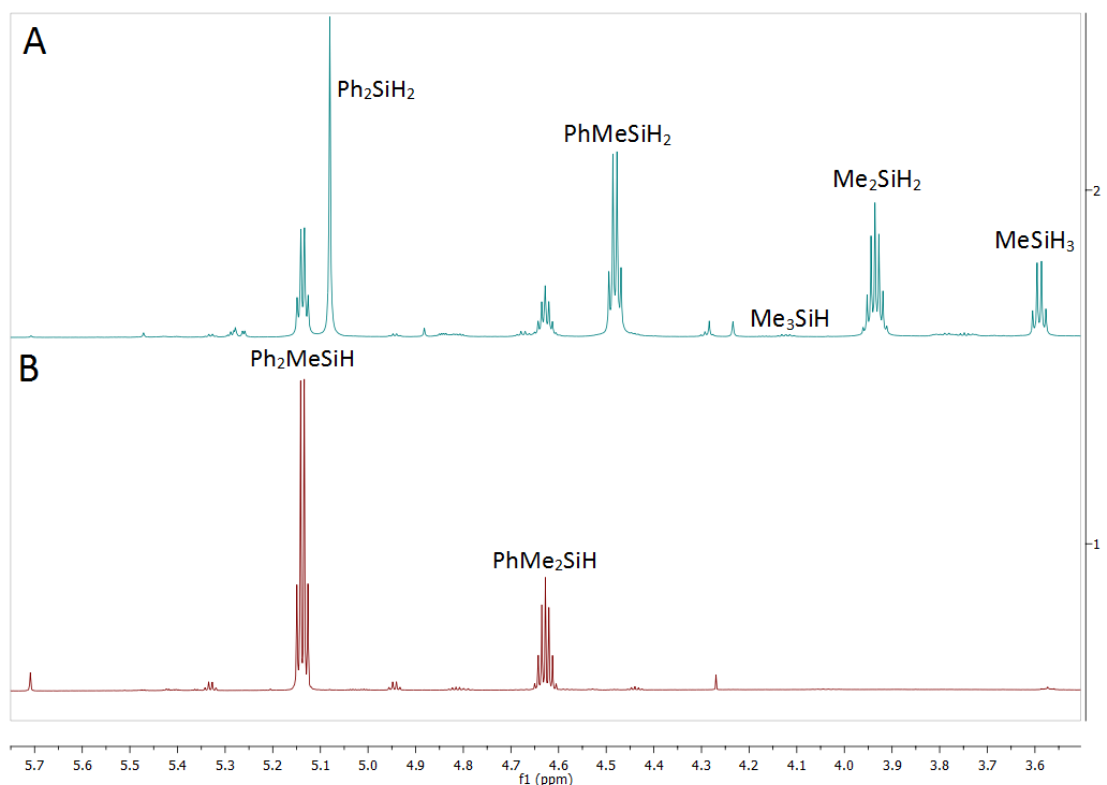


Figure 3.9 Reaction of 2 mol % **18** with PhMeSiH_2 after (A) 50 minutes and (B) 16 hours of reaction time

Reactions of the ^tBu compounds **19–21** with PhMeSiH_2 suffered from both incomplete conversion (24–74%) and poor selectivity for dehydrocoupling relative to redistribution. For this substrate, **20** and **21** were the most active (74% and 65% conversion, respectively), though their dehydrocoupling products accounted for a

maximum of only 20% of the product distribution and were limited to the simple disilane (PhMeSiH)₂. The major products of the ^tBu suite of compounds are Ph₂SiH₂ in reactions with **19** and **20** and PhMe₂SiH in reactions with **21** (Table 3.8).

Refluxing a toluene solution of Ph₂SiH₂ for 16 hours with **19**, **20**, or **21** yielded minimal conversion ($\leq 5\%$) to the redistribution product Ph₃SiH along with trace amounts ($\leq 1\%$) of the dehydrocoupling products (Ph₂SiH)₂ and PhSiH₂-SiPh₃. In contrast, treatment of Ph₂SiH₂ with 2 mol % of **18** at reflux for 16 hours in toluene solution gave complete consumption of the substrate and yielded the major products: Ph₃SiH (15%), Ph₃Si-SiH₂-SiPh₃ (18%) and Ph₃Si-PhSiH-SiHPh₂ (50%) as determined by ¹H-²⁹Si HSQC and ²⁹Si DEPT NMR spectroscopy.³⁸ In the reaction of PhSiH₃ with **18**, traces of trisilane, Ph₃Si-PhSiH-SiHPh₂, were detected via ¹H NMR spectroscopy, though this resonance integrated to $< 1\%$ of the products in that reaction (vide supra). Compound **18** initially redistributes PhSiH₃ to Ph₂SiH₂ and SiH₄, and the use of Ph₂SiH₂ as a substrate bypasses this initial redistribution, resulting in greater amounts of dehydrocoupling products capped with tri-substituted silanes. Other products include, (Ph₂SiH)₂ and Ph₃Si-SiH₂Ph (combined 5%), while the remaining products are likely disilane redistribution products that were only produced in trace amounts.

3.3. Conclusions

A series of iridium pincer compounds were shown to be active for both silane dehydrocoupling and redistribution with product selectivity primarily governed by steric considerations of both the substrate and catalyst. Most importantly, reaction conditions can govern dehydrocoupling versus redistribution reactivity. Under thermal conditions, reaction of primary and secondary silanes favor redistribution products for **18** unless a sterically demanding substrate is used. Under dynamic vacuum, reactions catalyzed by **18** also yield dehydrocoupling products.

The more sterically encumbered compounds **19–21** are active primary silane dehydrocoupling catalysts that undergo competitive redistribution with less hindered substrates to yield oligosilane products as determined by GPC. Effects of a functional group *para* to iridium in the POCOP ligand were also considered as a source of selectivity and activity in these reactions. It was determined that the *para* electron withdrawing compound **19** showed the lowest activity, though the highest selectivity for dehydrocoupling products, which is consistent with decreased Si–H bond activation. The electron rich compound **21** had the highest catalytic activity, but also showed the greatest propensity to yield redistribution products. To favor the production of dehydrocoupling products the use of an electron deficient metal center is advantageous, but this enhanced product selectivity comes at a cost of reduced catalytic activity.

These results described herein provide design parameters for dehydrocoupling catalysts to avoid competitive redistribution. Additionally, this work demonstrates that careful control of reaction conditions remains a pivotal factor for governing late-metal reactivity toward organosilanes.

3.4. Experimental Methods

General Considerations. All manipulations, unless otherwise stated, were performed under an atmosphere of dry nitrogen using Schlenk or in a M. Braun glovebox. Dry, oxygen-free solvents were employed throughout. NMR spectra were recorded on a Bruker AXR 500 MHz spectrometer where ^1H and ^{13}C NMR spectra were referenced to residual solvent resonances. ^{31}P and ^{29}Si NMR spectra were referenced to external 85% H_3PO_4 and tetramethylsilane standards, respectively. Benzene- d_6 was degassed and dried over NaK alloy. Elemental analyses were performed using an Elementar VarioMicro cube. The ligands, *ipr*(POCOP)- H^{41} , *p*-COOMe^{*tbu*}(POCOP)- H^{23} and *p*-NMe₂^{*tbu*}(POCOP)- H^{42} , and metal precursors, $[\text{Ir}(\text{COD})\text{Cl}]_2^{43}$ and $[\text{Ir}(\text{COE})_2\text{Cl}]_2^{43}$, were prepared as described in the literature. The substrates *o*-tolylsilane⁴⁴, mesitylsilane⁴⁵, naphthylsilane⁴⁶, and *n*-octylsilane,⁴⁷ were prepared by modified literature methods. The substrates PhSiH_3 , Ph_2SiH_2 , and PhMeSiH_2 were purchased from Acros Organics and were used as received. Gel Permeation Chromatography (GPC) data was collected using a Hewlett-Packard 1100 series HPLC equipped with a refractive index detector. Samples were

eluted through a Waters μ Styragel 103 Å (7.8×300 mm) column using tetrahydrofuran (THF) at a flow rate of 1 mL min^{-1} . The average molecular weights of the polysilane samples were determined relative to five polystyrene standards obtained from Waters with molecular weights ranging from 489–6480 amu.

(1) Typical Procedure for NMR-scale dehydrocoupling reactions.

A PTFE-valved NMR tube was charged with PhSiH_3 (28.3 mg, 0.262 mmol), catalyst (5.24 μmol), an internal standard of C_6Me_6 and approximately 0.5 mL of benzene- d^6 . After two freeze-pump-thaw cycles, an initial ^1H NMR spectrum was collected. The orange solution was then heated for 16 hours at 120°C , which resulted in the solution darkening to an orange-red color. After heating, ^1H and ^{29}Si NMR spectra were collected.

(2) Typical Procedure for reflux Schlenk dehydrocoupling reactions.

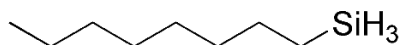
A Schlenk flask with an attached condenser was charged with catalyst (0.045 mmol), C_6Me_6 as an internal standard and (2.25 mmol, 50 equiv) silane, where upon a color change from dark red to light orange occurred. After an initial aliquot of the reaction mixture was analyzed by ^1H NMR, the reagents were diluted in ~ 2 mL toluene, and then refluxed for 16 hours under an N_2 atmosphere. After cooling the reaction mixture to ambient temperature, the reaction was diluted with toluene or hexanes (~ 5 mL) then

filtered through two narrow bore florisil columns to remove the catalyst. The resulting solution was dried under reduced pressure to afford the product as a viscous clear liquid, which was then analyzed by ^1H and ^{29}Si NMR spectroscopy.

(3) Typical Procedure for dehydrocoupling reactions under reduced pressure.

A 10 mL round bottom flask was charged with catalyst (7.20 μmol), C_6Me_6 as an internal standard, and (3.60 mmol, 500 equiv) silane, where upon immediate gas evolution and a color change from dark red to light orange occurred. After an initial aliquot of the reaction mixture was removed to be analyzed by ^1H NMR, the flask was equipped with a vacuum adapter and left under dynamic vacuum. Reaction start times were recorded as the time at which the flask was opened to full vacuum. Aliquots of the reaction mixture were collected at 0.5 hour, 1 hour, 2 hour, 3 hour, and 4 hour intervals; quenched via hexane elution (~ 5 mL) through two narrow bore florisil columns; and analyzed by ^1H NMR spectroscopy.

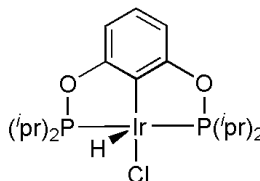
Modified preparation of (*n*-oct) SiH_3 :⁴⁷



A solution of (*n*-oct) $\text{Si}(\text{OEt})_3$ (15 mL, 46.5 mmol) in diethyl ether (25 mL) was added slowly to a stirred suspension of LiAlH_4 (5.47 g, 144.1 mmol) in diethyl ether (200 mL)

at -78 °C. The reaction mixture was then allowed to warm to ambient temperature and subsequently stirred for 12 h. The precipitate was separated and extracted with hexanes (2 × 100 mL), and the combined organic phases were distilled under N₂ to remove the solvent. Filtration to remove residual LiAlH₄ yielded (*n*-oct)SiH₃ as a clear oil. (4.79 g, 85.5% yield). ¹H NMR (500 MHz, 25 °C, C₆D₆): δ 3.64 (t, *J*_{SiH} = 191.7 Hz, 3 H, SiH₃), 1.34-1.22 (m, 12 H, 6 × CH₂), 0.91 (t, 3 H, CH₃), 0.56 (m, 2 H, CH₂(SiH₃)). ¹³C NMR (125.8 MHz, C₆D₆): δ 32.9 (s, C); 32.3 (s, C); 29.7 (s, 2C); 26.8 (s, C); 23.1 (s, C); 14.4 (s, C); 6.2 (s, C-SiH₃); ²⁹Si NMR (99 Hz): δ -60.0 (s)

Preparation of *p*-X^R(POCOP)IrHCl compounds:



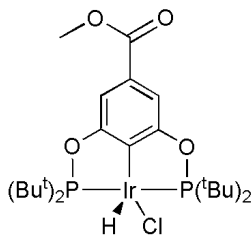
iprr(POCOP)IrHCl, **18**

A reaction tube was charged with *iprr*(POCOP)-H (0.348 g, 1.02 mmol) and [Ir(COE)₂Cl]₂ (0.444 g, 0.496 mmol) followed by 8 mL of toluene. After one freeze-pump-thaw cycle the tube was backfilled with H₂, sealed, then heated at 120 °C for 16 h. After cooling the reaction mixture to ambient temperature, the solution was dried under reduced pressure. The resulting red residue was brought up in pentane, then dried again under reduced pressure to ensure all cyclooctane was removed. The resulting orange powder was then

quickly washed with cold (-30 °C) pentane then filtered to give a yellow-orange powder (0.469 g, 0.823 mmol, 83%). ¹H NMR (500 MHz, 25 °C, C₆D₆): δ 6.80 (t, *J*_{HH} = 7.9 Hz, 1 H, *Ar*), 6.69 (d, *J*_{HH} = 7.9 Hz, 2 H, *Ar*), 2.65 (sept, 2 H, CH(CH₃)₂), 2.28 (m, 2 H, CH(CH₃)₂), 1.24 (dt, *J* = 8.7, 7.7 Hz, 6 H, CH₃), 1.14–1.06 (m, 12 H, CH₃), 1.01 (dt, *J* = 8.0, 7.3 Hz, 6 H, CH₃), -36.68 (br, 1 H, Ir-*H*). ¹³C NMR (125.8 MHz, C₆D₆): δ 166.2 (vt, *J*_{PC} = 6.5 Hz C_{Ar}OP); 128.4 (s, 4-C_{Ar}); 125.7 (s, 3,5-C_{Ar}); 105.6 (vt, *J*_{PC} = 5.4 Hz Ir-C_{Ar}); 31.5 [vt, *J*_{PC} = 14.7 Hz, 2 x PCH(CH₃)₂]; 29.4 [vt, *J*_{PC} = 16.5 Hz, 2 x PCH(CH₃)₂]; 17.4 (s, PCH(CH₃)₂); 17.0 (vt, *J*_{PC} = 4.2 Hz, PCH(CH₃)₂); 16.9 (br, PCH(CH₃)₂) 16.7 (s, PCH(CH₃)₂). ³¹P NMR (202.5 MHz): δ 173.0 (s). Anal. Calcd. for C₁₈H₃₂ClIrO₂P₂: C, 37.92; H, 5.66;. Found: C, 38.29; H, 5.76.

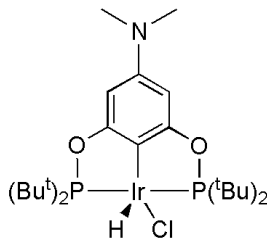
General Preparation²⁰ of *p*-X^{*ibu*}(POCOP)IrHCl Compounds

A reflux Schlenk flask was charged with 0.5 equiv of [(COD)IrCl]₂ and 1.05 equiv. of the respective *p*-X^{*ibu*}(POCOP)-H (X= COOMe, NMe₂) ligand. A small amount of toluene was added, and the solution was stirred in an oil bath for 16 h at 140 °C. The reaction mixture was cooled to room temperature, then the solvent and free (1, 5)-COD were removed under reduced pressure. The residue was extracted with a small amount of pentane via sonification (3 min). After filtration in air, the solid was washed with small amounts of cold pentane and dried under high vacuum to yield analytically pure samples.



p-COOMe^{tbu}(POCOP)IrHCl, **19**

From (0.269 g, 0.400 mmol) of [(COD)IrCl]₂ and (0.366 g, 0.802 mmol) of *p*-COOMe(POCOP)-H in 10 mL of toluene was obtained (0.483 g, 0.706 mmol, 88%) of **2** as an orange powder. ¹H NMR (500 MHz, 25 °C, C₆D₆): δ 7.70 (s, 2 H, Ar); 3.53 (s, 3 H, OCH₃); 1.22 (dt, *J* = 23.8 Hz, 7.2 Hz, 36 H, CH₃); -40.10 (t, *J* = 12.9 Hz, 1 H, Ir-*H*). ¹³C NMR (125.8 MHz, CDCl₃): δ 167.5 (s, C=O); 167.2 (vt, *J*_{PC} = 5.9 Hz C_{Ar}OP); 128.3 (m, br Ir-C_{Ar}); 127.8 (s, C_{Ar}COOMe); 106.0 (vt, *J*_{PC} = 5.3 Hz 3,5-C_{Ar}); 52.0 (s, OCH₃); 43.4 and 39.8 [vt, each *J*_{PC} = 11.4 and 12.6 Hz, 2 × P(*t*bu)₂]; 27.8 and 27.7 [vt, each *J*_{PC} = 3.1 Hz, 2 × P(*t*bu)₂]. ³¹P NMR (202.5 MHz): δ 176.5 (s). Anal. Calcd. for C₂₄H₄₂ClIrO₄P₂: C, 42.13; H, 6.19;. Found: C, 42.25; H, 6.22.



p-NMe₂^{tbu}(POCOP)IrHCl, **21**

From (0.262 g, 0.390 mmol) of [(COD)IrCl]₂ and (0.354 g, 0.802 mmol) of *p*-NMe₂(POCOP)-H in 10 mL of toluene was obtained (0.423 g, 0.632 mmol, 81%) of **21** as a purple powder. ¹H NMR (500 MHz, 25 °C, C₆D₆): δ 6.42 (s, 2 H, *Ar*); 2.52 (s, 6 H, CH₃); 1.37 (t, *J* = 7.2 Hz, 18 H, 2 × C(CH₃)₃) 1.31 (t, *J* = 7.3 Hz, 18 H, 2 × C(CH₃)₃), -41.13 (t, *J* = 13.3 Hz, 1 H Ir-*H*) ¹³C NMR (125.8 MHz, CD₂Cl₂): δ 168.4 (vt, *J*_{PC} = 6.1 Hz C_{Ar}OP); 151.4 (s, C_{Ar}N(CH₃)₂); 104.4 (m, br Ir-C_{Ar}); 91.2 (vt, *J*_{PC} = 5.1 Hz 3,5-C_{Ar}); 43.3 and 39.7 [vt, each *J*_{PC} = 11.4 and 12.6 Hz, 2 × P(CCH₃)₂]; 41.2 (s, N(CH₃)₂); 28.0 and 27.7 [vt, each *J*_{PC} = 3.1 and 3.1 Hz, 2 × P(CCH₃)₂] ³¹P NMR (202.5 MHz): δ 176.3 (s) Anal. Calcd. for C₂₄H₄₂ClIrNO₂P₂: C, 43.07; H, 6.78; N, 2.09. Found: C, 43.29; H, 6.77; N, 2.04.

3.5. References

- (1) Brook, M. A. *Silicon in Organic, Organometallic, and Polymer Chemistry*; John Wiley & Sons: New York, 2000.
- (2) Gauvin, F.; Harrod, J. F.; Woo, H. G. *Adv. Organomet. Chem.* **1998**, *42*, 363.
- (3) Waterman, R. *Cur. Org. Chem.* **2008**, *12*, 1322.
- (4) Corey, J. Y. *Adv. Organomet. Chem.* **2004**, *51*, 1.
- (5) Curtis, M. D.; Epstein, P. S. In *Adv. Organomet. Chem.*; Stone, F. G. A., Robert, W., Eds.; Academic Press: 1981; Vol. Volume 19, p 213.

- (6) Brown-Wensley, K. A. *Organometallics* **1987**, *6*, 1590.
- (7) Ojima, I.; Inaba, S.-I.; Kogure, T.; Nagai, Y. *J. Organomet. Chem.* **1973**, *55*, C7.
- (8) Lappert, M. F.; Maskell, R. K. *J. Organomet. Chem.* **1984**, *264*, 217.
- (9) Corey, J. Y.; Chang, L. S.; Corey, E. R. *Organometallics* **1987**, *6*, 1595.
- (10) Chang, L. S.; Corey, J. Y. *Organometallics* **1989**, *8*, 1885.
- (11) Rosenberg, L.; Davis, C. W.; Yao, J. *J. Am. Chem. Soc.* **2001**, *123*, 5120.
- (12) Rosenberg, L.; Kobus, D. N. *J. Organomet. Chem.* **2003**, *685*, 107.
- (13) Corey, J. Y.; Kraichely, D. M.; Huhmann, J. L.; Braddock-Wilking, J.; Lindeberg, A. *Organometallics* **1995**, *14*, 2704.
- (14) Okazaki, M.; Tobita, H.; Ogino, H. *Chem. Lett.* **1997**, *26*, 437.
- (15) Sangtrirutnugul, P.; Tilley, T. D. *Organometallics* **2007**, *26*, 5557.
- (16) Park, S.; Kim, B. G.; Göttker-Schnetmann, I.; Brookhart, M. *ACS Catal.* **2012**, *2*, 307.
- (17) Waterman, R.; Hayes, P. G.; Tilley, T. D. *Acc. Chem. Res.* **2007**, *40*, 712.
- (18) Tilley, T. D. *Comments Inorg. Chem.* **1990**, *10*, 37.
- (19) Choi, J.; MacArthur, A. H. R.; Brookhart, M.; Goldman, A. S. *Chem. Rev.* **2011**, *111*, 1761.
- (20) Göttker-Schnetmann, I.; White, P.; Brookhart, M. *J. Am. Chem. Soc.* **2004**, *126*, 1804.
- (21) Morales-Morales, D.; Redón, R. o.; Yung, C.; Jensen, C. M. *Inorg. Chim. Acta* **2004**, *357*, 2953.

- (22) Huang, Z. Ph.D. Thesis, The University of North Carolina, 2009.
- (23) Vabre, B.; Spasyuk, D. M.; Zargarian, D. *Organometallics* **2012**, *31*, 8561.
- (24) Göttker-Schnetmann, I.; White, P. S.; Brookhart, M. *Organometallics* **2004**, *23*, 1766.
- (25) Addison, A. W.; Rao, T. N.; Reedijk, J.; van Rijn, J.; Verschoor, G. C. *J. Chem. Soc., Dalton Trans.* **1984**, 1349.
- (26) Roddick, D. *Top. Organomet. Chem.* **2013**, *40*, 49.
- (27) Arunachalampillai, A.; Olsson, D.; Wendt, O. F. *Dalton Trans.* **2009**, 8626.
- (28) Denney, M. C.; Pons, V.; Hebden, T. J.; Heinekey, D. M.; Goldberg, K. *I. J. Am. Chem. Soc.* **2006**, *128*, 12048.
- (29) Gauvin, F.; Harrod, J. F. *Can. J. Chem.* **1990**, *68*, 1638.
- (30) Banovetz, J. P.; Stein, K. M.; Waymouth, R. M. *Organometallics* **1991**, *10*, 3430.
- (31) Tilley, T. D. *Acc. Chem. Res.* **1993**, *26*, 22.
- (32) Bratton, D.; Holder, S. J.; Jones, R. G.; Wong, W. K. C. *J. Organomet. Chem.* **2003**, *685*, 60.
- (33) Hengge, E.; Kovar, D.; Söllradl, H. *Monatsh Chem* **1979**, *110*, 805.
- (34) Aitken, C.; Harrod, J. F.; Gill, U. S. *Can. J. Chem.* **1987**, *65*, 1804.
- (35) Grimmond, B. J.; Corey, J. Y. *Organometallics* **1999**, *18*, 2223.
- (36) Hahn, J. Z. *Naturforsch.* **1980**, *35b*, 282.

- (37) Sadow, A. D.; Tilley, T. D. *Organometallics* **2003**, *22*, 3577.
- (38) Hassler, K.; Köll, W. *J. Organomet. Chem.* **1997**, *538*, 145.
- (39) Hassler, K. *Monatsh Chem* **1990**, *121*, 361.
- (40) Fryzuk, M. D.; Rosenberg, L.; Rettig, S. J. *Inorg. Chim. Acta* **1994**, *222*, 345.
- (41) Morales-Morales, D.; Grause, C.; Kasaoka, K.; Redón, R. o.; Cramer, R. E.; Jensen, C. M. *Inorg. Chim. Acta* **2000**, *300–302*, 958.
- (42) Lao, D. B.; Owens, A. C. E.; Heinekey, D. M.; Goldberg, K. I. *ACS Catal.* **2013**, *3*, 2391.
- (43) Herde, J. L.; Lambert, J. C.; Senoff, C. V.; Cushing, M. A. In *Inorganic Syntheses*; John Wiley & Sons, Inc.: 2007, p 18.
- (44) Manoso, A. S.; Ahn, C.; Soheili, A.; Handy, C. J.; Correia, R.; Seganish, W. M.; DeShong, P. *J. Org. Chem.* **2004**, *69*, 8305.
- (45) Söldner, M. S., M.; Schier, A.; Schmidbaur, H. *Chem. Ber./Recueil.* **1997**, *130*, 1671.
- (46) Minge, O. N., S.; Schmidbaur, H. *Z. Naturforsch., B: Chem. Sci.* **2004**, *59*, 153.
- (47) Hosomi, A.; Iijima, S.; Sakurai, H. *Chem. Lett.* **1981**, *10*, 243.

CHAPTER 4: FUTURE STUDIES AND CONCLUSIONS

This dissertation has focused on the transition metal catalyzed dehydrocoupling of main group elements. A theme common to both early and late metal dehydrocoupling catalysts examined in this dissertation was the pronounced effect steric considerations had on catalyst activity and product selectivity.

In chapter 2, dehydrocoupling of first generation bisphosphine substrates resulted in oligophosphine products and the eventual formation of insoluble hyperbranched polyphosphine materials. To overcome insolubility and facilitate product characterization, second generation linker molecules incorporating long chain solubilizing substituents were prepared. Catalytic reaction of alkoxy substituted bisphosphine molecules **10** and **11** with $(N_3N)Zr$, **1** resulted in sluggish conversion to diphosphine products. Reaction of the more active anionic zirconocene catalyst **2** with these substrates resulted in diphosphine products for **10** and sparingly soluble hyperbranched polyphosphine material with **11**. Despite the incorporation of alkoxy sidechains, the hyperbranched material resulting from **11** was still insoluble and further substrate design is necessary to produce soluble high molecular weight polyphosphines.

Future efforts on this project should focus on the installation of solubilizing substituents further away from the phosphine moieties in linker molecules. In substrates **10** and **11** sterically demanding functional groups *ortho* to the phosphine unnecessarily

crowded the molecule and likely stunted dehydrocoupling catalysis due to steric constraints.

In chapter 3, a series of POCOP iridium pincer compounds were demonstrated to be active for both silane dehydrocoupling and redistribution with product selectivity governed by steric considerations of both the catalyst and substrate. Most importantly, the work described in this chapter demonstrated that reaction conditions can govern dehydrocoupling vs. redistribution reactivity. For the ^{iPr}[Ir] compound **18**, thermal reaction conditions favored redistribution unless a bulky substrate was used. Conducting catalysis under dynamic vacuum conditions can turn off silane redistribution completely and solicit dehydrocoupling products instead.

The work in dissertation has demonstrated that effective dehydrocoupling catalysis depends on a concert of factors including appropriate substrate design, catalyst choice and reaction conditions. The results described herein offer researchers design parameters for consideration in designing future catalytic studies involving early metal phosphine or late metal silane dehydrocoupling. Ideally, this work could lead to the development of synthetic routes for preparing high molecular weight monodisperse polymers comprised of main group elements.

CHAPTER 5: COMPREHENSIVE BIBLIOGRAPHY

2014 ed.; Nobel Media AB: Nobelprize.org.

Addison, A. W.; Rao, T. N.; Reedijk, J.; van Rijn, J.; Verschoor, G. C. *J. Chem. Soc., Dalton Trans.* **1984**, 1349.

Aitken, C.; Barry, J. P.; Gauvin, F.; Harrod, J. F.; Malek, A.; Rousseau, D. *Organometallics* **1989**, *8*, 1732.

Aitken, C.; Harrod, J. F.; Gill, U. S. *Can. J. Chem.* **1987**, *65*, 1804.

Aitken, C.; Harrod, J. F.; Samuel, E. *J. Organomet. Chem.* **1985**, *279*, C11.

Arunachalampillai, A.; Olsson, D.; Wendt, O. F. *Dalton Trans.* **2009**, 8626.

Balaji, V.; Michl, J. *Polyhedron* **1991**, *10*, 1265.

Bande, A.; Michl, J. *Chem. Eur. J.* **2009**, *15*, 8504.

Banovetz, J. P.; Stein, K. M.; Waymouth, R. M. *Organometallics* **1991**, *10*, 3430.

Baumgartner, T.; Réau, R. *Chem. Rev.* **2006**, *106*, 4681.

Benito-Garagorri, D.; Kirchner, K. *Acc. Chem. Res.* **2008**, *41*, 201.

Bird, C. W. *Tetrahedron* **1985**, *41*, 1409.

Böhm, V. P. W.; Brookhart, M. *Angew. Chem. Int. Ed* **2001**, *40*, 4694.

Bratton, D.; Holder, S. J.; Jones, R. G.; Wong, W. K. C. *J. Organomet. Chem.* **2003**, *685*, 60.

Brook, M. A. *Silicon in Organic, Organometallic, and Polymer Chemistry*; John Wiley & Sons: New York, 2000.

Brown-Wensley, K. A. *Organometallics* **1987**, *6*, 1590.

Burkhard, C. A. *J. Am. Chem. Soc.* **1949**, *71*, 963.

- Cabelli, D. E.; Cowley, A. H.; Dewar, M. J. S. *J. Am. Chem. Soc.* **1981**, *103*, 3286.
- Chang, L. S.; Corey, J. Y. *Organometallics* **1989**, *8*, 1885.
- Choi, J.; MacArthur, A. H. R.; Brookhart, M.; Goldman, A. S. *Chem. Rev.* **2011**, *111*, 1761.
- Choi, N.; Onozawa, S.-y.; Sakakura, T.; Tanaka, M. *Organometallics* **1997**, *16*, 2765.
- Corcoran, E. W.; Sneddon, L. G. *J. Am. Chem. Soc.* **1984**, *106*, 7793.
- Corey, J. Y. *Adv. Organomet. Chem.* **2004**, *51*, 1.
- Corey, J. Y.; Chang, L. S.; Corey, E. R. *Organometallics* **1987**, *6*, 1595.
- Corey, J. Y.; Kraichely, D. M.; Huhmann, J. L.; Braddock-Wilking, J.; Lindeberg, A. *Organometallics* **1995**, *14*, 2704.
- Corey, J. Y.; Zhu, X. H.; Bedard, T. C.; Lange, L. D. *Organometallics* **1991**, *10*, 924.
- Corriu, R. J. P.; Enders, M.; Huille, S.; Moreau, J. J. E. *Chem. Mater.* **1994**, *6*, 15.
- Crabtree, R. H. *The Organometallic Chemistry of the Transition Metals*; 5th ed.; John Wiley & Sons, 2009.
- Curtis, M. D.; Epstein, P. S. In *Adv. Organomet. Chem.*; Stone, F. G. A., Robert, W., Eds.; Academic Press: **1981**; *19*, 213.
- Damewood, J. R.; West, R. *Macromolecules* **1985**, *18*, 159.
- Denney, M. C.; Pons, V.; Hebden, T. J.; Heinekey, D. M.; Goldberg, K. I. *J. Am. Chem. Soc.* **2006**, *128*, 12048.
- Dillon, K. B. *Phosphorus : the carbon copy : from organophosphorus to phospha-organic chemistry*; John Wiley: New York, 1998.
- Dioumaev, V. K.; Harrod, J. F. *J. Organomet. Chem.* **1996**, *521*, 133.
- Dioumaev, V. K.; Rahimian, K.; Gauvin, F.; Harrod, J. F. *Organometallics* **1999**, *18*, 2249.

Drury, A.; Maier, S.; Ruther, M.; Blau, W. J. *J. Mater. Chem.* **2003**, *13*, 485.

Etkin, N.; Fermin, M. C.; Stephan, D. W. *J. Am. Chem. Soc.* **1997**, *119*, 2954.

Etkin, N.; Hoskin, A. J.; Stephan, D. W. *J. Am. Chem. Soc.* **1997**, *119*, 11420.

Facchetti, A. *Chem. Mater.* **2011**, *23*, 733.

Fermin, M. C.; Stephan, D. W. *J. Am. Chem. Soc.* **1995**, *117*, 12645.

Fontaine, F.-G.; Kadkhodazadeh, T.; Zargarian, D. *Chem. Commun.* **1998**, 1253.

Fontaine, F.-G.; Zargarian, D. *Organometallics* **2002**, *21*, 401.

Fontaine, F.-G.; Zargarian, D. *J. Am. Chem. Soc.* **2004**, *126*, 8786.

Fryzuk, M. D.; Rosenberg, L.; Rettig, S. J. *Organometallics* **1991**, *10*, 2537.

Fryzuk, M. D.; Rosenberg, L.; Rettig, S. J. *Inorg. Chim. Acta* **1994**, *222*, 345.

Fukazawa, A.; Yamaguchi, S. *Chem. Asian J.* **2009**, *4*, 1386.

Gates, D. P. *Top. Curr. Chem.* **2005**, *250*, 107.

Gauvin, F.; Harrod, J. F. *Can. J. Chem.* **1990**, *68*, 1638.

Gauvin, F.; Harrod, J. F.; Woo, H. G. *Adv. Organomet. Chem.* **1998**, *42*, 363.

Ghebreab, M. B. Ph.D. Thesis, University of Vermont, 2013.

Ghebreab, M. B.; Bange, C. A.; Waterman, R. *J. Am. Chem. Soc.* **2014**, *136*, 9240.

Ghebreab, M. B.; Shalumova, T.; Tanski, J. M.; Waterman, R. *Polyhedron* **2010**, *29*, 42.

Gidron, O.; Varsano, N.; Shimon, L. J. W.; Leituss, G.; Bendikov, M. *Chem. Commun.* **2013**, *49*, 6256.

Gillon, B. H.; Noonan, K. J. T.; Feldscher, B.; Wissensz, J. M.; Kam, Z. M.; Hsieh, T.; Kingsley, J. J.; Bates, J. I.; Gates, D. P. *Can. J. Chem.* **2007**, *85*, 1045.

Gilman, H.; Atwell, W. H.; Schwebke, G. L. *J. Organomet. Chem.* **1964**, *2*, 369.

- Gilman, H.; Chapman, D. R. *J. Organomet. Chem.* **1966**, *5*, 392.
- Giordan, J. C.; Moore, J. H.; Tossell, J. A.; Kaim, W. *J. Am. Chem. Soc.* **1985**, *107*, 5600.
- Göttker-Schnetmann, I.; White, P.; Brookhart, M. *J. Am. Chem. Soc.* **2004**, *126*, 1804.
- Göttker-Schnetmann, I.; White, P. S.; Brookhart, M. *Organometallics* **2004**, *23*, 1766.
- Greenberg, S.; Stephan, D. W. *Chem. Soc. Rev.* **2008**, *37*, 1482.
- Grimmond, B. J.; Corey, J. Y. *Organometallics* **1999**, *18*, 2223.
- Günes, S.; Neugebauer, H.; Sariciftci, N. S. *Chem. Rev.* **2007**, *107*, 1324.
- Guo, X.; Baumgarten, M.; Müllen, K. *Prog. Polym. Sci.* **2013**, *38*, 1832.
- Gupta, M.; Hagen, C.; Flesher, R. J.; Kaska, W. C.; Jensen, C. M. *Chem. Commun.* **1996**, 2083.
- Hahn, J. Z. *Naturforsch.* **1980**, *35b*, 282.
- Halevi, E. A.; Winkelhofer, G.; Meisl, M.; Janoschek, R. *J. Organomet. Chem.* **1985**, *294*, 151.
- Han, L.-B.; Tilley, T. D. *J. Am. Chem. Soc.* **2006**, *128*, 13698.
- Harrah, L. A.; Zeigler, J. M. *Macromolecules* **1987**, *20*, 601.
- Hassler, K. *Monatsh Chem* **1990**, *121*, 361.
- Hassler, K.; Köll, W. *J. Organomet. Chem.* **1997**, *538*, 145.
- He, X.; Baumgartner, T. *RSC Adv.* **2013**, *3*, 11334.
- Heeger, A. J. *J. Phys. Chem. B* **2001**, *105*, 8475.
- Hengge, E.; Kovar, D.; Söllradl, H. *Monatsh Chem* **1979**, *110*, 805.
- Herde, J. L.; Lambert, J. C.; Senoff, C. V.; Cushing, M. A. *Inorganic Synth*; John Wiley & Sons, Inc.: **2007**, 18.

- Hide, F.; Díaz-García, M. A.; Schwartz, B. J.; Andersson, M. R.; Pei, Q.; Heeger, A. J. *Science* **1996**, *273*, 1833.
- Hillhouse, G. L.; Bercaw, J. E. *J. Am. Chem. Soc.* **1984**, *106*, 5472.
- Hissler, M.; Dyer, P. W.; Réau, R. *Coord. Chem. Rev.* **2003**, *244*, 1.
- Hoeben, F. J. M.; Jonkheijm, P.; Meijer, E. W.; Schenning, A. P. H. J. *Chem. Rev.* **2005**, *105*, 1491.
- Hosomi, A.; Iijima, S.; Sakurai, H. *Chem. Lett.* **1981**, *10*, 243.
- Huang, Z. Ph.D. Thesis, The University of North Carolina, 2009.
- Huang, Z.; Rolfe, E.; Carson, E. C.; Brookhart, M.; Goldman, A. S.; El-Khalafy, S. H.; MacArthur, A. H. R. *Adv. Synth. Catal.* **2010**, *352*, 125.
- Imori, T.; Lu, V.; Cai, H.; Tilley, T. D. *J. Am. Chem. Soc.* **1995**, *117*, 9931.
- Imori, T.; Tilley, T. D. *Polyhedron* **1994**, *13*, 2231.
- Imori, T.; Woo, H. G.; Walzer, J. F.; Tilley, T. D. *Chem. Mater.* **1993**, *5*, 1487.
- Izumi, T.; Kobashi, S.; Takimiya, K.; Aso, Y.; Otsubo, T. *J. Am. Chem. Soc.* **2003**, *125*, 5286.
- Jeffries-El, M.; Kobilka, B. M.; Hale, B. J. *Macromolecules* **2014**, *47*, 7253.
- Jiu, T.; Li, Y.; Liu, H.; Ye, J.; Liu, X.; Jiang, L.; Yuan, M.; Li, J.; Li, C.; Wang, S.; Zhu, D. *Tetrahedron* **2007**, *63*, 3168.
- Kanbara, T.; Takase, S.; Izumi, K.; Kagaya, S.; Hasegawa, K. *Macromolecules* **2000**, *33*, 657.
- Kapp, J.; Schade, C.; El-Nahasa, A. M.; von Ragué Schleyer, P. *Angew. Chem. Int. Ed.* **1996**, *35*, 2236.
- Katritzky, A. R.; Ramsden, C. A.; Joule, J. A.; Zhdankin, V. V. In *Handbook of Heterocyclic Chemistry*; Elsevier Science: Amsterdam, **2010**, 87.
- Kipping, F. S. *J. Chem. Soc. Trans.* **1924**, *125*, 2291.
- Kozima, S.; Kobayashi, K.; Kawanisi, M. *Bull. Chem. Soc. Jpn.* **1976**, *49*, 2837.

- Kraft, A.; Grimsdale, A. C.; Holmes, A. B. *Angew. Chem. Int. Ed* **1998**, *37*, 402.
- Kyba, E. P.; Liu, S. T.; Harris, R. L. *Organometallics* **1983**, *2*, 1877.
- Lao, D. B.; Owens, A. C. E.; Heinekey, D. M.; Goldberg, K. I. *ACS Catal.* **2013**, *3*, 2391.
- Lappert, M. F.; Maskell, R. K. *J. Organomet. Chem.* **1984**, *264*, 217.
- Less, R. J.; Melen, R. L.; Wright, D. S. *RSC Adv.* **2012**, *2*, 2191.
- Lucht, B. L.; St. Onge, N. O. *Chem. Commun.* **2000**, 2097.
- Manners, I. *Angew. Chem. Int. Ed.* **1996**, *27*, 1602.
- Manners, I. *J. Polym. Sci., Part A: Polym. Chem.* **2002**, *40*, 179.
- Manoso, A. S.; Ahn, C.; Soheili, A.; Handy, C. J.; Correia, R.; Seganish, W. M.; DeShong, P. *J. Org. Chem.* **2004**, *69*, 8305.
- Masuda, J. D.; Hoskin, A. J.; Graham, T. W.; Beddie, C.; Fermin, M. C.; Etkin, N.; Stephan, D. W. *Chem. Eur. J.* **2006**, *12*, 8696.
- McCullough, R. D.; Lowe, R. D.; Jayaraman, M.; Anderson, D. L. *J. Org. Chem.* **1993**, *58*, 904.
- McWilliams, A.; Dorn, H.; Manners, I. *Top. Curr. Chem.* **2002**, *220*, 141.
- Miller, R. D.; Michl, J. *Chem. Rev.* **1989**, *89*, 1359.
- Miller, R. D.; Sooriyakumaran, R. *Macromolecules* **1988**, *21*, 3120.
- Minge, O. N., S.; Schmidbaur, H. *Z. Naturforsch., B: Chem. Sci.* **2004**, *59*, 153.
- Morales-Morales, D.; Grause, C.; Kasaoka, K.; Redón, R. o.; Cramer, R. E.; Jensen, C. M. *Inorg. Chim. Acta* **2000**, *300–302*, 958.
- Morales-Morales, D.; Redón, R. o.; Yung, C.; Jensen, C. M. *Inorg. Chim. Acta* **2004**, *357*, 2953.
- Moulton, C. J.; Shaw, B. L. *J. Chem. Soc., Dalton Trans.* **1976**, 1020.
- Mu, Y.; Aitken, C.; Cote, B.; Harrod, J. F.; Samuel, E. *Can. J. Chem.* **1991**, *69*,

264.

Nakajima, Y.; Shimada, S. *RSC Adv.* **2015**, *5*, 20603.

Naseri, V.; Less, R. J.; Mulvey, R. E.; McPartlin, M.; Wright, D. S. *Chem. Commun.* **2010**, *46*, 5000.

Neale, N. R.; Tilley, T. D. *J. Am. Chem. Soc.* **2002**, *124*, 3802.

Neale, N. R.; Tilley, T. D. *J. Am. Chem. Soc.* **2005**, *127*, 14745.

Nešpůrek, S. *Mater. Sci. Eng., C* **1999**, *8–9*, 319.

Ojima, I.; Inaba, S.-I.; Kogure, T.; Nagai, Y. *J. Organomet. Chem.* **1973**, *55*, C7.

Okazaki, M.; Tobita, H.; Ogino, H. *Chem. Lett.* **1997**, *26*, 437.

Park, S.; Kim, B. G.; Göttker-Schnetmann, I.; Brookhart, M. *ACS Catal.* **2012**, *2*, 307.

Patra, A.; Bendikov, M. *J. Mater. Chem.* **2010**, *20*, 422.

Power, P. P. *Nature* **2010**, *463*, 171.

Reiter, S. A.; Nogai, S. D.; Schmidbaur, H. *Dalton Trans.* **2005**, 247.

Roddick, D. *Top. Organomet. Chem.* **2013**, *40*, 49.

Roering, A. J.; Davidson, J. J.; MacMillan, S. N.; Tanski, J. M.; Waterman, R. *Dalton Trans.* **2008**, 4488.

Roering, A. J.; Leshinski, S. E.; Chan, S. M.; Shalumova, T.; MacMillan, S. N.; Tanski, J. M.; Waterman, R. *Organometallics* **2010**, *29*, 2557.

Roering, A. J.; Maddox, A. F.; Elrod, L. T.; Chan, S. M.; Ghebreab, M. B.; Donovan, K. L.; Davidson, J. J.; Hughes, R. P.; Shalumova, T.; MacMillan, S. N.; Tanski, J. M.; Waterman, R. *Organometallics* **2008**, *28*, 573.

Roering, A. J.; Maddox, A. F.; Elrod, L. T.; Chan, S. M.; Ghebreab, M. B.; Donovan, K. L.; Davidson, J. J.; Hughes, R. P.; Shalumova, T.; MacMillan, S. N.; Tanski, J. M.; Waterman, R. *Organometallics* **2009**, *28*, 573.

Roncali, J. *Macromol. Rapid Commun.* **2007**, *28*, 1761.

Rosenberg, L.; Davis, C. W.; Yao, J. *J. Am. Chem. Soc.* **2001**, *123*, 5120.

- Rosenberg, L.; Kobus, D. N. *J. Organomet. Chem.* **2003**, 685, 107.
- Sadow, A. D.; Tilley, T. D. *Organometallics* **2003**, 22, 3577.
- Saito, A.; Matano, Y.; Imahori, H. *Org. Lett.* **2010**, 12, 2675.
- Saito, A.; Miyajima, T.; Nakashima, M.; Fukushima, T.; Kaji, H.; Matano, Y.; Imahori, H. *Chem. Eur. J.* **2009**, 15, 10000.
- Sandorfy, C. *Can. J. Chem.* **1955**, 33, 1337.
- Sangtrirutnugul, P.; Tilley, T. D. *Organometallics* **2007**, 26, 5557.
- Shirakawa, H.; Louis, E. J.; MacDiarmid, A. G.; Chiang, C. K.; Heeger, A. J. *J. Chem. Soc., Chem. Commun.* **1977**, 578.
- Sloan, M. E.; Staubitz, A.; Clark, T. J.; Russell, C. A.; Lloyd-Jones, G. C.; Manners, I. *J. Am. Chem. Soc.* **2010**, 132, 3831.
- Smith, E. E.; Du, G.; Fanwick, P. E.; Abu-Omar, M. M. *Organometallics* **2010**, 29, 6527.
- Smith, R. C.; Protasiewicz, J. D. *J. Am. Chem. Soc.* **2004**, 126, 2268.
- Söldner, M. S., M.; Schier, A.; Schmidbaur, H. *Chem. Ber./Recueil.* **1997**, 130, 1671.
- Son, H. J.; He, F.; Carsten, B.; Yu, L. *J. Mater. Chem.* **2011**, 21, 18934.
- Staubitz, A.; Sloan, M. E.; Robertson, A. P. M.; Friedrich, A.; Schneider, S.; Gates, P. J.; Günne, J. r. S. a. d.; Manners, I. *J. Am. Chem. Soc.* **2010**, 132, 13332.
- Tilley, T. D. *Comments Inorg. Chem.* **1990**, 10, 37.
- Tilley, T. D. *Acc. Chem. Res.* **1993**, 26, 22.
- Torsi, L.; Dodabalapur, A.; Rothberg, L. J.; Fung, A. W. P.; Katz, H. E. *Science* **1996**, 272, 1462.
- Trefonas, P.; West, R. *J. Polym. Sci. Polym. Chem. Ed.* **1985**, 23, 2099.
- Trefonas, P.; West, R.; Miller, R. D. *J. Am. Chem. Soc.* **1985**, 107, 2737.

- Trujillo, R. E. *J. Organomet. Chem.* **1980**, *198*, C27.
- Vabre, B.; Spasyuk, D. M.; Zargarian, D. *Organometallics* **2012**, *31*, 8561.
- van Mullekom, H. A. M.; Vekemans, J. A. J. M.; Havinga, E. E.; Meijer, E. W. *Mater. Sci. Eng., R* **2001**, *32*, 1.
- Waterman, R. *Organometallics* **2007**, *26*, 2492.
- Waterman, R. *Cur. Org. Chem.* **2008**, *12*, 1322.
- Waterman, R. *Chem. Soc. Rev.* **2013**, *42*, 5629.
- Waterman, R. *Organometallics* **2013**, *32*, 7249.
- Waterman, R.; Hayes, P. G.; Tilley, T. D. *Acc. Chem. Res.* **2007**, *40*, 712.
- Waterman, R.; Tilley, T. D. *Angew. Chem. Int. Ed* **2006**, *45*, 2926.
- West, R.; David, L. D.; Djurovich, P. I.; Stearley, K. L.; Srinivasan, K. S. V.; Yu, H. *J. Am. Chem. Soc.* **1981**, *103*, 7352.
- Williams, J. W. *J. Phys. Chem.* **1931**, *36*, 437.
- Woo, H. G.; Freeman, W. P.; Tilley, T. D. *Organometallics* **1992**, *11*, 2198.
- Woo, H. G.; Tilley, T. D. *J. Am. Chem. Soc.* **1989**, *111*, 8043.
- Woo, H. G.; Tilley, T. D. *J. Am. Chem. Soc.* **1989**, *111*, 3757.
- Woo, H. G.; Walzer, J. F.; Tilley, T. D. *J. Am. Chem. Soc.* **1992**, *114*, 7047.
- Wright, V. A.; Gates, D. P. *Angew. Chem. Int. Ed* **2002**, *41*, 2389.
- Wright, V. A.; Patrick, B. O.; Schneider, C.; Gates, D. P. *J. Am. Chem. Soc.* **2006**, *128*, 8836.
- Xin, S.; Woo, H. G.; Harrod, J. F.; Samuel, E.; Lebuis, A.-M. *J. Am. Chem. Soc.* **1997**, *119*, 5307.
- Yajima, S.; Hayashi, J.; Omori, M. *Chem. Lett.* **1975**, *4*, 931.
- Yamaguchi, S.; Itami, Y.; Tamao, K. *Organometallics* **1998**, *17*, 4910.

Zhang, X.-H.; West, R. *J. Polym. Sci. B Polym. Lett. Ed.* **1985**, 23, 479.

APPENDIX 1: CRYSTALLOGRAPHY DATA

Table A.1: Crystallographic Data for *p*-X^R[Ir] Compounds

Compound	18	19	21
Chemical formula	C ₁₈ H ₃₂ ClIrO ₂ P ₂	C ₂₄ H ₄₂ ClIrO ₄ P ₂	C ₂₄ H ₄₅ ClIrNO ₂ P ₂
Formula Weight	570.06	684.16	669.2
Temperature (K)	125(2)	125(2)	125(2)
Wavelength (Å)	0.71073	0.71073	0.71073
Crystal system	triclinic	monoclinic	orthorhombic
Space group	P-1	P2 _{1/c}	Pbcn
a (Å)	8.3060(19)	10.6097(14)	34.451(3)
b (Å)	12.205(3)	26.515(4)	11.035(9)
c (Å)	12.335(3)	20.822(3)	14.4669(12)
α (deg)	119.410(2)	90	90
β (deg)	96.267(3)	91.087	90
γ (deg)	98.328(3)	90	90
Z	2	8	8
Unit cell vol. (Å³)	1054.0(4)	5856.5(13)	5499.8(8)
μ (mm⁻¹)	6.621	4.785	5.089
ρ calcd (g cm⁻³)	1.796	1.552	1.616
θ Range (deg)	1.923 to 27.186	1.244 to 25.200	1.182 to 25.026
R₁^a [I > 2σ(I)]	0.0342	0.0301	0.0195
wR₂^b [I > 2σ(I)]	0.0887	0.0609	0.0372
R₁ [all data]	0.0391	0.0443	0.0238
GOF	1.079	1.019	1.107

^aR₁ = ||F_o| - |F_c|| / Σ |F_o|. ^bwR₂ = {Σ[w(F_o² - F_c²)²] / Σw(F_o²)²]^{1/2}.

APPENDIX 2: MASTER LIST OF SILANE ^1H AND ^{29}Si NMR δ

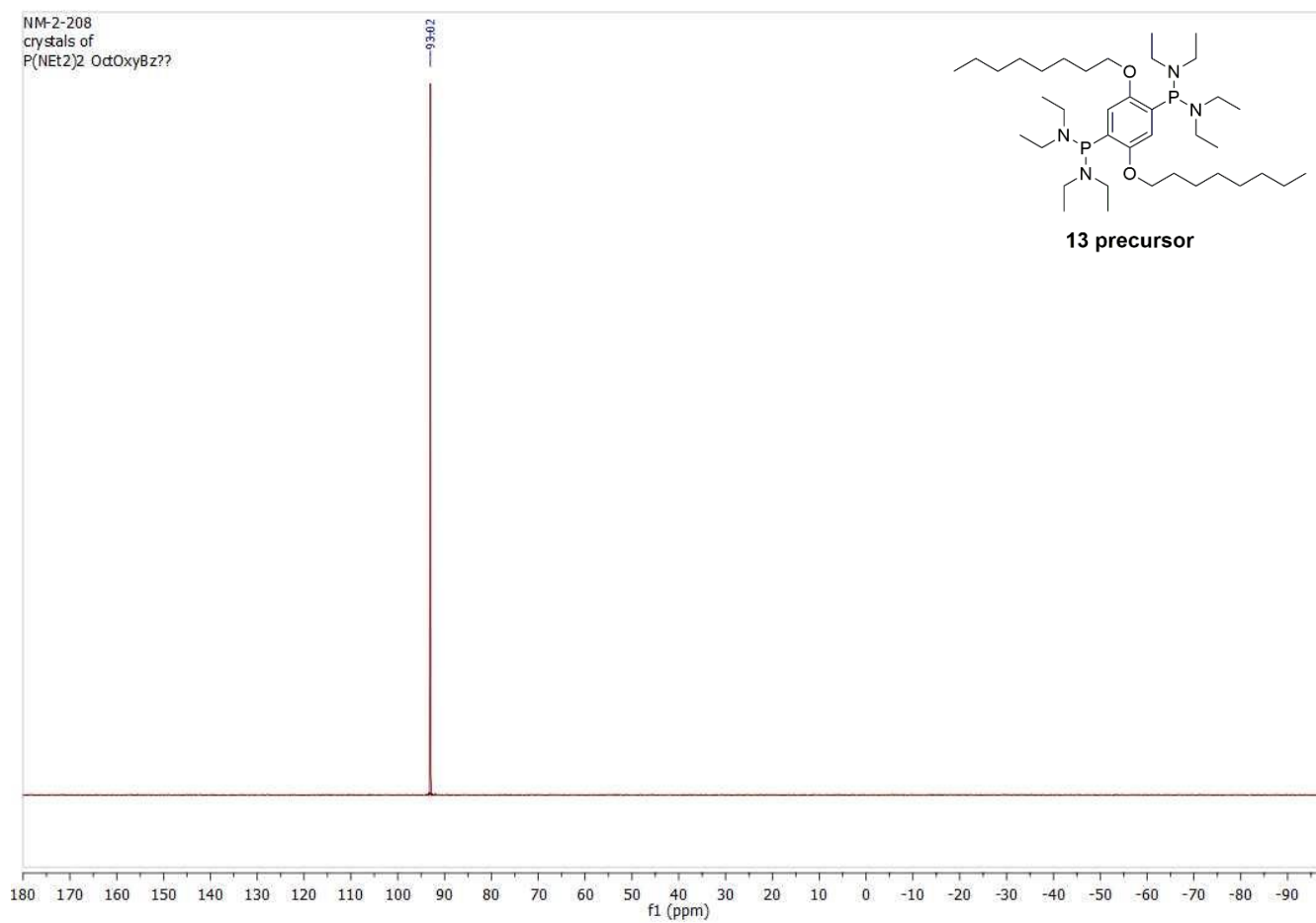
All spectra were recorded in benzene- d^6 :

Table A.2: Mucha's Master Silane List

Compound	^1H δ	^{29}Si δ
	(* Si and H δ is listed first)	
PhSiH ₃	4.23	-59.7
Ph ₂ SiH ₂	5.08	-33.7
Ph ₃ SiH	5.71	-17.7
<i>o</i> -tolyl SiH ₃	4.24	-64.1
(<i>o</i> -tolyl) ₂ SiH ₂	5.13	-39.9
[(<i>o</i> -tolyl)SiH ₂] ₂	4.51	-65.3
MesSiH ₃	4.27	-78.0
(MesSiH ₂) ₂	4.57	-79.6
Mes ₂ SiH ₂	5.29	-62.1
(Mes ₂ SiH) ₂	5.87	??
NapSiH ₃	4.48	-62.8
Nap ₂ SiH ₂	5.72	-39.4
(NapSiH ₂) ₂	4.85	-63.7
<i>n</i> -octylSiH ₃	3.65	-59.9
(<i>n</i> -octyl) ₂ SiH ₂	3.98	-28.7
[(<i>n</i> -octyl)SiH ₂] ₂	3.80	-63.8
PhMeSiH ₂	4.46, q	
Ph ₂ MeSiH	5.13, q	
(PhMeSiH) ₂	4.63 q, 4.64 q	
HPhMeSi–SiPhMe–SiPhMeH	4.71, - 4.74 overlap q	
PhMe ₂ SiH	4.63, sept	
Me ₃ SiH	4.16, sept	
Me ₂ SiH ₂	3.93, sept	
MeSiH ₃	3.55, q	-65.2
SiH ₃ –SiH ₃	3.17	-102.8
Si*H ₃ –SiH ₂ Ph	3.28, 4.33	-100.3, -62.9
Si*H ₃ –SiHPh ₂	3.41, 5.14	-99.5, -34.4

Si*H ₃ -SiPh ₃	3.65	-98.9, -18.9
SiH ₂ Ph-SiH ₂ Ph	4.49	-61.2
Si*H ₂ Ph-SiHPh ₂	4.64, 5.31	-60.7, -34.0
Si*H ₂ Ph-SiPh ₃	4.82	-60.3, -20.8
SiHPh ₂ -SiHPh ₂	5.47	-34.5
Si*HPh ₂ -SiPh ₃	5.61	-33.3, -22.2
SiPh ₃ -SiPh ₃	N/A	-26.6
HPh ₂ Si*-SiPh ₂ -SiPh ₂ H	?	-31.9, -42.4
H ₂ PhSi*-Si**PhH-SiPh ₂ H		-58.7, -67.7, -31.5
H ₂ PhSi*-SiH ₂ -SiPhH ₂	?	-60.1, -110.6
H ₂ PhSi*-SiPhH-SiPhH ₂	4.61 m	-58.7, -68.1
H ₂ PhSi*-SiPh ₂ -SiPhH ₂	?	-58.2, -41.7
PhSiH ₂ *-(SiH ₂) ₂ -SiPhH ₂	4.44, 3.32	-59.0, -110.3
SiH ₃ *-(SiH ₂) ₂ -SiH ₃	3.30, 3.18	-99.1, -111.9
PhSiH ₂ *-(PhSiH) ₂ -SiPhH ₂	4.61 m, 4.71 m	-64.5, -65.1 & -58.5, -58.6

APPENDIX 3: PHOSPHINE SUBSTRATE NMR DATA FROM CHAPTER 2



141

Figure A3.1 ³¹P NMR spectrum of the diethylaminophosphine precursor to **13** in benzene-*d*₆

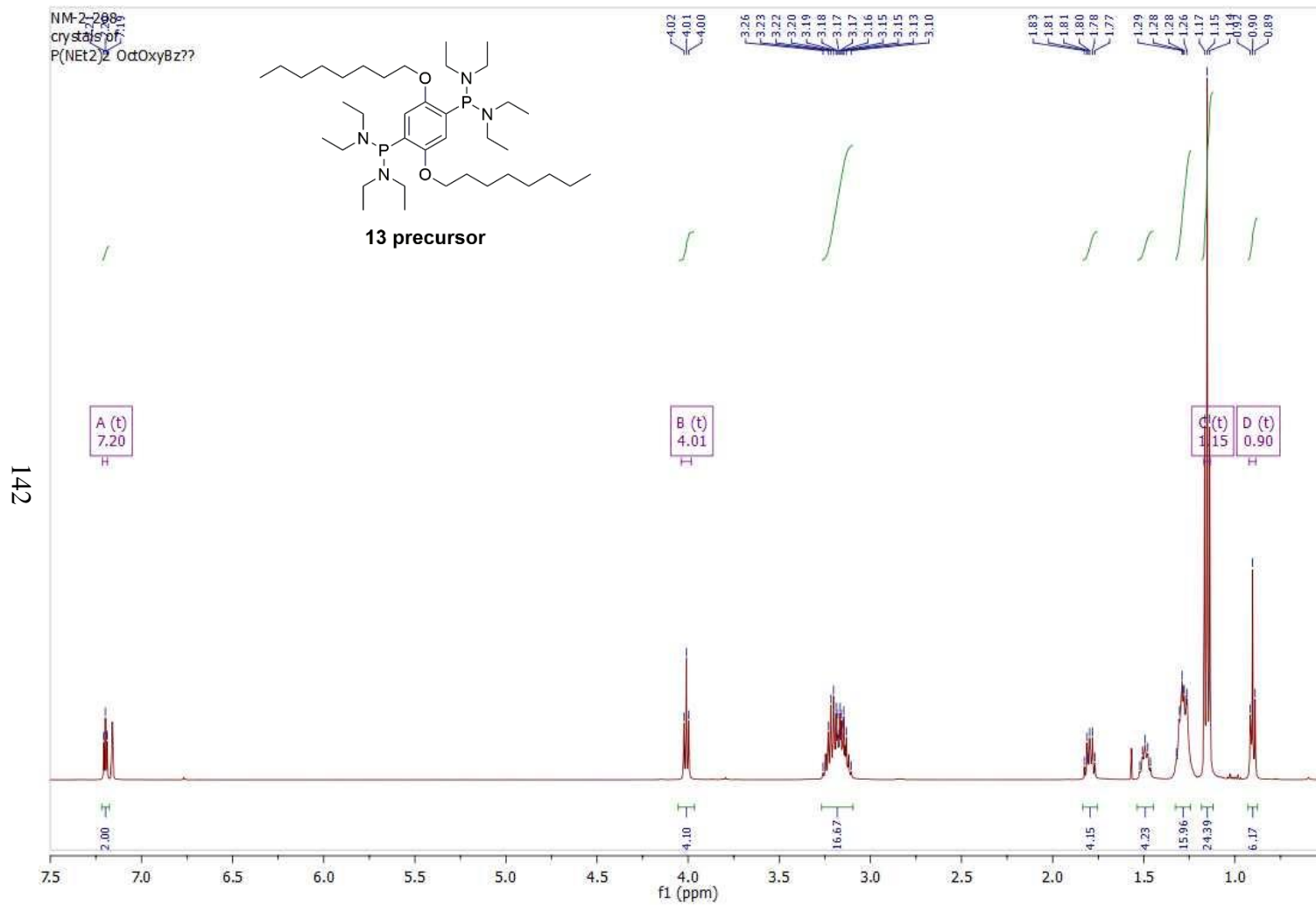


Figure A3.2 ¹H NMR spectrum of the diethylaminophosphine precursor to **13** in benzene-*d*₆

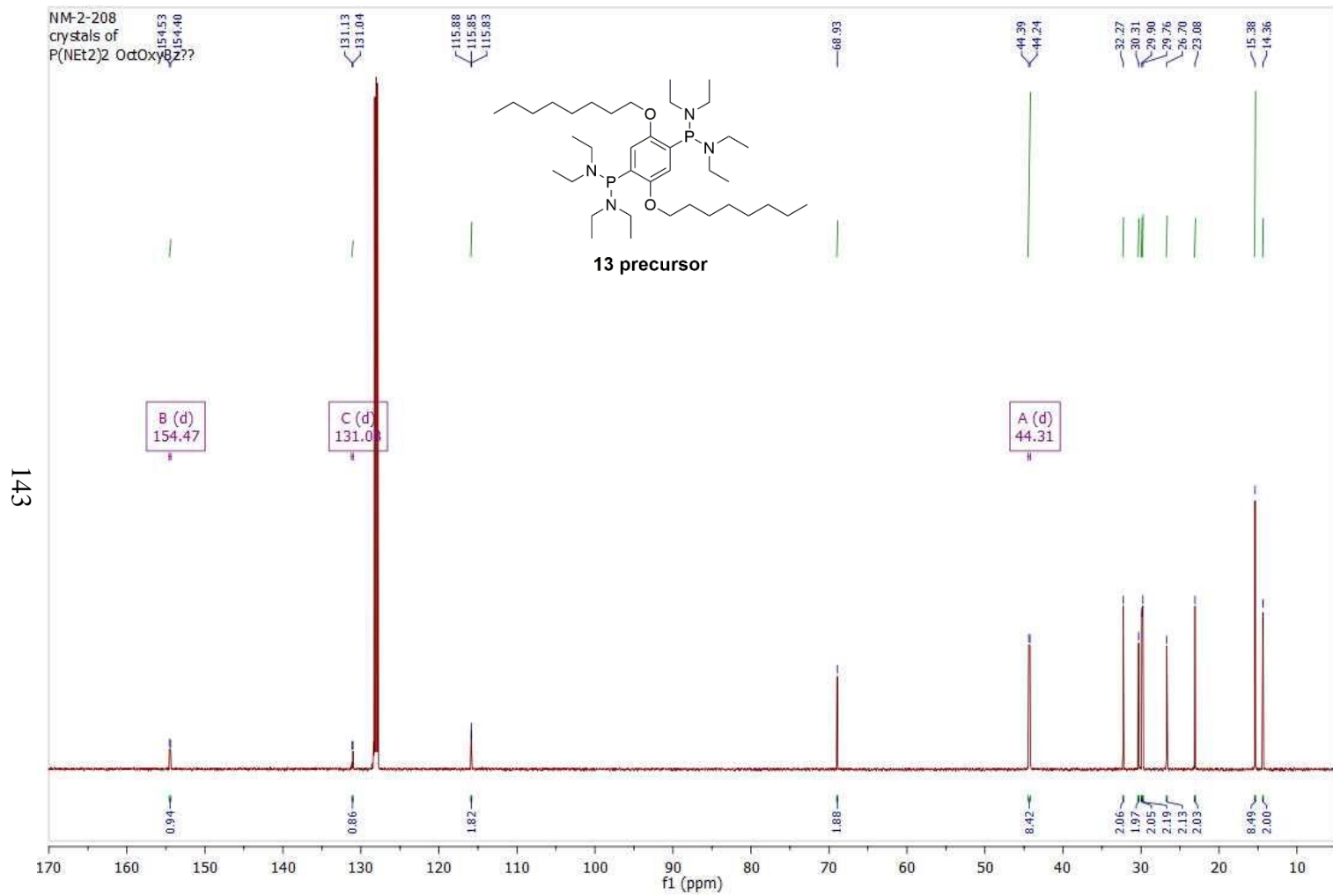


Figure A3.3 ¹³C NMR spectrum of the diethylaminophosphine precursor to **13** in benzene-*d*₆

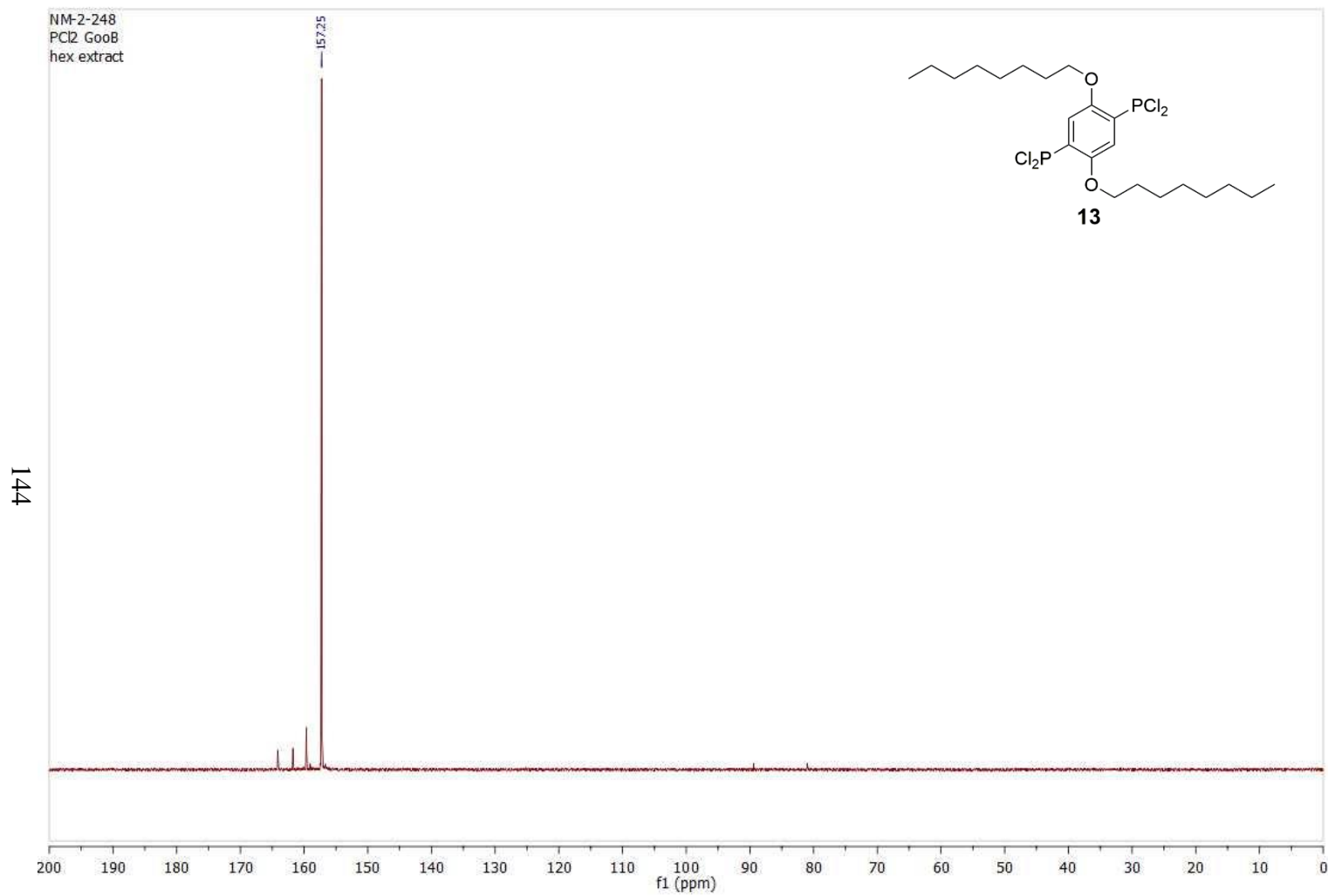


Figure A3.4 ³¹P NMR spectrum of **13** in benzene-*d*₆

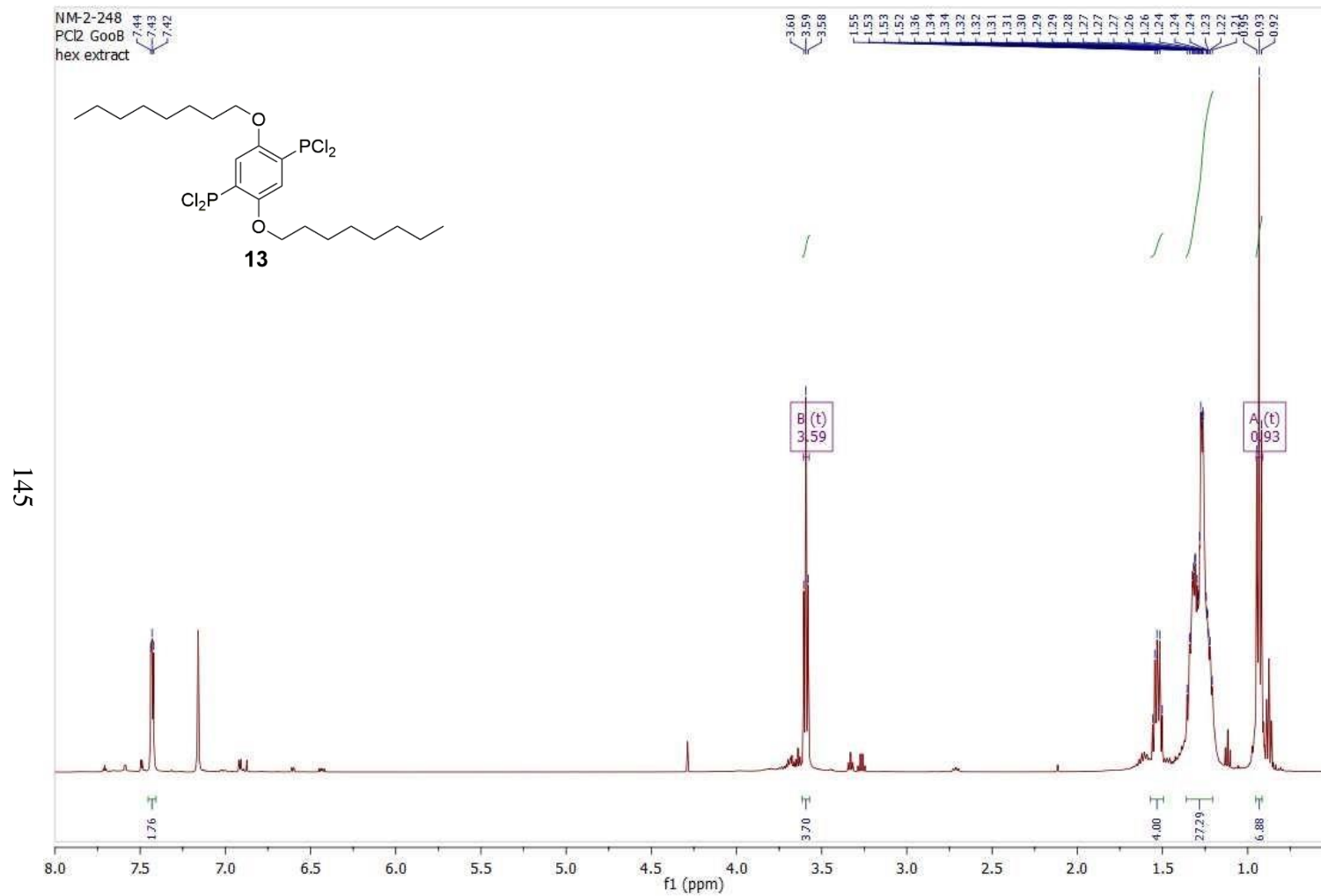


Figure A3.5 ¹H NMR spectrum of 13 in benzene-*d*₆

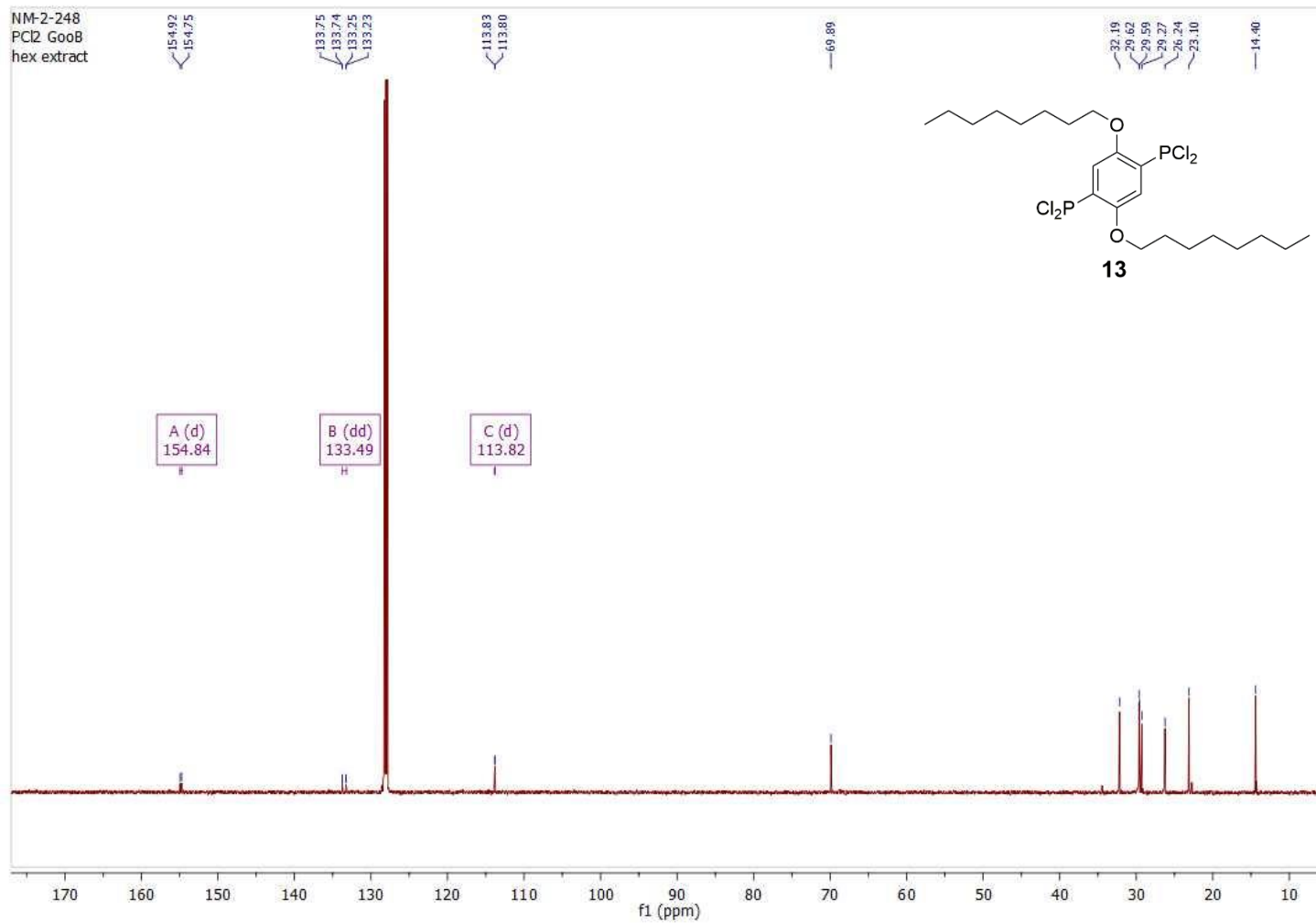


Figure A3.6 ¹³C NMR spectrum of **13** in benzene-*d*₆

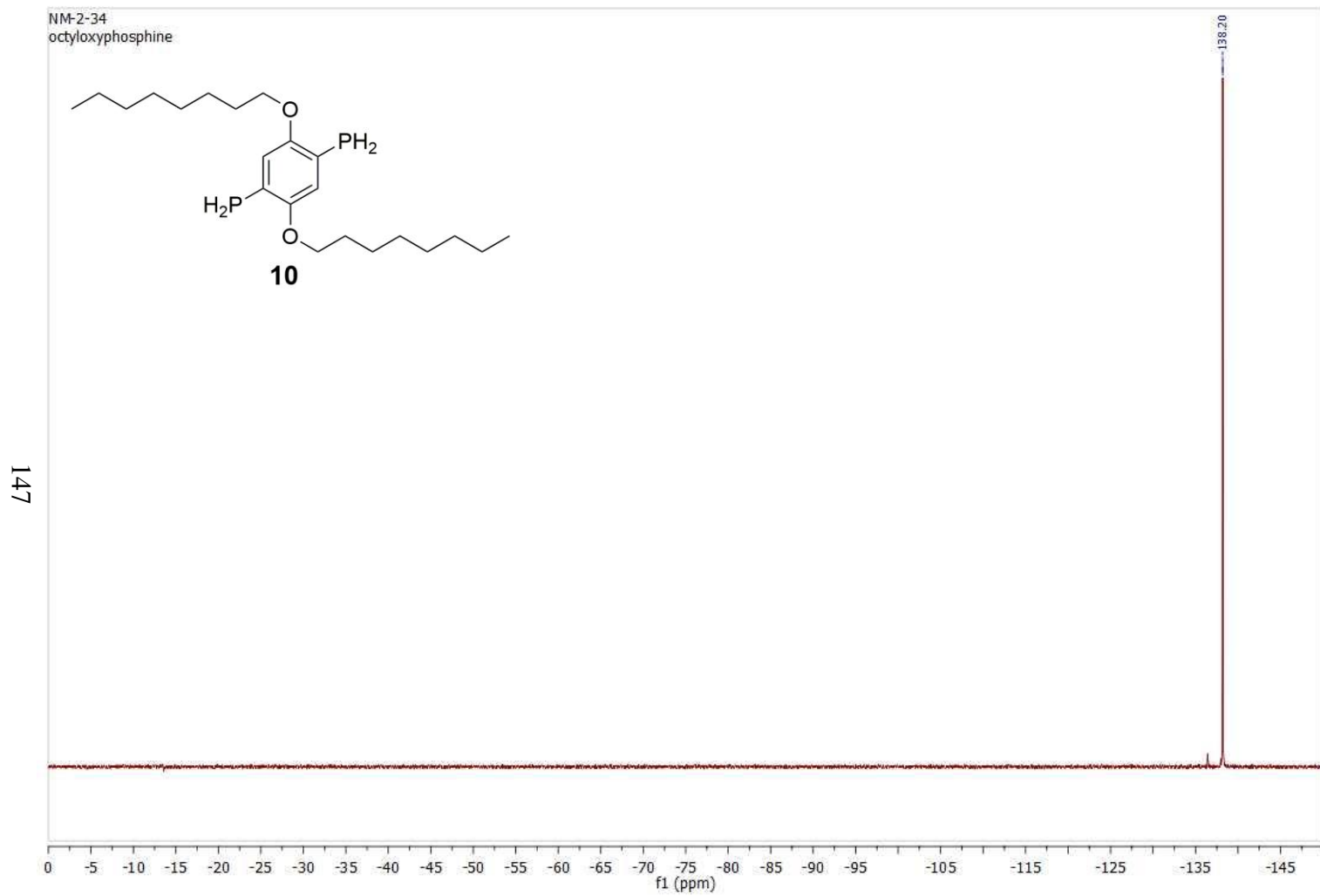


Figure A3.7 ^{31}P NMR spectrum of **10** in benzene- d_6

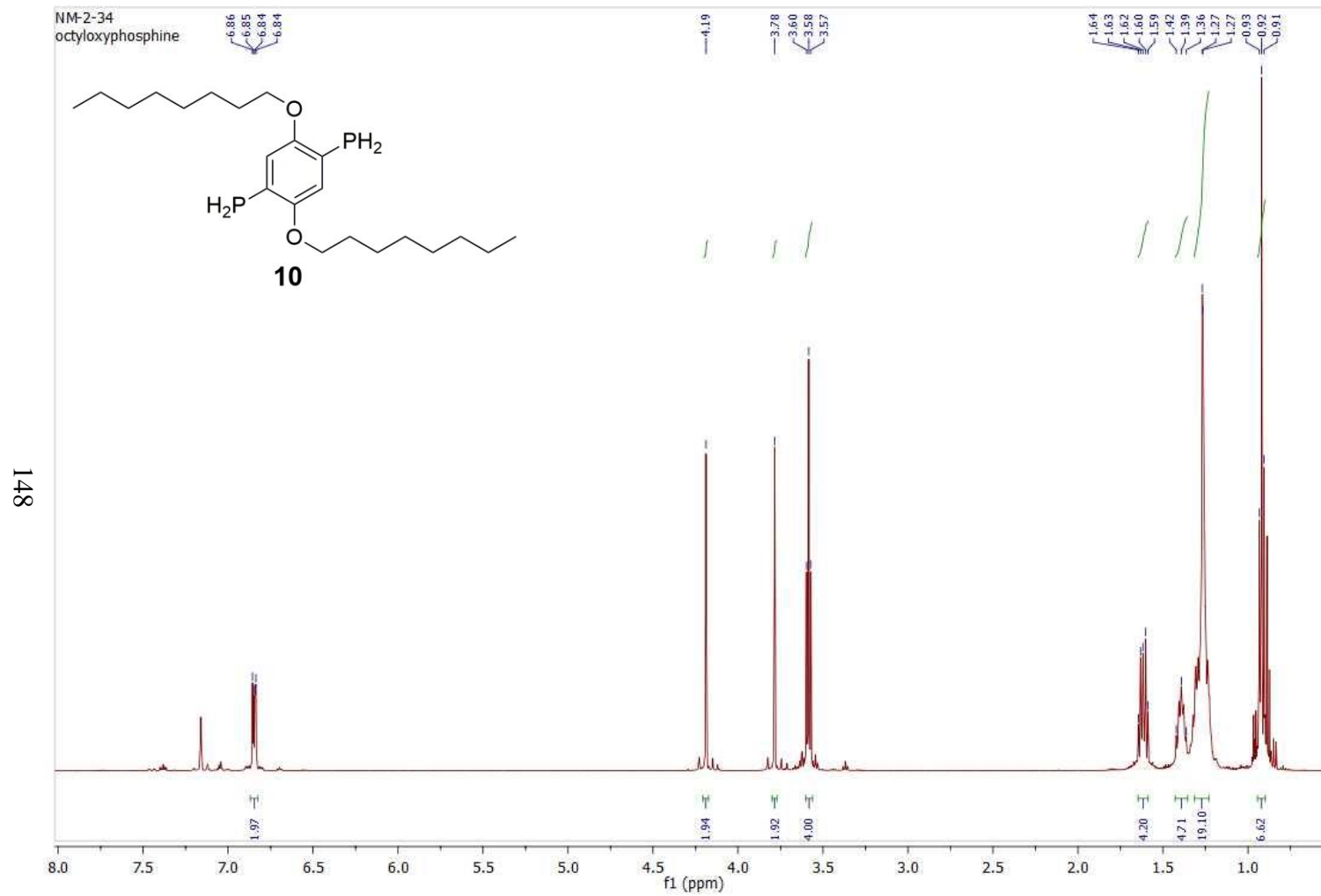


Figure A3.8 ^1H NMR spectrum of **10** in benzene- d_6

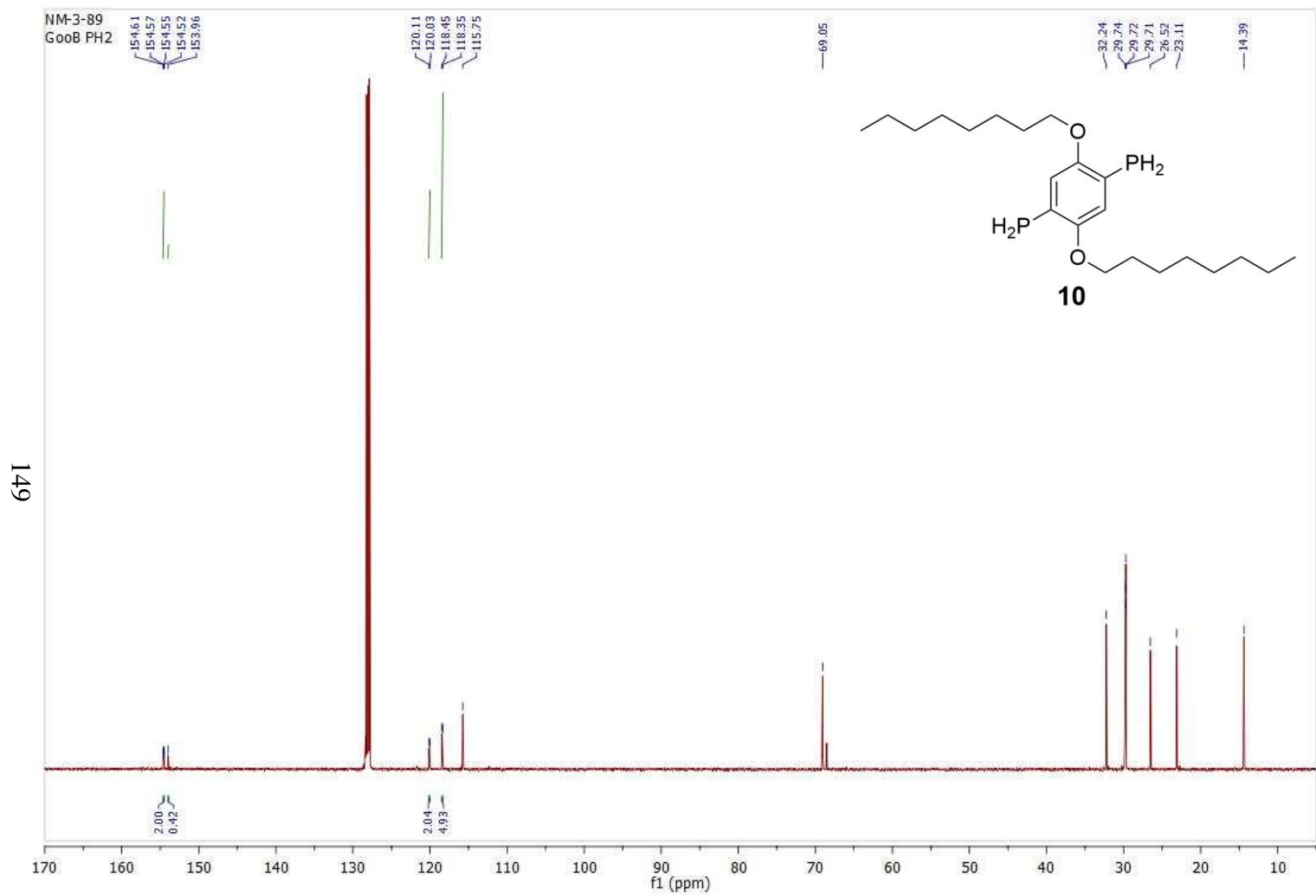


Figure A3.9 ^{13}C NMR spectrum of **10** in benzene- d_6

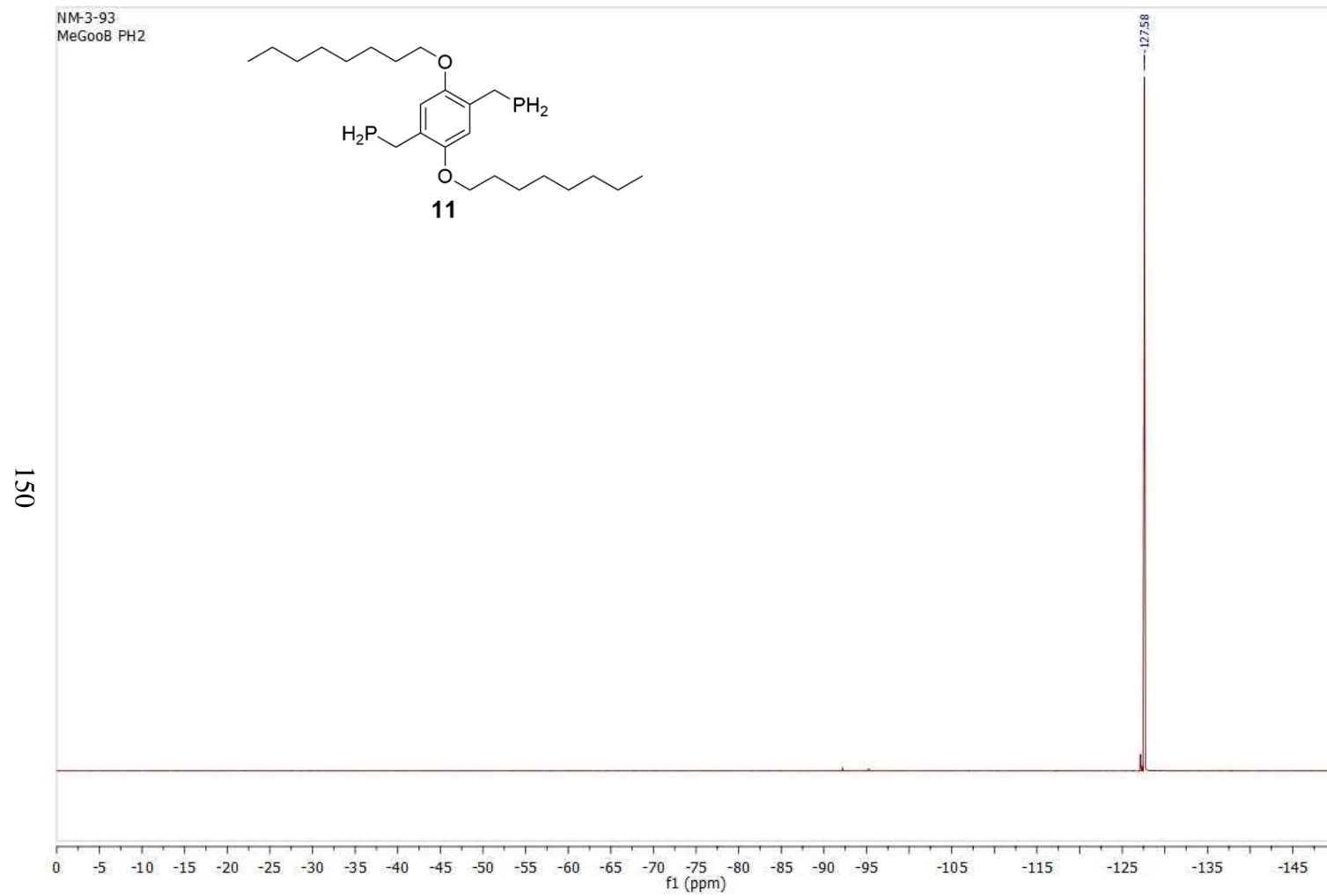


Figure A3.10 ^{31}P NMR spectrum of **11** in benzene- d_6

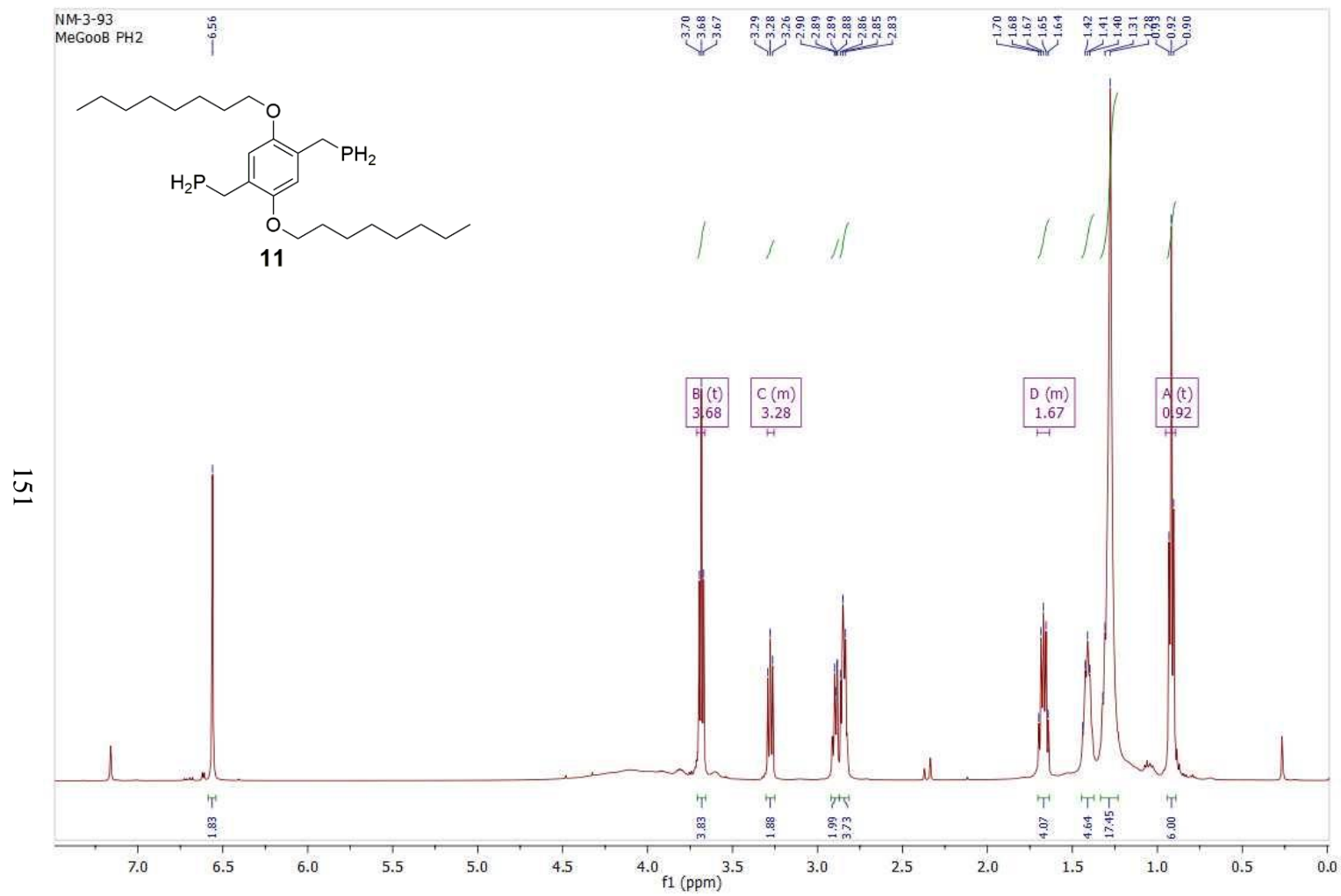


Figure A3.11 ^1H NMR spectrum of **11** in benzene- d_6

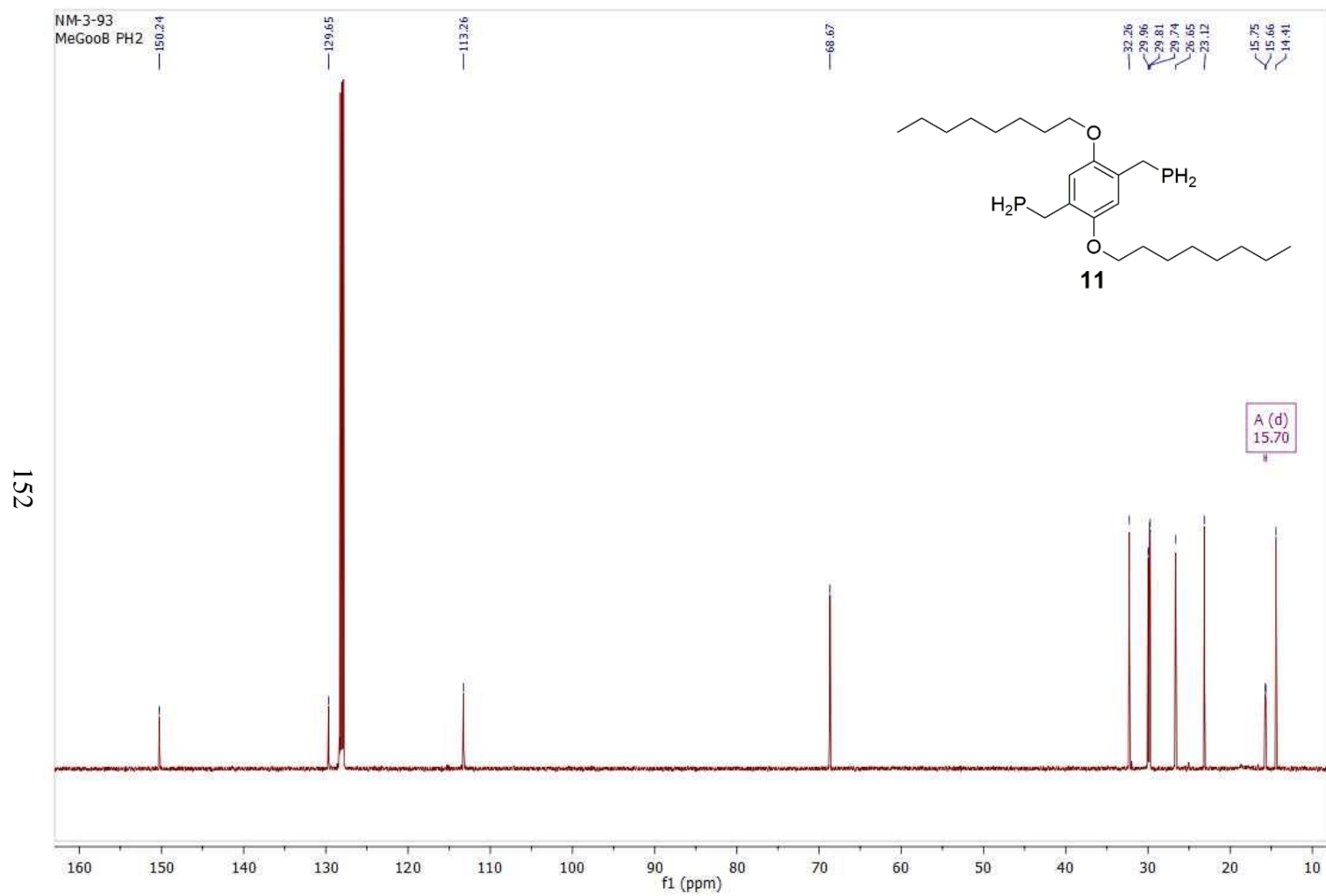


Figure A3.12 ^{13}C NMR spectrum of **11** in benzene- d_6